Characterization of Caytaxin protein in animal models of cerebellar dysfunction

by

Kristine M. Ito-Smith

A dissertation submitted in partial fulfillment
of the requirements for the degree of
Doctor of Philosophy
(Cellular and Molecular Biology)
in the University of Michigan
2012

Doctoral Committee:

Professor Margit Burmeister, Chair
Professor Henry L. Paulson
Associate Professor Michael Hortsch
Associate Professor Andrew P. Lieberman
Assistant Professor Vikram Shakkottai
Assistant Professor Hisashi Umemori

Dedication

To my dad, my eternal hero

To my sister, my forever best friend

To my brother, my radiant superstar

&

To my mom, 143 always

Acknowledgments

I would like to acknowledge my mentors, Drs. Michael Hortsch and Margit Burmeister, who endlessly supported my graduate training and always encouraged critical thinking and resourcefulness. I am grateful to the members of the Hortsch and Burmeister labs for their warm smiles and wonderful friendships, especially Dr. Vita Strumba, Dr. Cindy Schoen, Randi Burns, Ela Sliwerska, and Dr. Sandra Villafuerte. In their help in building my scientific foundation, I thank Dr. Zoia Stoycheva, Dr. Les Hanakahi and Dr. Alan Lau.

A warm thank you to my committee members Dr. Hank Paulson, Dr. Vikram Shakkottai, Dr. Hisashi Umemori, and Dr. Andy Lieberman for their continuous support and invaluable advice during the development and execution of my research. I am also grateful to those who provided additional mentorship and support, especially Dr. Jessica Schwartz, Dr. Katiuska Molina-Luna, and Dr. Ken Balazovich. I would like to acknowledge my support from PIBS, the Rackham Graduate School, the Program in Cellular and Molecular Biology, the Molecular and Behavioral Neuroscience Institute, and the department of Cell and Developmental Biology.

I thank my incredible friends and family, especially my dad Rodney, Nicole, Nickolas, and Nana for their love, faith, and for always being there despite the distance. A very special thank you to Ken and Emily for their endless encouragement, kindness, and open arms. Most of all, I thank my husband Matt – whose resplendent optimism has been my light in the darkness, and whose unwavering support has helped me become the person I am proud to be today.

Table of Contents

List of Figures

List of Tables

List of Appendices

List of Key Terms and Abbreviations

ARCA	Autosomal Recessive Cerebellar Ataxia
ARDA	Autosomal Dominant Cerebellar Ataxia
Arg	Arginine, amino acid, positively charged
AUG	aka ATG, translational start site
BAC	Bacterial Artificial Chromosome
BCH	BNIP-2 and Cdc42GAP Homology
BNIP-2	BCL2/adenovirus E1B 19kDa Interacting Protein 2
BNIP-H	BNIP-2 Homologous
cDNA	Complementary DNA
C-term	Carboxy-terminal, 3' end
CHIP	Carboxyl Terminus of Hsp70-Interacting Protein, E3 ubiquitin ligase
CHLC	Cooperative Human Linkage Center
cM	Centimorgan
DNA	Deoxyribonucleic Acid
ECL	Enhanced Chemiluminescence
ENU	N-ethyl-N-nitrosourea
ESP	Exome Sequencing Project
EVS	Exome Variant Server
GSP	Gene-Specific Primer
His	Histidine, amino acid
IAP	Intracisternal A Particle
kDa	Kilodalton
KGA	Kidney-type Glutaminase
KLC	Kinesin Light Chain, a component of Kinesin-1
Leu	Leucine, amino acid, common non-methionine start site
LTR	Long Terminal Repeat
mAb	Monoclonal Antibody (antibody)
Mb	Megabase
Met1	Mutation of first methionine to threonine
Met10	Mutation of second methionine to threonine
Met1+10	Mutation of both methionines to threonines
mRNA	Messenger RNA
N-term	Amino-terminal, 5' end
NGF	Nerve Growth Factor
NMD	Nonsense-Mediated Decay
ORF	Open Reading Frame
PAG	Phosphate-Activated Glutaminase
PAHO	Pan American Health Organization

Pin1	Peptidyl-Prolyl cis/trans-isomerase
PCR	Polymerase Chain Reaction
PTD	Primary Torsion Dystonia
PTM	Post-Translational Modification
qRT-PCR	Quantitative Real-Time PCR
RACE	Rapid Amplification of cDNA Ends
RNA	Ribonucleic Acid
Scn8A	Sodium Channel, voltage gated, type VIII, alpha subunit
SDS-PAGE	SDS Polyacrylamide Gel Electrophoresis
SEM	Standard Error of the Mean
Ser	Serine, amino acid, neutral
SINE	Short Interspersed Element
SNP	Single Nucleotide Polymorphism
Scn8A	aka Nav1.6, sodium channel, voltage gated, type VIII, alpha subunit
STRP	Short tandem repeat polymorphism
upORF	Upstream Open Reading Frame
UTR	Untranslated Region
Val	Valine, amino acid, common non-methionine start site

Gene and Mouse Nomenclature

Atcay	Mouse gene
ATCAY	Human gene
Caytaxin	Protein product of *Atcay/ATCAY*, human: 371aa, mouse: 372 aa
dystonic	aka *dt,* dystonic rat, IAP elements in intron 1
hes/*hes*	*hesitant* homozygote, mutant
hesitant	*Atcay*^{hes}, C3H-*Atcay*$^{ji\text{-}hes}$/J, IAP element in intron 1
ji/*ji*	*jittery* homozygote, mutant
jittery	*Atcay*^{ji}, B6.C(Cg)-*Atcay*^{ji}/BurJ, B1 element in exon 4
sidewinder	*Atcay*^{swd}, 2 base pair deletion in exon 5
swd/*swd*	*sidewinder* homozygote, mutant
wobbley	ENU-induced *Atcay* mouse mutation, lacking exon 4
wt/*ji*	*jittery* heterozygote, wild type
wt/*swd*	*sidewinder* heterozygote, wild type
wt/*hes*	*hesitant* heterozygote, wild type
BAC^{+}	Transgenic mouse, positive for the transgene
BAC^{-}	Transgenic mouse, negative for the transgene
BAC^{E9}	Transgenic line, *ATCAY* exon 9 mutation
BAC^{I9}	Transgenic line, *ATCAY* intron 9 mutation
BAC^{EI9}	Transgenic line, *ATCAY* exon 9 and intron 9 mutations
wtBAC	Transgenic line, Full-length *ATCAY*

Mouse videos

Video recordings of phenotypes of all lines described above are available upon request to the author or the Burmeister laboratory.

Chapter I.

Introduction

Ataxia is a disease of motor dysfunction

Since the 5th century B.C., physicians have identified and reported diseases which manifest as a lack of motor coordination. Greek patients presented with what they termed *ataksia*, *tabes dorsalis*, and *tabes* ossis sacri; the English and Germans instead described it as *ataxy*, *dorsal consumption*, *progressive spinal paralysis*, and *paraplegia*; French doctors observed *ataxia locomotrice progressive*. Today, over 2,000 years later, the term '*ataxia*' has evolved to represent a class of neurological disorders associated with hundreds of diseases, both acquired and inherited. Interestingly, the name itself remains relatively true to its origins.

The word 'ataxia' is composed of the Greek privative alpha (*a*), to indicate negation or absence, and the word '*taksia'* to describe order. Consistent with this, it is used clinically to describe a type of movement that seems to occur 'without order'. In 1837, the use of microscopes enabled more detailed descriptions of the pathological anatomy of diseases. A number of cellular abnormalities were identified in some ataxic patients, including wasting of spinal nerve-fibers,

presence of amyloid corpuscles, and proliferation of connective tissue [2]. Attempts at establishing a universal classification for ataxic disorders were unsuccessful even through the mid-20th century. Early documentation of hereditary ataxias consisted predominantly of reports from single cases or families, many of which were given different labels despite their similarity with previously-described incidences.

In 1847, Dr. Robert Bentley Todd described the physical symptoms resulting from these cellular abnormalities in one of his patients as a:

> "…diminution or total absence of power of coordinating movements. While considerable muscular power remained, the patient found great difficulty in walking, and the gait was so tottering and uncertain that his center of gravity was easily displaced." [3].

In 1858, French neurologist M. Duchenne de Boulogne described a disease which he called "*ataxia locomotrice progressive*" ("*progressive locomotor ataxia*"), characterized by atrophy of the roots of the sensory nerves, and the inability to take the bearings of external surfaces [2]. In an 1869 review by Sir Thomas Clifford Allbutt, he reminds medical practitioners that ataxia is not a disease in itself, but rather a symptom which is "...common to many diseases, or, indeed, in its widest sense, to all diseases, and that, in fact, it simply means '*disorder'."* [4]. In a 1983 article by Dr. A. E. Harding, she comically states that "…there are as many classifications of [hereditary ataxias] as there are authors on the subject." [5].

The evolution of ataxia classification continues today and the term “ataxia” is still used to describe both a symptom and a disease. However, cerebellar *ataxias* are now generally categorized as either “inherited” or “non-inherited”. Non-inherited (acquired) ataxia can be caused by a variety of physical cerebellar insults or appear as a secondary symptom to an underlying disease [6-8]. These include, but are not limited to, alcohol abuse, chemical toxicity, vitamin deficiencies, stroke, and physical brain trauma [9]. The category of inherited cerebellar ataxias encompasses a wide range of disorders characterized by cerebellar Purkinje cell degeneration, resulting in ataxia or loss of balance and coordination [10]. Many are caused by either gain-of-function or loss-of-function mutations in genes; however, the associated gene has only been identified in roughly half of inherited disorders [11].

Inherited cerebellar ataxias can further be classified based on their mode of inheritance, with the smallest groups comprising X-linked and mitochondrial ataxias, and the largest groups consisting of autosomal dominant cerebellar ataxias (ADCAs) and autosomal recessive cerebellar ataxias (ARCAs) [5, 12]. ADCAs are usually slowly progressive and often associated with cerebellar atrophy [12]. The predominant group of ADCAs, the spinocerebellar ataxias (SCAs), encompass 36 known types of SCAs, which are given numbers referring to the chronological order in which they were linked to a specific chromosome [12, 13]. The second largest group of inherited ataxias, ARCAs, is similar to ADCA’s in heterogeneity and complexity but differ in mode of inheritance [14].

Autosomal recessive cerebellar ataxias

ARCAs are recessively-inherited neurological disorders characterized by the degeneration or abnormal development of the cerebellum and spinal cord [9]. This group encompasses a large number of diseases, the most notable being Friedreich ataxia [9]. In a 1984 report, Dr. A. E. Harding suggests the separation of certain ARCAs based on age of onset and pathological mechanisms [5, 15]. In addition to progressive (degenerative) ataxias which worsen over time due to degeneration of cerebellar and spinal pathways [9], she also proposes a category of non-progressive congenital ataxias, which are present from birth and are associated with impaired development of the cerebellum and its connections. Under this classification system, relatively few conditions have been identified and described which cannot be classified as degenerative or involving defects in metabolism or DNA repair. The most recently discovered of these syndromes has been termed “Cayman ataxia”.

Cayman ataxia

Cayman ataxia was first described in 1978 by Dr. Arthur Bloom, a pediatrician and geneticist from Columbia University, who was asked to travel to the Cayman Islands by the Pan American Health Organization (PAHO) in 1976 [15]. He was asked to assess for genetic disorders in the Cayman Islands due to an alarming observation made by a public health nurse who was sent to the islands by PAHO a year earlier. She reported that 8.3% of newborns in the Cayman Islands had obvious physical abnormalities [15, 16]. It was determined by Dr. Bloom that

continual consanguinity had occurred in the Cayman Islands over a period of approximately 150 years, resulting in an increase in autosomal recessive genetic disorders [17]. Through data gathered from Dr. Bloom's study, three disorders were identified – only two of which had been previously described as Sanfilippo A and Usher syndrome [17]. The third was a unique form of ataxia only present in a small region of Grand Cayman Island, which was initially termed "Cayman Disease" and later renamed "Cayman ataxia" [15].

Based on family studies performed by Dr. Bloom, Cayman ataxia was characterized as an autosomal recessive disorder of the cerebellum (ARCA). The Cayman government reports that imaging studies in Cayman ataxia patients show cerebellar hypoplasia [15, 18], indicating an abnormal development of the cerebellum. Interestingly, while most ARCA cases appear before the age of 20 [15], Cayman ataxia is present from birth (congenital) with no signs of progression throughout the affected individual's lifetime (non-progressive) [17], making it unique among this class of ataxias.

Clinical symptoms of Cayman ataxia include a number of defects caused by cerebellar dysfunction which can be observed through general physical assessment. The most notable of these symptoms is variable psychomotor retardation characterized by both mental retardation and markedly delayed motor milestones [15]. A presence of hypotonia and a lack of motor control results in an uncoordinated wide-based ataxic gait, truncal ataxia, and intention tremors. Additionally, these patients present with pes planus (flat feet) and scoliosis

(abnormal spine curvature), which likely contribute to difficulties in moving and walking [15]. Lack of motor control also manifests in facial muscles, which causes a slurred dysarthric speech and marked ocular abnormalities. These include nystagmus (slow and quick phase oscillatory eye movements) [15, 16], and exo- or esotropia (outward or inward deviation of the eyes, respectively) [15], which may only be worsened by occasional paralysis of the eye muscles. The presence of nystagmus but the absence of retinal degeneration or detachment is unique to Cayman ataxia, among other ARCAs [15, 16]. Interestingly, despite their handicaps, the majority of these individuals often lived past 40 years and were able to hold steady jobs involving the application of simple vocational skills, with the aid of programs established by the Cayman Islands Government [18].

As of a 2004 report on genetic disorders in the Cayman Islands, 26 individuals were diagnosed with Cayman ataxia. An additional 6 cases were accounted for based on data obtained through personal interviews and limited public records [19]. Of these 32 total cases, a founder effect was evident as the lineage of 20 of these individuals could be linked to a single person [20]. In 1995, Dr. Paul Benke led a study which aimed to identify the affected genetic region common in all individuals with the disease [19]. Of the 26 living individuals, 19 of them contributed DNA for testing. Markers from affected samples were compared with those collected from unaffected siblings and parents of affected individuals through a DNA pooling approach. Short tandem repeat polymorphism (STRPs) developed by the Cooperative Human Linkage Center (CHLC) were used to amplify alleles in each pool via PCR [18, 21]. A difference in allele pattern

between control and affected pools was observed in a chromosome 19 marker. Further genotyping and pedigree analysis identified the common distal and proximal markers flanking the affected region, which narrowed the disease interval a region less than 2.0Mb on chromosome 19p13.3 [18].

The causative gene was identified in 2003, 8 years after Dr. Benke began his study, through comparative mapping with common DNA markers on mouse chromosome 10, which is homologous to human chromosome 19p13.3 [18]. At the time of this study, three ataxic mouse mutants had been identified, but the causative gene had not yet been characterized; however two of the mutations had been previously mapped to a region on mouse chromosome 10 [21]. Critical intervals within the affected regions on both human and mouse chromosomes were compared and an overlap was identified which spanned 150kb covering 7 genes. Sequencing of this interval revealed mutations in one common region which mapped to a single unknown predicted gene, thereafter hence termed *Atcay*/*ATCAY* for ‘ataxia, Cayman type’ [18].

The *Atcay*/*ATCAY* gene and its encoded protein Caytaxin

The human *ATCAY* gene contains a total of 13 exons, with the protein coding region spanning exons 2-13 [22]. Through a collaborative effort by Bomar *et al*, additional sequencing of exons and exon-intron boundaries of the *ATCAY* gene found that individuals with Cayman ataxia are homozygous for two mutations in *ATCAY* [18]. A mutation in exon 9 was identified as a single nucleotide

substitution from cytosine to guanine (C to G), resulting in a non-conserved serine to arginine (Ser to Arg) conversion in the amino acid sequence. The second mutation was also identified as a single nucleotide change, but in intron 9 of *ATCAY* near the exon 9-intron 9 splice junction. While this has no direct effect on amino acid sequence, it was hypothesized to cause a disruption of normal splicing [18].

To identify whether these two mutations were unique to Cayman ataxia, DNA sequences were compared between affected individuals and controls. The ancestry of the Cayman Islanders can be traced back to British and Jamaican origins [23] with specific Jamaican heritage originating from the west coast of Africa [18, 23]. Control DNA was chosen to represent these origins, and included samples from American-Europeans, ethnically diverse Americans, British individuals, Jamaican individuals, and West African Akan (from Ghana) and Bamileke (from Cameroon) [16]. A human mutation screen was developed by utilizing two restriction enzyme recognition sites *Alu* I and *Tsp* RI, which are eliminated by the presence of the exon 9 mutation and intron 9 mutation, respectively [18]. The data output from this screen provided DNA banding patterns unique to each mutation which could be compared across the controls.

Interestingly, neither mutation was identified in any of the control samples, indicating that both mutations are unique to Cayman ataxia and are unlikely to represent natural polymorphisms. At the time of this 2003 study, large-scale sequencing projects such as the NHLBI GO Exome Sequencing Project (ESP)

either did not yet exist or provided limited information regarding single nucleotide polymorphism (SNP) origins. To date, neither *ATCAY* variant has been identified and published in the Exome Variant Server (EVS) [24] . This poses the pressing question: do both of the mutations contribute to the disease phenotype?

Based on the location and nature of the *ATCAY* mutations, Bomar *et al* postulated that the exon mutation, despite causing a non-conserved amino acid change, would not interfere with the structure of the encoded protein [18]. The intron mutation, however, lies within a region critical for proper RNA splicing, thereby potentially decreasing this sites ability to serve as a splice donor [18]. They confirmed aberrant splicing around exon 9 by expressing a sub-cloned DNA fragment from affected individuals *in vivo* and observing banding patterns indicative of exon 9 skipping. The encoded protein was predicted to either be truncated or expressed at lower levels [18].

Abnormal gene products for ataxias are generally referred to as ‘”ataxins”, thus the protein encoded by the *Atcay*/*ATCAY* gene was termed “Caytaxin”. The human protein is comprised of 371 amino acids (372 residues in mouse) with 91% sequence similarity between human and mouse orthologs [25]. The first published analysis of *Atcay*/*ATCAY* mRNA localization was in mouse, and predicted Caytaxin expression to be robust but restricted to the nervous system [18, 26]. *In situ* hybridization of mouse adult brain and embryo indicated strong expression in all brain regions, including the cortex, cerebellum, and olfactory bulbs. In the embryo, *Atcay* was expressed predominantly in the brain, but was

also detected in regions of the nervous system such as trigeminal, sphenopalatine and dorsal root ganglia; as well as the nasal cavity and enteric system [18].

The highly-specific localization and high concentration of *Atcay*/*ATCAY* mRNA suggests that Caytaxin plays a critical role within the nervous system. Thus, decreases in Caytaxin expression caused by mutations in *Atcay*/*ATCAY* could explain the motor, physical and cognitive defects observed in animals and individuals who harbor mutations in the gene.

Atcay **mutations in animal models**

Thus far, Cayman ataxia is the only human disease that has been linked to mutations in the *ATCAY* gene. However, mutations in the mouse and rat *ATCAY* ortholog (*Atcay*) have been identified to cause dystonia and/or ataxia [18, 26, 27]. Of these models, the effect of *Atcay* mutations on Caytaxin expression has only been sparingly described for the dystonic *Atcay* mutant rat, $Atcay^{dt}$.

The genetically dystonic rat arose as a spontaneous autosomal recessive mutation in the Sprague-Dawley rat strain, and was given the name *dystonic* (*dt*) by Lorden *et al* who first described the mutation in 1984 [26]. Originally identified as an animal model for dystonia musculorum deformans [28], now referred to as primary torsion dystonia (PTD), the disease manifests in rats 9 days after birth as a stiff gait, frequent falling, and twisting of the neck [26]. The disease progresses rapidly and symptoms evolve to include tail rigidity and truncal hyperflexion, with

a severity that prevents rat survival beyond post-natal day 40 [26]. The cause of the disease could not be linked to physical brain anomalies due to the absence of gross morphological abnormalities and a lack of degeneration in the central and peripheral nervous systems. However, biochemical and physiological analyses suggested that the cause of the disease originates from abnormal cerebellar output. This hypothesis was confirmed by LeDoux *et al* who performed cerebellectomies on affected rats, which successfully eliminated the majority of dystonic symptoms and resulted in a sustained long-term improvement in motor function [28].

Chromosomal mapping and subsequent gene sequencing of rat *Atcay* found a down-regulation in mutant *Atcay* gene expression due to an insertion of a 3'-long terminal repeat (3'-LTR) of rat intracisternal A particle (IAP) elements in *Atcay* intron 1 [27]. This insertion results in an addition of 435bp to intron 1, and a dramatic reduction in *Atcay* RNA transcript within cerebellar and cerebral cortical tissues. Due to the limited availability of reliable antibodies for detecting Caytaxin protein at the time of this study, LeDoux *et al* generated two anti-Caytaxin polyclonal antibodies in rabbit and mouse which were raised against different portions of rat Caytaxin. Western blotting with these antibodies on cerebellar samples detected markedly reduced levels of Caytaxin protein in the *dystonic* mutants but intermediate levels in heterozygous littermates, compared to wild type controls [27]. Not only was this the first study examining Caytaxin protein expression within the brain, but it supports the hypothesis that mutations in *Atcay*/*ATCAY* may cause disease by affecting Caytaxin expression and function.

In addition to the *Atcay*^{dt} rat, four ataxic mouse mutants have been identified that harbor unique mutations in mouse *Atcay* [18, 29-32]. While Caytaxin expression has not been described in these *Atcay* mutant mice, characterization of their mutations predicted that the protein is either decreased or absent [18, 32]. In three of these mouse lines, the *Atcay* mutation arose spontaneously; the fourth mutation was induced by chemical mutagenesis. These *Atcay* mutant mice differ from the rat model in that dystonia is not their primary symptom; they instead each display a distinct phenotype, with varying levels of both ataxia and dystonia [18, 29-32].

Atcay^{ji} (*jittery)* was the first *Atcay* mutant mouse discovered in 1941 by Dr. Kenneth B. DeOme, who described *jittery* in his 1945 manuscript as a spontaneous mutation occurring in the Bagg albino mouse strain (now known as BALB/c) [33]. He reports that *jittery* homozygotes display muscular incoordination (ataxia) by post-natal day 10 (P10), which manifests as righting difficulties and imbalance while walking or running. By P16, epileptic seizures and tetany (dystonia) present as an up-and-down beating of the limbs. At this point, mice lose the ability to obtain food and water and usually die of starvation and dehydration by 4 weeks of age without special care [33].

Dr. George D. Snell also published a report on the *jittery* mice in 1945 after drawing from Dr. DeOme's description of the *jittery* phenotype [31]. He tested for linkage of the *jittery* mutation with other known genes and mapped *ji* within 15-25cM distal to the *waltzing* mutation, which was discovered in the early 1900's in

mice from Japan that display circling, head-tossing, deafness, and hyperactivity [29, 34]. Information gathered from additional mapping efforts by Dr. Margaret C. Green in 1968 [29], Sweet and Davisson in 1993 [34], and Kapfhamer *et al* in 1996 [30], further narrowed the *ji* locus to a region on mouse Chromosome 10. The affected gene and mutation were not discovered until the 2003 Cayman ataxia study by Bomar *et al* from the laboratory of Dr. Margit Burmeister. It was here that the identification of *Atcay*/*ATCAY* enabled the characterization of the *Atcay* mouse mutations [18]. These mutations and their observed or putative effect on Caytaxin expression are summarized in Figure 1.1

jittery mutants harbor a B1 element – a non-LTR retro-transposon, short interspersed element (SINE) – insertion in exon 4 of the *Atcay* gene [18, 35]. This insertion results in a larger mRNA species expressed at markedly reduced levels compared to wild type controls, but equivalent with non-affected heterozygote littermates. Two proteins are expected to be translated, with the smallest protein predicted to encode only 83 residues out of the normal 372, 21 of which are missense [18] (Fig 1.1 B, starred). Expression of the larger species is predicted to be extremely low, made up of 298 amino acids and missing exon 4 [18] (Fig 1.1B).

The second spontaneous *Atcay* mutation, *Atcay*$^{ji\text{-}hes}$ (*hesitant*), arose at The Jackson Laboratory in 1987 [36]. Originating in the C3H/HeJ-ca strain, homozygous mutant mice can be identified by P14 due to their smaller size, imbalance (ataxia), and slight hesitation upon walking. By P21, affected mice

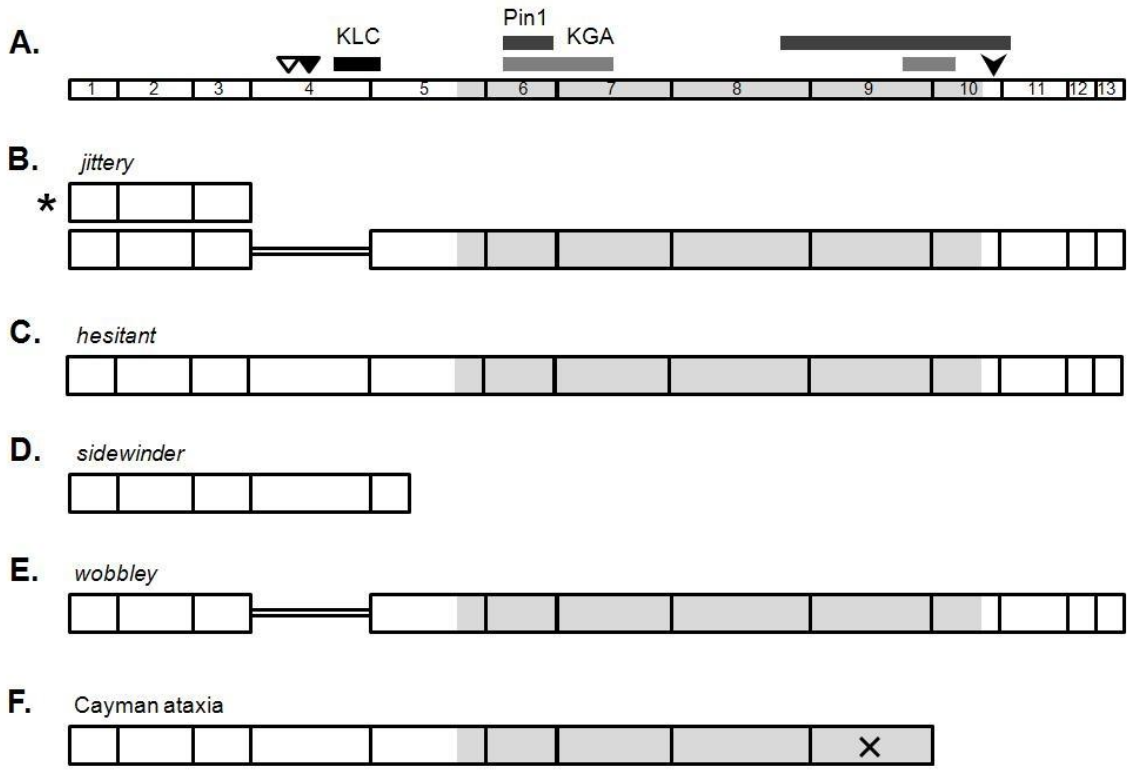

Figure 1.1. Effects of *Atcay*/*ATCAY* mutations on conserved Caytaxin domains.
Putative effects of mouse and human *Atcay*/*ATCAY* mutations on Caytaxin based on known interactions sites and conserved domains. **(A)** shows full-length Caytaxin separated into its 13 exons. The conserved BCH domain (shaded) spans the end of E5 into E10. Interaction sites for CHIP (open triangle), caspase-3 (filled triangle), and the putative nuclear export signal (filled arrowhead) are marked. Binding regions for kinesin light chain (black bar), Pin1 (dark grey bars), and glutaminase (light grey bars) are indicated. **(B)** The mutation in *jittery* produces protein truncated at E4 (starred) and low levels of a protein missing E4. **(C)** The *hesitant* mutation produces low levels of full length Caytaxin. **(D)** The *sidewinder* mutation produces a protein which is truncated within E5. **(E)** The *wobbley* mutation produces a protein missing exon 4 (not observed). **(F)** The Cayman ataxia mutations produce a protein truncated after E9 due to the intron 9 mutation. The E9 amino acid conversion (**X**) is not expected to effect Caytaxin expression.

display a more pronounced phenotype characterized by exaggerated stepping of the hind limbs due to a sustained stiffness of the legs [21, 36], later described as dystonia. Despite their unusual symptoms, *hesitant* mutant mice have a normal life span, and are able to reproduce and rear offspring [36]. *hesitant* defects are caused by an intracisternal A particle (IAP) element insertion into intron 1 of *Atcay*, which affects normal RNA splicing, resulting in larger mutant transcripts and significantly less normal transcript [30, 36]. It had been hypothesized that the low amounts of normal transcript could produce an amount of Caytaxin sufficient for partial function (Fig 1.1C), thereby explaining the less-severe *hesitant* phenotype [18].

The third spontaneous *Atcay* mutation, *Atcay*^{swd} (*sidewinder*), was identified in 1999 by The Jackson Laboratory, where allelism with *jittery* was established through complementation tests [18]. These mice were then sent to Dr. Margit Burmeister at the University of Michigan (whose laboratory performed the 2003 mapping of *jittery)* where they were described as phenotypically similar to *jittery* and found to harbor a 2 base pair deletion in exon 5 of *Atcay* [18]. This was expected to cause a frame shift and the introduction of a premature stop codon, predicting a Caytaxin protein of only 200 amino acids, the last 19 of which differ from the original sequence (Fig 1.1D). Similar to *jittery*, the functional capacity of this mutant Caytaxin was not discussed [18].

The fourth mutant mouse *Atcay* allele, *wobbley*, is the only known chemically-induced mutation of *Atcay*, and was created by Dr. Bruce Beutler's laboratory at

UT Southwestern Medical Center through N-ethyl-N-nitrosourea (ENU) mutagenesis [32]. Although *wobbley* has not been published by this group, the mouse has been deposited into the MUTAGENETIX™ database, which contains phenotypes and mutations produced through random germ line mutagenesis with ENU (http://mutagenetix.utsouthwestern.edu/). Dr. Beutler's group posted the *wobbley* record in 2008, and the description of the phenotype is reminiscent of *hesitant* and *sidewinder*; symptoms appear around P21 and include an abnormal gait with exaggerated stepping of the hind legs, frequent imbalance, and difficulty righting [32]. Affected mice are able to successfully breed and access food and water; however, disease progression prevents survival beyond 8 months of age. The causative mutation was identified to be a T to A conversion in the donor splice site of *Atcay* intron 4, expected to result in skipping of exon 4 [32] (Fig 1.1E).

Within the four different *Atcay* mutant mouse strains, different mutations in *Atcay* produce different phenotypes. Interestingly, the phenotype of these mice is distinct and individual strains can be identified simply based on their visible motor phenotypes; however this may in part also be influenced by the genetic background on which they are maintained. Although all of these mouse mutations were predicted to result a decrease or an absence of Caytaxin [37], the level of Caytaxin protein expression in mutant animals has not been characterized prior to the work described in this dissertation. A large body of data, however, has been generated by multiple groups regarding Caytaxin protein interactions and protein processing.

Identification of Caytaxin protein domains and interactions

In some reports, Caytaxin has also been referred to as BNIP-H (BNIP-2 homologous) since it shares 52% amino acid sequence identity and an overall 69% sequence similarity with BNIP-2 (BCL2/adenovirus E1B 19kDa interacting protein 2) [38]. In addition to BNIP-H, three other proteins make up the BNIP-2 protein family based on a conserved domain at the C-terminus of all BNIP-2 proteins [38, 39]. This region, the BNIP-2 and Cdc42GAP homology (BCH) domain, has been found to impart a wide range of cellular functions such as apoptosis [38, 40-42], cell migration [43], intracellular trafficking [38, 40], and cell differentiation [44]. Phylogenetic mapping of BCH domains found in various vertebrate Caytaxin protein orthologs indicates a high level of amino acid similarity [39, 41], and potentially a shared physiological function of the different Caytaxin proteins across species. While it has not been determined whether the BCH domain of Caytaxin is involved in any of the functions mentioned above, many groups have identified Caytaxin's BCH domain as a region targeted by a number of neuronal factors [38, 40, 44-46]. These interactions and their location within *Atcay*/*ATCAY* are summarized in Figure 1.1A.

The first protein found to interact with Caytaxin was the E3 ubiquitin ligase, CHIP (carboxyl terminus of Hsp70-interacting protein), which was identified in a screen for CHIP protein interactions. This ligase was found to directly bind and poly-ubiquinate Caytaxin *in vitro* [44], suggesting a mechanism for Caytaxin protein regulation. Another protein interaction screen performed by Buschdorf *et al*

specifically sought to identify Caytaxin cellular binding partners to gain insight into its physiological function. Through a GST-Caytaxin pull-down assay, they identified kidney-type glutaminase (KGA), the only isoform of phosphate-activated glutaminase (PAG) expressed in the brain [47], as a protein that directly binds Caytaxin at two separate regions within its BCH domain [38]. KGA is an enzyme that converts glutamine to glutamate, an excitatory neurotransmitter essential for synaptic transmission within the brain that is excitotoxic at high concentrations [48, 49]. Buschdorf *et al* also found that over-expression of Caytaxin appeared to regulate KGA levels, activity, and localization [38]. They hypothesized that without Caytaxin, KGA levels in the axon terminals would decrease, resulting in elevated glutaminase activity and an overall increase in glutamate levels – which could potentially affect neurotransmission or cause toxicity.

Through a candidate screen for proteins which could bind to a conserved serine/threonine motif within the BCH domain of Caytaxin, Buschdorf *et al* identified peptidyl-prolyl cis/trans-isomerase (Pin1) [27]. Pin1, a factor that is known to affect structure, phosphorylation status, and stability of proteins involved in cell cycle control and has been linked to a number of neurodegenerative disorders such as Alzheimer's and Parkinson disease [48, 50]. Buschdorf *et al* found that upon stimulation by nerve growth factor (NGF), which is thought to release Caytaxin's intramolecular interactions, Pin1 binds at two different sites within the BCH domain [40]. Together these proteins localize to neurites in differentiating neurons. The functions that Pin1 could impart on

Caytaxin due to this direct interaction were not discussed; however Buschdorf *et al* suggested that this data provides evidence for possible post-translational functions for Caytaxin [40].

In their own examination of Caytaxin function, Aoyama *et al* utilized a yeast two-hybrid screen to identify binding partners for Caytaxin [45]. They found that kinesin light chain (KLC), a component of Kinesin-1, directly binds Caytaxin at its N-terminal region and transports it along axons towards distal regions of neurites by a microtubule-dependent kinesin mechanism [45]. The KLC recognition site on Caytaxin lies at the N-terminus upstream of the BCH domain and is highly conserved among Caytaxin homologues and among the other BNIP-2 family proteins [45]. This led Aoyama *et al* to hypothesize that Caytaxin functions as a scaffold between KLC's and various cargo, such as those required for cell signaling.

The most recent investigation into Caytaxin protein binding partners stems from a study led by Dr. Toshiyuki Nakagawa. Originally designed as a screen for proteins involved in synaptic apoptosis, they performed a caspase cleavage assay and identified a single positive clone as Caytaxin [46]. This finding evolved into two separate studies. In one study by Itoh *et al* [46], they confirmed that Caytaxin is cleaved by caspase-3, a protease involved in apoptosis and cell signaling cascades [51]. At a recognition site in the N-terminus of Caytaxin, upstream of the BCH domain, caspase-3 cleaves the protein and produces a C-terminal fragment capable of inhibiting MEK2 (MAPK) signaling [46]. The residual

N-terminal fragment, now missing a putative nuclear export signal, no longer localizes to the cytosol but instead remains primarily in the nucleus. Based on this data, Itoh *et al* hypothesized that Caytaxin regulates glutamate neurotransmission though both its full-length and cleaved forms [46].

In a second report from Dr. Nakagawa's laboratory, Hayakawa *et al* [52] attempted to characterize Caytaxin expression and localization. Two anti-Caytaxin polyclonal antibodies were raised against the N-terminus or the C-terminus of the protein to examine Caytaxin localization within the mouse brain. They found predominant expression of Caytaxin in the cerebellum, which increased between ages P14-P28; robust expression in the olfactory bulb, cerebral cortex, basal ganglia, and hippocampus; and lower expression in brain stem and spinal cord [52]. Within the sub-regions of the brain, they detected predominant expression in the molecular layer of the cerebellum more specifically in presynaptic neurons [52]. They demonstrate that Caytaxin is expressed in presynaptic granule cells, and hypothesize that it is involved in synaptic transmission, likely via a highly-conserved protein binding domain.

Optimizing tools for studying Caytaxin function

So far, studies investigating Caytaxin protein properties and function within relevant animal models have been limited, and more commonly involve *in vitro* assays or *in vivo* (cell culture) systems. Advancements in identifying Caytaxin protein binding partners and characterizing regions which may impart specific

functions have been instrumental in contributing to the overall characterization of Caytaxin. However, the function of Caytaxin remains poorly understood. Four mouse models and one rat model have been identified to actually harbor mutations in *Atcay*. Of these, Caytaxin expression has only been briefly characterized in the dystonic rat, whose *Atcay* mutation and symptoms significantly differ from those of the human disorder [53].

The significance of identifying the role of Caytaxin within the nervous system becomes apparent when one considers the various symptoms associated with Cayman ataxia resulting from two seemingly innocuous mutations. The broad range of *Atcay* mutations in rodent systems indicate that even single mutations or insertions within the gene can cause an array of phenotypes which vary in severity. Together, this suggests that Caytaxin indeed plays a critical role in neuronal function. Since Cayman ataxia is a rare disease, limited information and resources can be utilized to study Caytaxin. Thus, in advancing toward an understanding of its function, the establishment and optimization of reliable tools and reproducible methods are critical. By further examining Caytaxin expression in *Atcay* mutant mouse models, a link can be established between phenotype and genotype.

We hypothesize that biochemical analysis of Caytaxin in appropriate ataxic model animals is essential to elucidate the overall function of Caytaxin within the nervous system. This function may be highly dependent on both level of expression and presence of a complete BCH binding domain – two

factors that are likely affected by mutations within the *Atcay/ATCAY* gene. Using representative *Atcay* mutant and humanized mice to characterize the effect of *Atcay/ATCAY* mutations on Caytaxin expression will establish reliable experimental paradigms; thus providing a novel approach to examining Caytaxin function.

Summary

The studies described in subsequent chapters greatly expand the number of tools for examining Caytaxin function and present novel methods for more accurate assessment of protein expression. In Chapter II, we generate monoclonal antibodies (mAb) specific for the Caytaxin protein as well as transgenic mouse lines expressing human Caytaxin. Caytaxin expression was assessed in multiple model systems including cell lines, wild type and *Atcay* mouse mutants, and transgenic *ATCAY* mouse lines. These analyses describe a conservation of function between Caytaxin orthologs and establish a link between protein expression and disease phenotype. In Chapter III, we examine the effect of the Cayman ataxia intron 9 variant on *ATCAY* gene and Caytaxin protein expression. This analysis reveals that while this mutation causes a truncation of Caytaxin, the protein retains its functionality, and may require the exon 9 variant for abrogation of function. By comparing data from Chapters II and III with previous studies characterizing Caytaxin protein interactions, further evidence was gathered suggesting the requirement of an intact BCH domain for Caytaxin function. Additionally, these studies reveal a potentially important role

for regions both upstream and downstream of the conserved region. Overall, this study highlights the importance for previously-unknown Caytaxin characteristics that must be accounted for in future studies of Caytaxin protein function and describes novel systems and methods for these studies.

Chapter II.

Expression of Caytaxin protein in Cayman ataxia mouse models correlates with phenotype severity

Introduction

Mutations in *Atcay*/*ATCAY* are predicted to decrease or eliminate Caytaxin expression within the nervous system, as evidenced by the four ataxic mouse mutants that harbor unique mutations in the mouse homologue of *ATCAY* (*Atcay*) [18, 32, 33]. The B1 element insertion in *Atcay* of the severely ataxic *jittery* mutants is predicted to result in a reduction of mRNA levels and truncation of Caytaxin [18]. Similarly, the 2 base pair deletion in *Atcay* of *sidewinder* mutants is expected to produce a truncated non-functional protein due to a frame shift [18]. This also leads to a drastic reduction in mRNA, likely due to nonsense-mediated decay (NMD) [18]. Conversely, the intracisternal A particle (IAP) insertion *in Atcay* of the mildly ataxic *hesitant* mutant mice is expected to affect splicing [18]. This is observed in the mutant dystonic rat strain (SD-dt:JFL) which also harbors an IAP insertion in intron 1 of the *Atcay* rat homologue, resulting in a marked reduction of cerebellar Caytaxin levels [42, 54, 55].

These known rodent and human *Atcay*/*ATCAY* mutations differ in gene location and how they affect the genomic sequence and its protein product, each resulting

in pronounced defects in motor coordination. However, the effects of different mutations on Caytaxin expression had not been characterized. While the role of Caytaxin in the nervous system remains poorly understood, protein homology mapping has identified highly-conserved domains, such as the BCH domain, and interactions with Pin1, glutaminase, kinesin, and CHIP, that may be critical for its function [38, 40, 44-46]. Phylogenetic analysis of various vertebrate Caytaxin orthologs indicates a high level of amino acid similarity [39], suggesting a potentially shared physiological function across these species.

While these data suggest that Caytaxin plays an important role at synapses and/or during neuronal differentiation, it remains unclear how mutations in the *Atcay* gene affect the ability of Caytaxin to properly function and maintain normal motor control. Thus, we sought to characterize Caytaxin expression in the spontaneous mutants *sidewinder*, *jittery*, and *hesitant* using novel monoclonal antibodies (mAbs) specific for Caytaxin. We also investigated the potentially conserved function of Caytaxin by rescuing the ataxic phenotype in transgenic *sidewinder* and *jittery* mice through over-expression of human *ATCAY*. Through the use of mouse models which display an assayable phenotype resulting from mutations in *Atcay*, we demonstrate that a more direct link between Caytaxin expression and function can be established. Further investigation into motor defects in these mouse models represents a promising approach in elucidating the physiological function of Caytaxin within the nervous system.

Results

Monoclonal antibodies generated against full-length Caytaxin detect multiple protein bands

To examine Caytaxin protein expression, mAbs were generated against full-length human Caytaxin protein (described in Materials and methods). A human Caytaxin fusion protein was expressed and purified from bacteria, which was subsequently used as an immunogen in mice to ultimately generate anti-Caytaxin secreting hybridoma cell lines. Using SDS polyacrylamide gel electrophoresis (SDS-PAGE) and a Western blot-based screen, whole brain lysate from wild type C57BL/6J mice were probed with hybridoma cell line supernatants (Fig 2.1), and compared to polyclonal antiserum that was obtained from the immunized mouse that was used for the generation of hybridoma cell lines (Fig 2.1, lane 2). This polyclonal antiserum reacts with three distinct protein bands ranging in size from 50-60kDa and an additional protein band of approximately 67kDa. Hybridoma cell line supernatants 1E2, 4E3, and 8F4 all react with the same three 50-60kDa protein bands, which are also detected by the polyclonal anti-Caytaxin antiserum, but did not react with the 67kDa band (Fig 2.1, lanes 3-5).

Based on their amino acid sequences, the calculated molecular weights for human and mouse Caytaxin are 42.12kDa and 42.18kDa, respectively [56]. The three protein bands, which are detected by the polyclonal antibody and the three selected hybridoma supernatants, have apparent molecular weights that are not only larger than 42.18kDa, but appear as distinct bands. The two larger protein species are 58kDa and 55kDa in apparent molecular size and the smallest

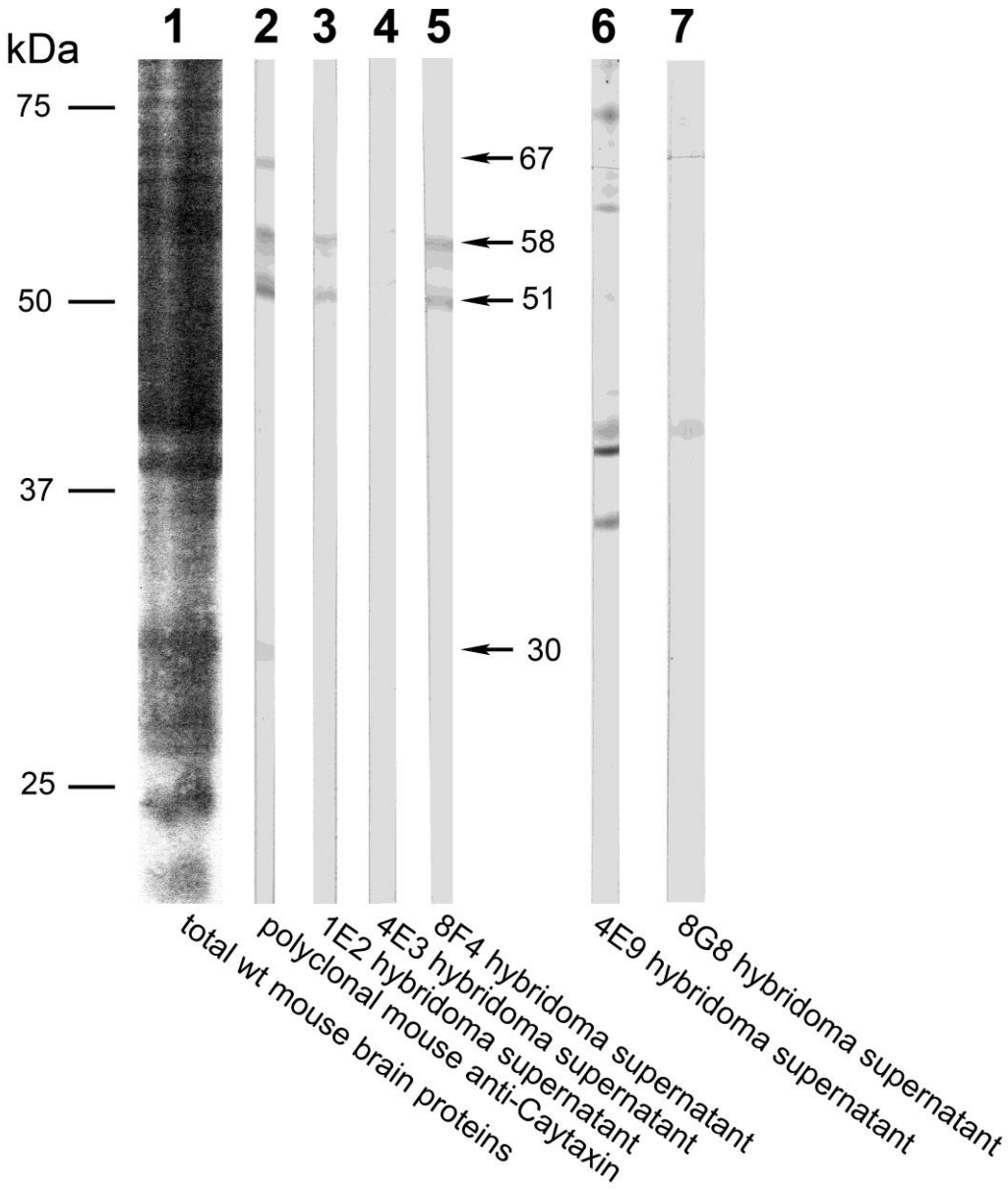

Figure 2.1. Caytaxin monoclonal antibody screen.
Western blots with wild type mouse whole brain protein extracts were used to screen hybridoma supernatants for anti-Caytaxin antibody activity. Lanes 2-7 were developed with DAB. **Lane 1**, total wild type mouse brain protein as detected by Ponceau S staining; **lane 2**, pattern of polyclonal mouse serum from mouse sacrificed for the fusion protocol; **lanes 3, 4 and 5**, patterns from hybridoma wells 1E2, 4E3, and 8F4 respectively; **lanes 6 and 7**, hybridoma supernatants 4E9 and 8G8 were later determined not to contain any anti-Caytaxin activity, but rather reacted with unknown proteins of different molecular weights. Data and figure generated by LaGina Nosavanh.

protein band is around 50kDa. Since all three of these bands were not recognized by control hybridoma supernatants (Fig 2.1, lanes 6 & 7), we hypothesized that the three selected hybridoma supernatants are specific for Caytaxin and detect three different Caytaxin isoforms. Thus, hybridoma cell lines 1E2, 4E3 and 8F4 were sub-cloned and further investigated as potential candidates for secreting antibodies specific for the Caytaxin protein.

Caytaxin protein expression is absent or reduced in homozygous *Atcay* mouse mutants

We next sought to determine the specificity of our selected mAbs and to confirm that all three protein bands detected by the hybridoma supernatants represent Caytaxin protein. The mutant *Atcay* mouse lines, *sidewinder*, *jittery*, and *hesitant* each harbor unique mutations in the mouse *Atcay* gene, which were predicted to affect Caytaxin protein expression [18]. Homozygous *jittery* and *sidewinder* mutant mice display a severely ataxic phenotype and were predicted to produce a truncated non-functional Caytaxin protein [18]. In contrast, homozygous *hesitant* mutant mice exhibit a mild ataxic/dystonic phenotype and due to a defect in RNA processing, were expected to have a reduced level of Caytaxin protein [18, 36]. A comparison of the Caytaxin protein expression pattern of wild type versus affected littermates from these mutant lines suggests that all three protein bands detected by our mAbs are indeed Caytaxin isoforms (Fig 2.2).

The Western blot shown in Figure 2.2A contains total brain lysates from wild type

(wt/wt), heterozygous (*swd*/wt), and mutant (*swd*/*swd*) littermates from the *sidewinder* mouse line. In wild type mice, all three putative Caytaxin protein isoforms are strongly expressed, but are absent in severely ataxic homozygous *swd*/*swd* littermates (Fig 2.2A, lanes 1 & 3). Caytaxin protein expression was decreased in heterozygous littermates, which harbor one normal allele and do not show signs of ataxia nor dystonia (Fig 2.2A, lane 2). This result confirms that each of the three isoforms detected by our mAbs is Caytaxin protein.

Similar to *swd*/*swd* mice, mice homozygous for the *jittery* mutation (*ji*/*ji*) do not express Caytaxin protein (Fig 2.2B & C, lanes 3 & 4). In contrast, *hesitant* mutant mice (*hes*/*hes*) express Caytaxin protein at a very low, but detectable level – at least 10-fold reduced, when compared to wild type littermates (Fig 2.2B, lanes 1 & 2). Caytaxin protein was only detectable in protein extracts from *hesitant* homozygous mice after over-exposing ECL-probed Western blots (Fig2.2C, lane 2). Table 2.1 summarizes each *Atcay* mouse mutation with corresponding phenotype and Caytaxin expression.

Multiple Caytaxin isoforms are observed across species

To characterize the trans-species reactivity of our anti-Caytaxin mAbs and probe for the existence of multiple Caytaxin protein isoforms in other animal model systems, Caytaxin protein expression was examined by Western blotting in cell lysates from *Drosophila melanogaster* (fruit fly), *Danio rerio* (zebrafish), *Xenopus laevis* (frog), *Gallus gallus* (chicken), and *Mus musculus* (mouse) (Fig 2.3A). This analysis revealed no cross reactivity of our antibodies with the Caytaxin orthologs

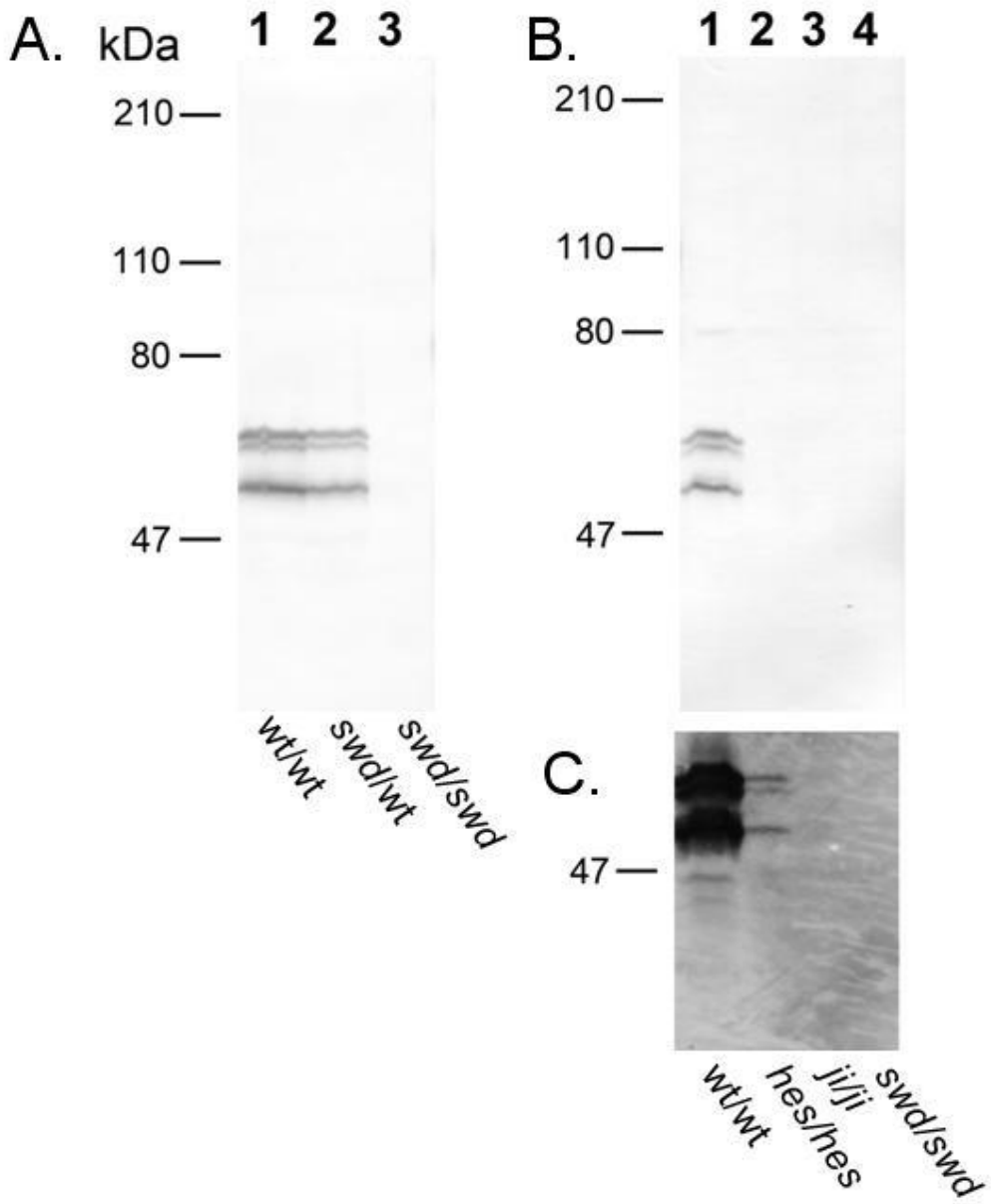

Figure 2.2. Caytaxin protein expression in *Atcay* mouse mutants.
(A) Western blot depicting Caytaxin expression in *sidewinder* littermates using anti-Caytaxin mAb 8F4, developed with DAB. Lane 1, wild type (wt/wt); lane 2, heterozygote (*swd*/wt); lane 3, homozygote (*swd*/*swd*). **(B)** Caytaxin expression in *Atcay* mutant mouse lines using anti-Caytaxin mAb 1E2, developed with DAB. Lane 1, wild type (wt/wt); lane 2, *hesitant* mutant (*hes*/*hes*); lane 3, *jittery* mutant (*ji*/*ji*); lane 4, *sidewinder* mutant (*swd*/*swd*). **(C)** Blot from (B) re-probed with mAb 1E2 and developed with ECL. All lanes contain 60µg total protein from frozen mouse brain lysates. Figure generated by Michael Tysor.

Mutant Allele	Mouse Line	Mutation	Location in *Atcay*	Phenotype	Caytaxin Protein Expression
Atcay$^{ji\text{-}hes}$	*hesitant*	IAP insertion	Intron 1	Mild ataxia and dystonia	Markedly reduced
Atcay^{ji}	*jittery*	B1 insertion	Exon 4	Severe ataxia	Absent
Atcay^{swd}	*sidewinder*	2bp deletion	Exon 5	Severe ataxia	Absent
(unknown)	*wobbley*	Point mutation	Intron 4	Progressive ataxia and dystonia	(unknown)

Table 2.1. Summary of *Atcay* mouse mutations.
Known mouse mutants containing mutations in the *Atcay* gene which cause ataxia and/or dystonia. **Column 1**, mutant allele; **column 2**, name of the mouse line; **column 3**, type of mutation; **column 4**, location of the mutation in *Atcay*; **column 5**, resulting phenotype in mice homozygous for mutation; **column 6**, Caytaxin protein expression. *hesitant*, *jittery*, and *sidewinder* are spontaneous mutations. *wobbley* is an ENU-induced mutation.

in the fruit fly, zebrafish, or frog (Fig 2.3A, lanes 1-3), likely due to a lower amino acid sequence similarity with human Caytaxin (50%, 77%, and 86%, respectively) [25]. However, our mAb detected Caytaxin in chicken nervous system protein extracts (an 88% amino acid sequence similarity with human Caytaxin) as three separate protein isoforms (Fig 2.3A, lane 4).

We next assessed whether Caytaxin protein expression is restricted to specific cell types within the nervous system and if our mAbs are able to detect human Caytaxin protein. Protein extracts from a panel of neural cell lines were analyzed using Western blots. Caytaxin protein was detected in mouse pituitary and rat adrenal medulla cytomas (Fig 2.3B, lanes 1 & 2), as well as human and mouse neuroblastomas (Fig 2.3B, lanes 6 & 7). However, we were unable to detect any Caytaxin protein in non-neuronal rat cells or human glioma cell lines (Fig 2.3B, lanes 3-5).

Our analyses performed with both mAbs 1E2 and 8F4 consistently detected a pattern of three differently-sized Caytaxin protein isoforms. These three isoforms were observed in nervous system and neuronal cell samples from bird and various mammalian species, including humans. The apparent molecular weights of the two largest Caytaxin isoforms are very similar in all species tested. However, the apparent molecular weight of the third and smallest isoform is higher in human and rat samples when compared to chicken and mouse tissues (Fig 2.3A, lanes 4 versus 5; Fig 2.3B, lanes 2 & 7 versus lanes 1 & 8).

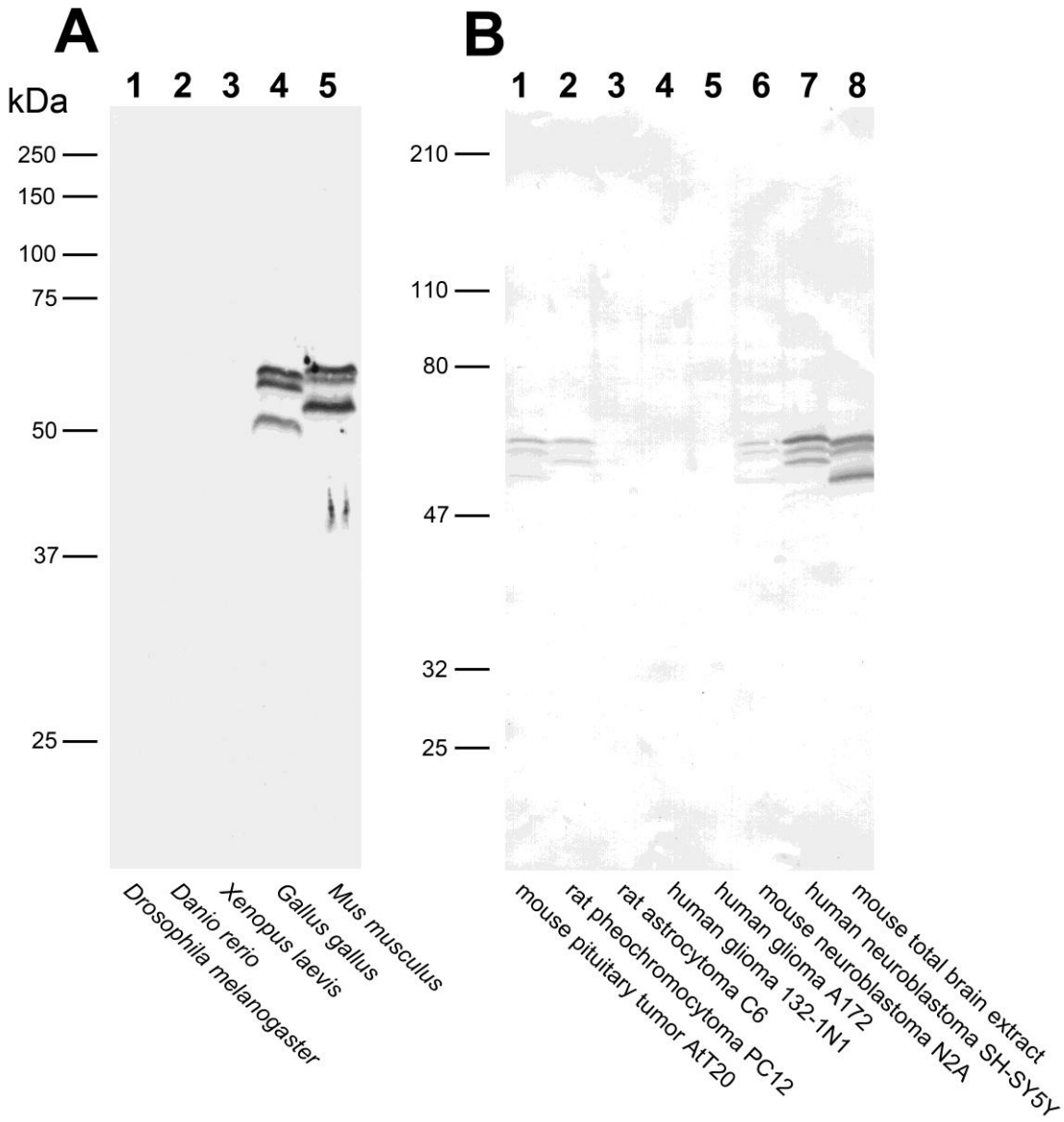

Figure 2.3. Caytaxin protein expression in various species and cell lines. Each lane contains approximately 60µg total protein. **(A) Lane 1**, total *Drosophila* embryo extract; **lane 2**, Zebrafish nervous system; **lane 3**, *Xenopus* adult brain; **lane 4**, chicken brain; and **lane 5**, mouse adult brain. Probed with anti-Caytaxin mAb 1E2 and developed with ECL. **(B)** Total protein lysates from frozen cell line pellets. **Lane 1**, AtT20 (mouse corticotroph pituitary tumor); **lane 2**, PC12 (rat pheochromocytoma); **lane 3**, C6 (rat astrocytoma); **lane 4**, 132-1N1 (human glioma); **lane 5**, A172 (human glioma); **lane 6**, N2A (mouse neuroblastoma); **lane 7**, SH-SY5Y (human neuroblastoma); and **lane 8**, wild type mouse brain. Probed with anti-Caytaxin mAb 8F4 and developed with DAB. Figure generated by Michael Tysor.

The two largest Caytaxin isoforms originate from alternative methionine start sites

Western blot analyses consistently detect Caytaxin as three distinct protein isoforms in unique, species-specific patterns. Therefore, we tested whether these three Caytaxin protein isoforms are the result of either RNA splicing or co- or post-translational protein modifications. Potential protein modifications were predicted based on the amino acid sequences of both mouse and human Caytaxin using online tools to search sites susceptible for sumoylation (http://www.abgent.com/tools/), glycosylation, sulfation, phosphorylation, acetylation, and ubiquitination [57-61]. Though these tools predicted the possibility of phosphorylation and ubiquitination, Western blot analyses for these modifications gave no indication of either the addition of ubiquitin (not shown) or phosphate (Appendix I) as causes of the multiple Caytaxin protein products. To elucidate the origin of the multiple Caytaxin protein isoforms, we employed a mammalian *in vitro* transcription/translation protein expression system. Using this system eliminates most post-translational protein modifications or differential RNA splicing processes, thus identifying only native unmodified Caytaxin protein. *In vitro* transcripts were generated from plasmid constructs containing the entire mouse or human *Atcay*/*ATCAY* open reading frame under control of an SP6 promoter. Subsequently, *in vitro*-translated *Atcay*/*ATCAY* mRNAs were translated in the presence of ^{35}S-labeled methionine using a rabbit reticulocyte lysate. Radioactively labeled protein products were separated by SDS-PAGE and detected by autoradiography (Fig 2.4A). Separate reactions without DNA or with T7 RNA polymerase were used as negative controls and did not result in

detectable protein products (Fig 2.4A, lanes 1-4). Both mouse and human *Atcay*/*ATCAY* cDNA constructs produce the identical three-protein-isoform patterns *in vitro* (Fig 2.4A, lanes 5 & 6) that are observed on Western blots of wild type mouse brain and human SH-SY5Y neuroblastoma cell protein lysates (Fig 2.4B, lanes 1 & 2, respectively).

These results, combined with the high similarity of the protein sequences in various Caytaxin orthologs, suggest that the origin of the protein isoforms resides in the DNA/mRNA or protein sequence. An amino acid alignment of human and mouse Caytaxin protein sequences revealed two highly conserved methionine residues (Met1 and Met10) at the predicted amino terminus separated by 8 amino acids (approximately 5.5kDa) (Fig 2.4D). Both ATG codons adhere to Kozak consensus sequence predictions (discussed further in Chapter IV) and could account for two separate protein translation start sites. Given the consistency of expression and the conserved apparent molecular weight of the two largest protein isoforms, we sought to determine whether these methionine residues could both serve as protein translation start sites.

Using site-directed mutagenesis, we created single and double nucleotide changes in the Met1 and Met10 methionine-encoding ATG codons in mouse *Atcay* cDNA by converting them to ACG codons (threonine) (Fig 2.4D, 'Met to Thr mutations'). Each mutation was designed to abolish the ability of the respective methionine residue(s) to serve as (a) translation start site(s), thereby resulting in the absence of the corresponding protein isoform(s). Three mutant

Atcay cDNA constructs (Met1Thr, Met10Thr, and the double mutant Met1+10Thr) were tested in the coupled transcription/translation system (Fig 2.4C), with wild type mouse *Atcay* cDNA serving as a positive control. Caytaxin protein translated from the Met1Thr construct (mutation of the first methionine Met1) abolished the largest Caytaxin isoform, as expected, however only the second largest protein isoform remained visible (Fig 2.4C, lane 3 compared to lane 1). Translation from the Met10Thr construct (mutation of the second methionine Met10) produced a Caytaxin product lacking only the second largest Caytaxin isoform. However, the Met10Thr mutation was also accompanied by an upshift of the size of the third protein species compared to the corresponding isoform in wild type *Atcay* cDNA construct (Fig 2.4C, lane 4 compared to lane 1). Finally, consistent with results from the single-mutant constructs, the construct harboring both mutations Met1+10Thr failed to produce any detectable Caytaxin protein (Fig 2.4C, lane 5). Common non-methionine start sites, leucine (Leu) and valine (Val), downstream of the second conserved methionine were identified as potential alternative start codons [42, 54, 55], and were also examined (Leu24, Val34, Leu37, and Val41). Similar to methods used to test Met1 and Met10, point mutations were created to disrupt each potential non-methionine start site and the cDNA was processed *in vitro* to observe the resultant translated protein. While the point mutations did have some effect on the apparent molecular weight and/or intensity of this third Caytaxin protein isoform, none of the sites tested could be confirmed as a starting amino acid (Appendix II). Additionally, employing a similar method to delete 58 residues from the C-terminus of Caytaxin had no effect on the

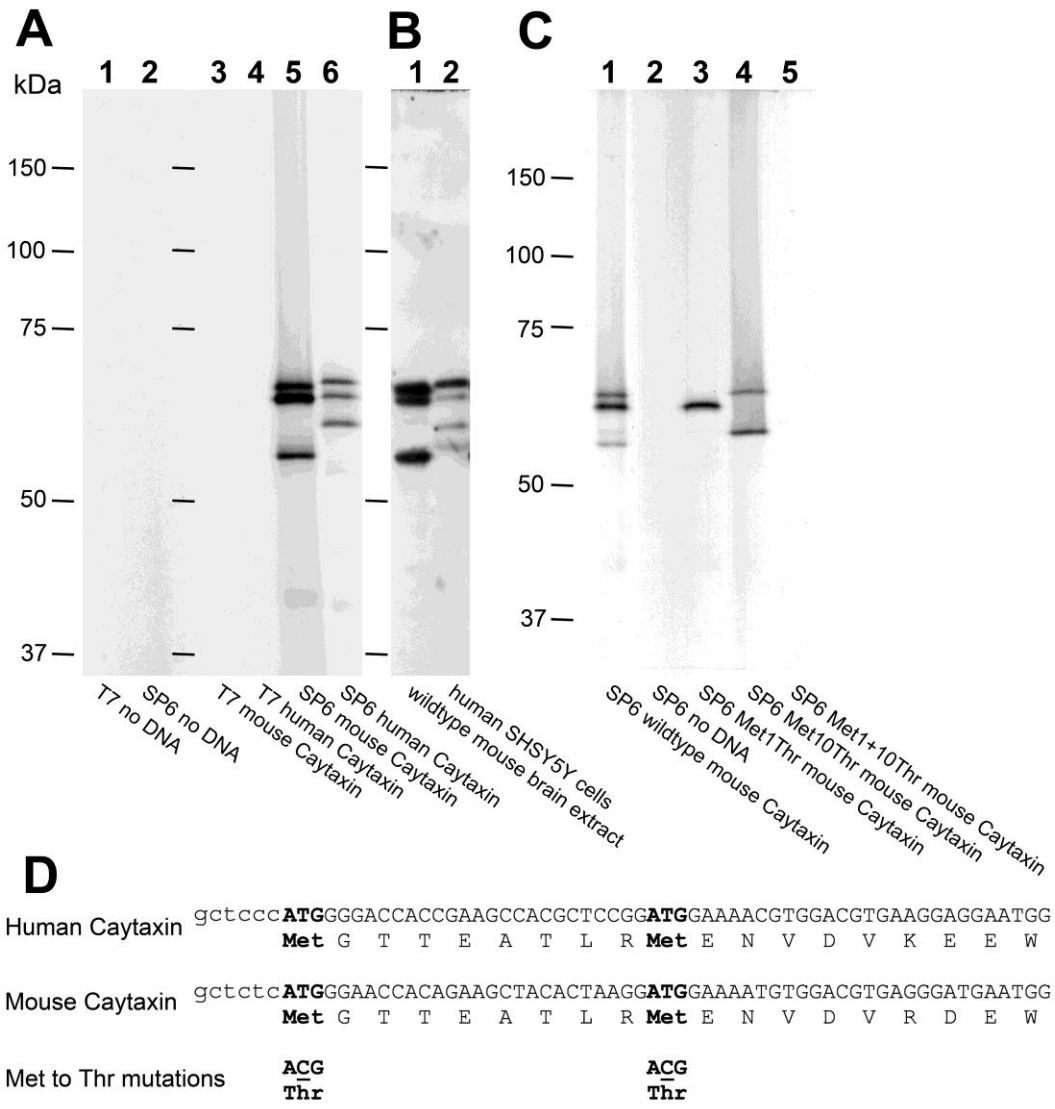

Figure 2.4. *In vitro* translation of wild type and mutant Caytaxin.
(A) autoradiogram of Caytaxin protein produced from *Atcay*/*ATCAY* cDNA *in vitro* (Materials and methods). **Lane 1**, T7 RNA Polymerase, no DNA; **lane 2**, SP6 RNA polymerase, no DNA; **lane 3**, T7 RNA polymerase, *Atcay* cDNA; **lane 4**, T7 RNA polymerase, *ATCAY* cDNA; **lane 5**, SP6 RNA polymerase, *Atcay* cDNA; and **lane 6**, SP6 RNA polymerase, *ATCAY* cDNA. **(B)** Western blot from adjacent part of the gel in (A) probed with anti-Caytaxin mAb 8F4, ECL detection. **Lane 1**, 30µg wild type mouse brain and **lane 2**, $1x10^6$ human SH-SY5Y cells. **(C)** Caytaxin protein from methionine mutant constructs by SP6 RNA polymerase *in vitro* translation. **Lane 1**, wild type *Atcay* cDNA; **lane 2**, no DNA; **lane 3**, mutation of first methionine; **lane 4**, mutation of second methionine; and **lane 5**, mutation of both methionines. **(D)** Nucleotide and amino acid sequence comparison between mouse and human Caytaxin. Met1 and Met 10 (bold) are separated by 8 amino acids.

appearance of the third Caytaxin protein isoform. This excluded the possibility of the third isoform originating from C-terminal protease cleavage of either of the larger isoforms as (Appendix IV).

Caytaxin expression in the mouse nervous system peaks at 3 months after birth

We found no significant differences in the ratio of each isoform relative to the others upon examination of Caytaxin protein expression in major brain regions from wild type mice (Fig 2.5) or among different neuronal cell types (Fig 2.3). Therefore, we analyzed Caytaxin levels from postnatal day 1 (P1) throughout adulthood to examine whether the expression of the three isoforms is subject to regulation throughout postnatal development.

Protein lysates were prepared from whole brains of wild type mice at various ages ranging from P1 to 10 months, and analyzed by Western blots. Caytaxin protein levels were determined relative to tubulin protein expression from the same sample (Fig 2.6, A & B). All Caytaxin protein isoforms were consistently expressed at comparable ratios at each time point (Fig 2.6A). Although amount of total Caytaxin varied somewhat between individual mice for most time points, a steady temporal pattern was maintained overall. Similar to previous reports [52, 53], total Caytaxin protein levels were modulated during postnatal rodent development (Fig 2.6C). Shortly after birth, Caytaxin protein is expressed at its lowest postnatal level (Fig 2.6, lanes 1 & 2) and begins to rise around P10 to its highest level around 1-3 months (Fig 2.6, lanes 3 & 6-8). At this point, protein

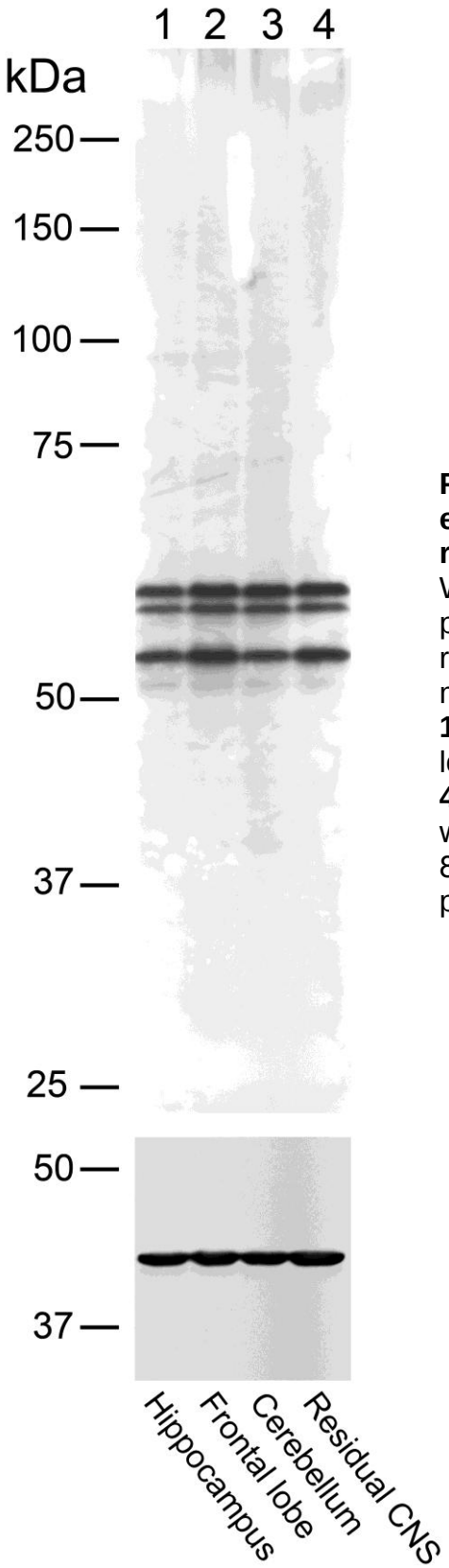

Figure 2.5. Caytaxin protein expression in major brain regions.
Western blot with 30µg of total protein extracts from different brain regions of a 25-month-old wild type mouse, developed with ECL. **Lane 1**, hippocampal area; **lane 2**, frontal lobe; **lane 3**, cerebellum; and **lane 4**, residual brain matter. The blot was probed with α-Caytaxin mAb 8F4 (upper panel) and α-actin (lower panel).

expression is largely stable at a robust level until it decreases slightly at the more advanced ages of 10 months and beyond (Fig 2.6, lane 12). No significant differences in the relative quantities of the three Caytaxin isoforms were observed during postnatal development.

The function of mouse and human Caytaxin is conserved

The Caytaxin family of proteins shares a high degree of amino acid sequence conservation, including a well-preserved BCH domain, which appears to play important roles in protein-protein interactions and function [42, 54, 55]. An amino acid sequence alignment of mouse and human Caytaxin reveals a 91% overall sequence similarity and a 96% sequence similarity between BCH domains (Fig 2.7). This high degree of sequence homology suggests that the physiological function of mammalian Caytaxin proteins may also be conserved.

To examine this hypothesis, we performed genetic complementation tests to assess the ability of human *ATCAY* DNA to rescue the severe ataxic phenotype of *Atcay* mouse mutants. Transgenic mice were generated that express a Bacterial Artificial Chromosome (BAC) containing *Homo sapiens* chromosome 19 clone CTB-171N13, which includes the complete coding region for the human *ATCAY* gene and at least 20kb of upstream sequence; this is expected to be sufficient to direct tissue-specific expression irrespective of insertion location. These mice were bred with the two severely ataxic lines *sidewinder* and *jittery* to obtain two different transgenic BAC lines homozygous for the respective mutant alleles (*swd*/*swd* BAC+ & *ji*/*ji* BAC^{+}). These mice did not express mouse

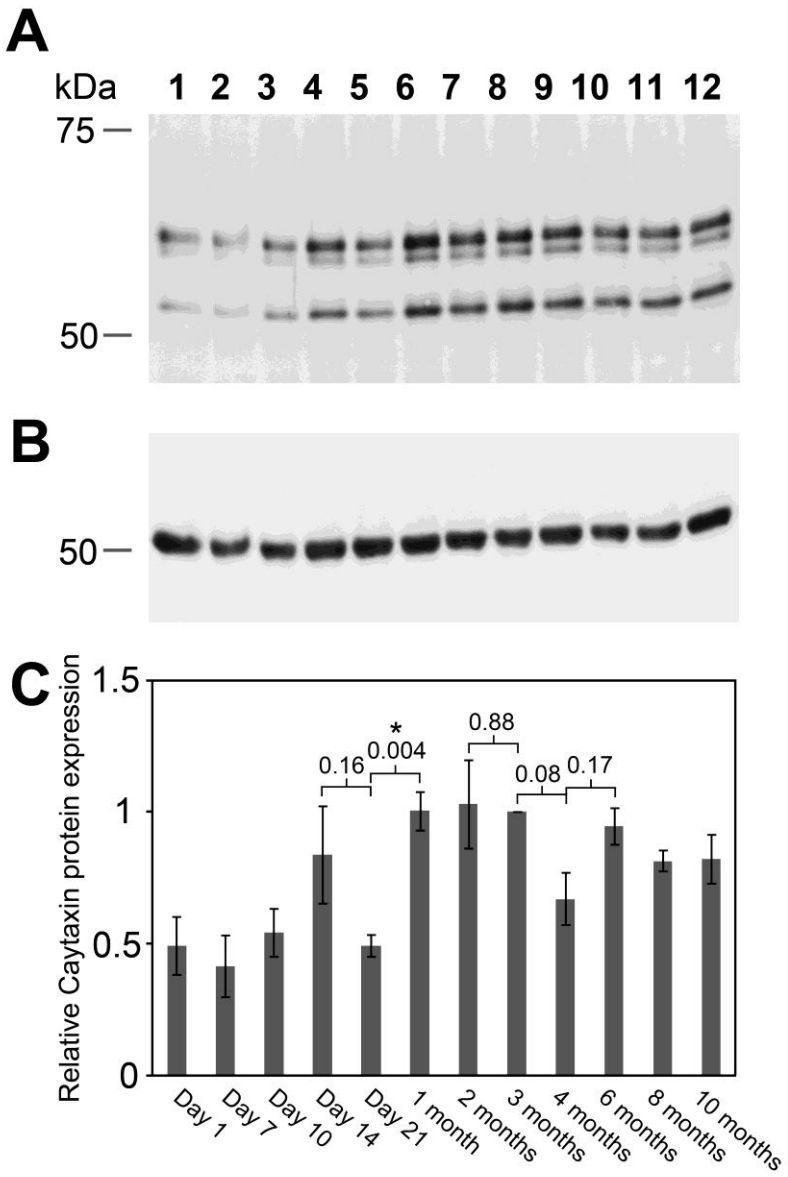

Figure 2.6. Caytaxin protein expression throughout mouse brain development.
Each lane contains 30µg of total brain protein extract obtained from wild type mice at post-natal ages Day 1 (**lane 1**), Day 7 (**lane 2**), Day 10 (**lane 3**), Day 14 (**lane 4**), Day 21 (**lane 5**), 1 month (**lane 6**), 2 months (**lane 7**), 3 months (**lane 8**), 4 months (**lane 9**), 6 months (**lane 10**), 8 months (**lane 11**), and 10 months (**lane 12**). **(A)** Western blot probed with anti-Caytaxin mAb 8F4 and re-probed with anti-β-tubulin as a loading control **(B)**. **(C)** Calculations for density of all protein bands described in materials and methods. Densities were averaged among all mice per time point (n=3, except at 10 months where n=2), and plotted with error bars representing ± SEM. Caytaxin was normalized to β-tubulin and plotted relative to average density at 3 months.

```
H. SAPIENS      MGTTEATLRMENVDVKEEWQDEDLPRPLPETGVELLGSPVEDTSS
M. MUSCULUS     MGTTEATLRMENVDVRDEWQDEDLPRPLPEDTGVERLGGAVEDSSS

H. SAPIENS      PPNTLNFNGAHRKRKTLVAPEINISLDQSEGSLLSDDFLDTPDDLD
M. MUSCULUS     PPSTLNLSGAHRKRKTLVAPEINISLDQSEGSLLSDDFLDTPDDLD

H. SAPIENS      INVDDIETPDETDSLEFLGNGNELEWEDDTPVATAKNMPGDSADLF
M. MUSCULUS     INVDDIETPDETDSLEFLGNGNELEWEDDTPVATAKNMPGDSADLF

H. SAPIENS      GDGTTEDGSAANGRLWRTVIIGEQEHRIDLHMIRPYMKVVTHGGYY
M. MUSCULUS     GDGSAEDGSAANGRLWRTVIIGEQEHRIDLHMIRPYMKVVTHGGYY

H. SAPIENS      GEGLNAIIVFAACFLPDSSLPDYHYIMENLFLYVISSLELLVAEDY
M. MUSCULUS     GEGLNAIIVFAACFLPDSSSPDYHYIMENLFLYVISSLELLVAEDY

H. SAPIENS      MIVYLNGATPRRRMPGIGWLKKCYQMIDRRLRKNLKSLIIVHPSWF
M. MUSCULUS     MIVYLNGATPRRRMPGIGWLKKCYHMIDRRLRKNLKSLIIVHPSWF

H. SAPIENS      IRTVLAISRPFISVKFINKIQYVHSLEDLEQLIPMEHVQIPDCVLQ
M. MUSCULUS     IRTVLAISRPFISVKFISKIQYVHSLEELERLIPMEHVQLPDCVLQ

H. SAPIENS      YEEERLKARRESAR-PQPEFVLPRSEEKPEVAPVENRSALVSEDQE
M. MUSCULUS     YEEQRLRAKRESTRPPQPEFLLPRSEEKPETVEEEDRAAEATEDQE

H. SAPIENS      TSMS
M. MUSCULUS     TSMS
```

Figure 2.7. Sequence similarity between human and mouse Caytaxin.
Amino acid alignment of the coding region for human (*H. sapiens*) and mouse (*M. musculus*) Caytaxin with BCH domain (underlined) and non-conserved amino acids (bold).

Caytaxin (Fig 2.2B, lanes 3 & 4), but over-expressed human Caytaxin (Figure 2.9A, lanes 3 & 4) with no ectopic expression in non-neuronal organs, such as heart, lungs, liver, kidney, or spleen (Fig 2.8).

The pattern of the Caytaxin isoforms expressed from the BAC was consistent with the human Caytaxin protein pattern detected in human neuroblastoma cells (Fig 2.9A, lane 2). However, the size of the Caytaxin protein from BAC transgenic mice was slightly larger than endogenous Caytaxin from human neuronal cell lines (Fig 2.9, lane 2 vs. 3 & 4). This was caused by a duplication of exon 10 in human *ATCAY* DNA, likely during the bacterial cloning phase of the BAC (Fig 2.10). This duplication of exon 10 results in an insertion of 9 amino acids at the C-terminus of Caytaxin (Fig 2.10B), but does not disrupt the reading frame.

Initial observations of movement and motor coordination in *swd*/*swd* BAC^+ and *ji*/*ji* BAC^+ mice suggested gross phenotype rescue and functional complementation. Mice containing the human *ATCAY* BAC on an *Atcay* mutant background exhibited no visible signs motor dysfunction, incoordination, or gait abnormalities (data not shown), no difficulties accessing food or water, successfully bred and reared offspring, and lived beyond 1.5 years (data not shown). To confirm and quantify this phenotypic rescue, 3-5 month-old mixed-gender *swd*/*swd* BAC^+ and *swd*/wt controls were tested in a rotarod performance test.

The experimental setup was designed to examine both motor coordination and

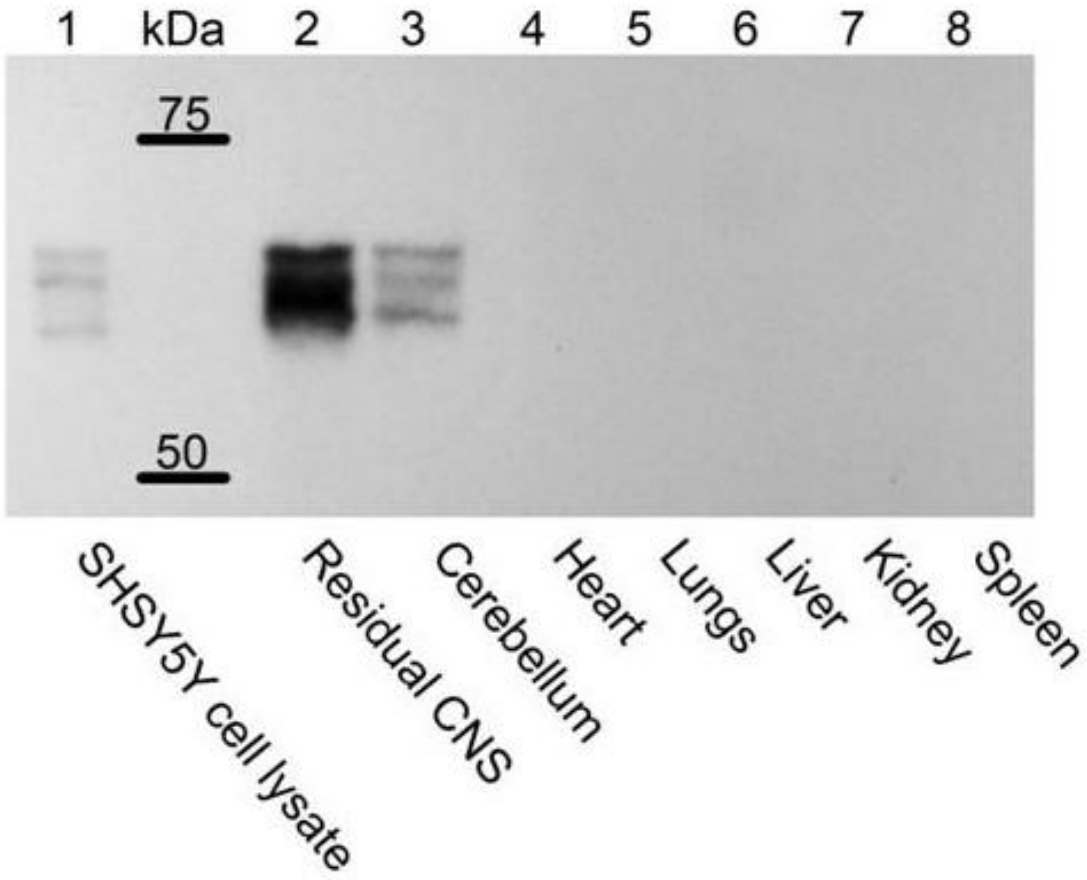

Figure 2.8. Caytaxin expression in major wtBAC$^+$ organs.
Western blot with approximately 30µg of protein loaded. Probed with monoclonal anti-Caytaxin antibody 8F4 and detected via ECL. Brain and organ lysates prepared from BAC$^+$ transgenic mouse line. **Lane 1**, wild type SH-SY5Y human neuroblastoma cells; **lane 2**, brain lysate without the cerebellum; **lane 3**, cerebellar-only lysate; **lane 4**, lysate from whole heart; **lane 5**, lysate prepared from both lungs; **lane 6**, lysate prepared from a single liver lobe; **lane 7**, prepared from both kidneys; and **lane 8**, prepared from a spleen.

learning functions, two major phenotypic aspects displayed by human individuals with Cayman ataxia [15]. We recorded the length of time that individual mice stayed on an accelerating rotating rod, with each mouse tested three times per day over a total of three days. Homozygous mutant mice that do not express the human *ATCAY* BAC are completely unable to coordinate grip, walk, or balance (data not shown). Additionally, without special housing conditions and specific accommodations to allow access to food and water (discussed in Chapter IV), these mice usually die after 3 weeks [21]. Due to the severity of the phenotype, we were unable to test their performance in this experimental paradigm.

Results obtained from the rotarod tests confirmed our earlier phenotype observations. We detected no significant difference ($p>0.05$ in each trial) in either motor coordination or learning and memory in *swd*/*swd* BAC^+ mice when compared to wild type controls (Fig 2.9B). *swd*/*swd* BAC^+ mice were not only capable of maintaining their balance, but they were also able to adjust their balance when the rod began to accelerate. Their total time on the rotating rod was comparable to wild type littermates (Fig 2.9B). In addition, rotarod performance for both wild type and BAC-rescued mice significantly increased between the first and third day of testing ($p=0.0002$ and 0.0024, respectively), reflecting their ability to learn from previous testing experiences.

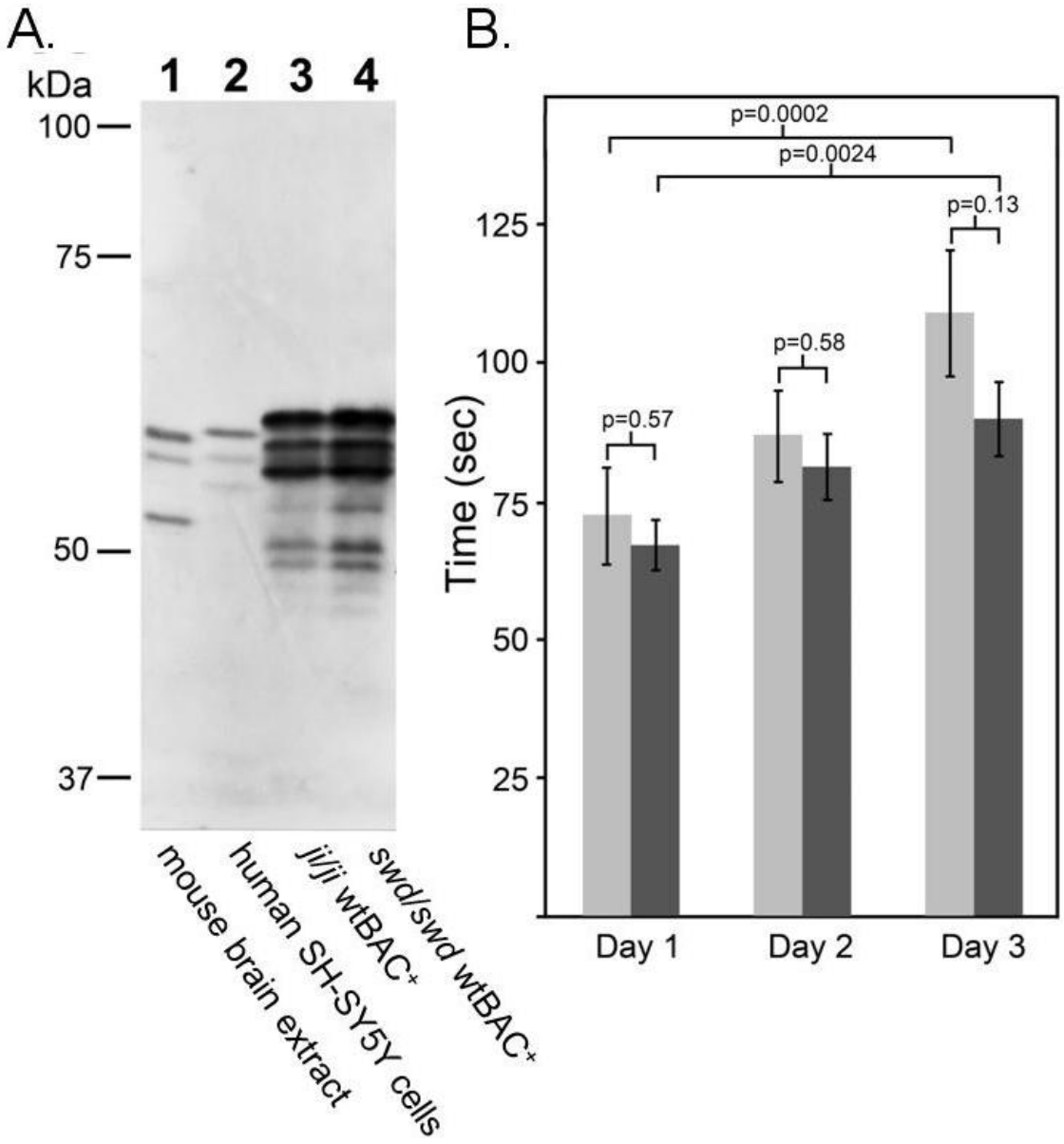

Figure 2.9. Caytaxin expression and functional rescue in transgenic *ATCAY* BAC$^+$ mice.

(A) Western blot with 30µg protein loaded, probed with anti-Caytaxin mAb 8F4 and developed using ECL. **Lane 1**, wild type mouse brain; **lane 2**, human SH-SY5Y cell lysate; **lane 3**, total brain protein from *ji/ji ATCAY* BAC$^+$; and **lane 4**, *swd*/*swd ATCAY* BAC$^+$. **(B)** Average time on a rotating rod per day, over 3 days, was plotted with error bars representing ± SEM. Wild type control +/*swd* BAC$^-$ mice (light grey bars, n=7), and transgenic rescue *swd*/*swd* BAC$^+$ mice (dark grey bars, n=10). P-values between the control and the rescued group performance and between Day 1 and Day 3 are indicated above the columns.

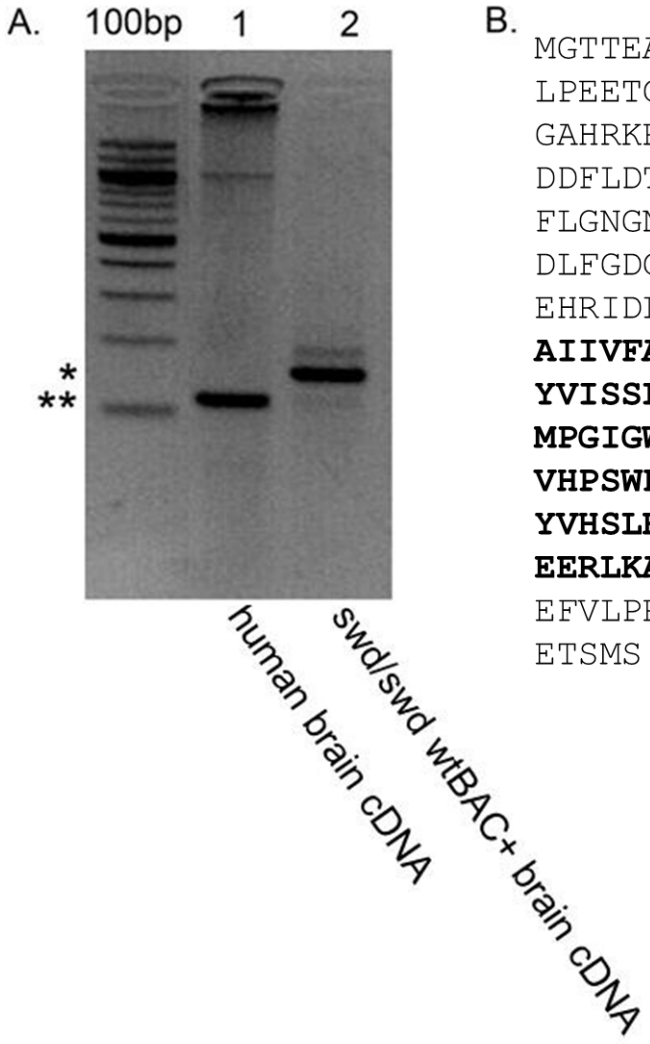

Figure 2.10. Exon 10 duplication in wild type *ATCAY* transgene.
(A) PCR for exon 10 from human (lane 1) and wtBAC^{+} (lane 2) brain cDNA. Expected size of exon 10 fragment (**), size of fragment in transgenic BAC (*). **(B)** shows the human Caytaxin amino acid sequence with the BCH domain (bold). Extra amino acids due to the exon 10 duplication (underlined).

Discussion

Individuals suffering from Cayman ataxia are homozygous for two mutations in the *ATCAY* gene and display marked motor and cognitive defects [15]. However it is unknown how these two mutations affect Caytaxin protein expression and cause ataxia. We report the use of monoclonal antibodies specific for Caytaxin to investigate Caytaxin protein expression in mutant *Atcay* mouse models. Our results demonstrate that mutations in the *Atcay* gene cause decreases in Caytaxin expression, and that the severity of ataxia is correlated with Caytaxin protein expression. Additionally, our data from transgenic *Atcay* mutant mice showing that over-expressing the human *ATCAY* gene rescues the *Atcay* mutant phenotype suggest that the high sequence homology between human and mouse Caytaxin also reflects a conservation of protein function.

While two of our monoclonal antibodies are specific for Caytaxin (Fig 2.2), their utility is limited to detecting Caytaxin protein on Western blots. *In vivo* staining experiments indicated that the third anti-Caytaxin monoclonal antibody 4E3 might also cross-react with unidentified protein(s) and we therefore did not use this antibody for further analyses (Fig 2.11). Previous reports utilized anti-Caytaxin polyclonal antibodies that were raised against small regions of rat Caytaxin or antibodies against affinity-tagged Caytaxin. These reports found Caytaxin to be expressed as one or two isoforms on Western blots [46], with the doublet hypothesized to be a result of protein post-translational modifications (PTM) or RNA splicing [46]. Our analysis reveals that in one avian and several mammalian

species, Caytaxin is actually expressed as three distinct isoforms of approximately 58, 55, and 50kDa, which are all derived from a single transcript. Due to the small difference in size between these protein isoforms, complete resolution of all three Caytaxin isoforms requires large SDS-PAGE gels (~10" long separating gel), high acrylamide concentrations (10-12%), and a longer run-time at a constant current (15-30mA). It may be for these reasons that the multiple isoforms of the Caytaxin protein have not been reported previously.

Our initial investigation into the origin of these three Caytaxin isoforms revealed that Caytaxin is one of few proteins consisting of multiple isoforms that are generated by different methionine translational start sites (Fig 2.4C & D). This is more often found in yeast [62] and viruses [63, 64], whose mRNAs are either polycistronic or lack a 5' cap. In mammals, the production of multiple proteins from a single mRNA transcript has been best described in for the transcription factors C/EBPβ and *c-Myc* [65]. Interestingly, the mechanism in which multiple start methionines encode two of the three Caytaxin bands closely resembles that for *c-Myc,* where three isoforms of 69kDa, 65kDa, and 50kDa originate from one non-AUG and two alternative AUG codons in a single mRNA transcript [66-68]. The proteins encoded by this gene are multifunctional nuclear phosphoproteins [69], suggesting that Caytaxin isoforms may also serve independent functions.

Assessment of whether expression of total Caytaxin protein is modulated during

mouse postnatal development revealed consistent expression of individual isoforms, but variation in total protein levels from P1 throughout adulthood. The peaks observed in Caytaxin protein expression throughout development closely follow developmental milestones and major mouse life events such as eye opening at Day 13, weaning at Day 21, and sexual maturity at 5 weeks (Fig 2.6, lanes 4-8) – all of which induce changes in neuronal gene expression [53, 70]. Reports from Hayakawa *et al* also found disparity between mRNA levels and Caytaxin protein expression upon examination of *Atcay* mRNA levels throughout development [52]; this indicates that our observed fluctuations in protein levels may be due to protein processing or degradation of total Caytaxin levels. Further investigation towards understanding the underlying pathways that regulate the Caytaxin gene and its protein product will be instrumental for pinpointing the role of this protein in nervous system development.

While we identified two independent AUG start codons responsible for the production of the two larger Caytaxin isoforms, we were unable to identify the source of the smallest Caytaxin isoform. Translation of both mouse and human Caytaxin in the wheat germ-based *in vitro* system failed to produce the third isoform in both species (Appendix V). This may further allude to a mammalian-specific protease or the presence of leaky ribosomal scanning. In this case, a proportion of ribosomal scanning complexes fail to initiate at the first AUG and continues scanning to the next AUG or an alternative start codon (commonly ACG, CUG, or GUG) [71]. Further examination into the origin of the third

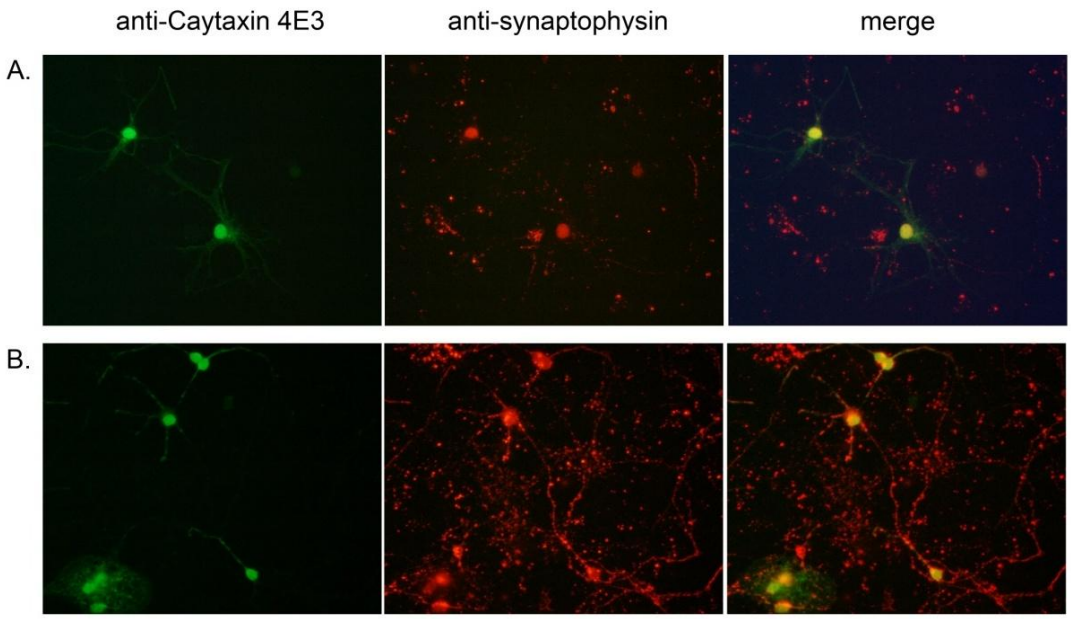

Figure 2.11. anti-Caytaxin mAb 4E3 is not specific for Caytaxin.
Immunofluorescence for Caytaxin (green, left panels) and neuronal marker synaptophysin (red, middle panels) in primary granule cell cultures from **(A)** wild type wt/*swd* mice and **(B)** mutant *swd*/*swd* mice. Right panels show Caytaxin and syntaptophysin panels merged to indicate regions of co-localization (yellow, right panels).

variable isoform ruled out mRNA splicing, a third ATG start site, and non-specific post-translational protease degradation (Appendix III and X). Common non-methionine start sites downstream of the second conserved methionine were also examined, but yielded inconclusive results (Appendix II). As an expansion on previous work by Kozak, Goosen and Hentze, and Wang and Wessler [72-74], a recent study by Kochetov *et al* revealed that stability of mRNA structure around a non-AUG site can cause preferential translation at that site, despite the presence of an upstream AUG with strong Kozak context [75]. The lack of an obvious third start site (i.e. downstream AUG or non-AUG) led us to examine the structure of *Atcay/ATCAY* mRNA and Caytaxin protein which could affect access of translation start sites or regions targeted by proteases, respectively. We utilized an *in silico* method to compare wild type and mutant *Atcay* mRNA harboring the two methionine point mutations (Appendix VIII), and found that these mutations affect local structure at the 5' end but do not result in the formation of complex RNA structures (Appendix VIII, arrows). This suggests that mRNA secondary structure is not a primary mechanism for regulating translation initiation for Caytaxin. Parallel experiments did not provide evidence for a significant role in protein secondary structure (Appendices IX and X) or C-terminal cleavage (Appendix IV).

Additional efforts to identify the source of the third Caytaxin isoform included protein purification and N-terminal sequencing (Appendix XI). Whether the third isoform is produced from an alternative start codon or from another mechanism, the origin lies at the amino-terminus of the protein. Determining the first amino

acids of the smallest protein via N-terminal sequencing will help to elucidate the mechanism responsible for its generation. Thus far, a nickel affinity tag system has produced a significant amount of pure Caytaxin, but not enough of sufficient purity for sequencing (Appendix XI). The physiological significance of three distinct proteins produced from a single transcript remains unknown. It will be of interest to elucidate whether the different Caytaxin protein isoforms differ in molecular function, protein-protein interactions, and/or subcellular localization.

Previous studies correlating Caytaxin protein expression with phenotype in animal models have been limited to a single report in the dystonic rat line [27]. We report that the *jittery* and *sidewinder* mice, which display a severe ataxic/dystonic phenotype [18, 33, 39], do not produce any detectable Caytaxin protein. In contrast, the low levels of normal *Atcay* RNA expressed by the mildly ataxic/dystonic *hesitant* mice are sufficient for producing small amounts of normal Caytaxin protein (Fig 2.2B, lane 2). Published observations report that severely ataxic *jittery* and *sidewinder* mice rarely live beyond 3-4 weeks [18, 33]. The causes of their deaths have been described as starvation and dehydration, leading to the interpretation that their ataxia is too severe for them to survive. However our experience with these models suggests that this conclusion is overly simplistic as we have observed that ataxic mice are able to live beyond 1 year. The eventual cause of their death is not starvation or dehydration; rather, they often suffer from infections originating from sores or wounds obtained as they attempt to travel around their cage (data not shown). Importantly, to prevent dehydration and starvation, ataxic mice require special care including extended

weaning time, co-housing with at least one non-ataxic littermate, soft diet gel supplementation or food pellets scattered on the cage floor, and an extended-lixit water bottle. With proper care, ataxic mice are also able to reproduce, but may experience difficulties during childbirth and are incapable of successfully rearing offspring. Based on these observations, current descriptions of *Atcay* mouse mutants are insufficient in their portrayal of the phenotype. By establishing a quantifiable phenotypic readout using assays such as those described in Chapter III, standards can be set which aid in more precisely correlating protein expression with severity of ataxia.

Correlation between Caytaxin expression and phenotype severity is also observed in our humanized transgenic *sidewinder* and *jittery* mice which over-express human Caytaxin and no longer display early lethality or ataxia. Based on our Western blot data and quantitative PCR analysis, these transgenic mice harbor ~12 copies of the BAC (data not shown) and over-express human Caytaxin protein by approximately 11-fold compared to wild type controls (data not shown). This over-expression does not appear to result in any leaky expression in non-neuronal tissues (Fig 2.9) or aberrant gain-of-function phenotype (data not shown). However, it remains unclear whether Caytaxin expressed from a single copy of the *ATCAY* transgene (similar to *sidewinder* and *jittery* heterozygotes) is sufficient to rescue the ataxic phenotype. It should be noted that while our transgenic mice express *ATCAY* containing a duplication of exon 10 (Fig 2.10B), the amino acid composition of the BCH domain is undisturbed.

Data obtained from the three *Atcay* mutant mouse models indicate that Caytaxin is critical for normal nervous system function, and retains some level of functionality at relatively low levels. Additionally, analysis of the transgenic BAC mice indicates a conservation of Caytaxin function between human and mice. Phylogenetic and evolution mapping of BNIP proteins and the BCH domain of Caytaxin suggest that this protein may play a similar role within the nervous systems of many related vertebrates and potentially also invertebrates [39]. Thus, the conserved function of Caytaxin may extend beyond *Homo sapiens* and *Mus musculus* to include other Caytaxin orthologs as potential animal models.

This report introduces new tools and methods to examine Caytaxin expression and function in complex animal systems. These approaches revealed that Caytaxin is actually expressed as multiple isoforms. It remains to be elucidated whether these multiple Caytaxin isoforms also impart multiple protein functionalities or differ in cellular localization. Our report also represents the first study characterizing Caytaxin expression in mutant *Atcay* mice and demonstrates that the severity of their ataxia is directly correlated with Caytaxin protein levels. The conservation of function between human and mouse Caytaxin confirms the validity of mouse models for use in understanding the etiology of Cayman Ataxia as a human neurological condition.

Acknowledgements

Monoclonal anti-Caytaxin antibodies generated by the University of Michigan Hybridoma Core, and screened by LaGina Nosavanh (Fig 2.1). Figures 2.2 & 2.3 generated by Michael Tysor, University of Michigan, Cell and Developmental Biology. Prameela Kantheti and Joyce Iping greatly contributed to the generation and screening of transgenic BAC founders. They performed PCR screens and to characterize the wild type BAC mice by exon amplification, and provided invaluable support in the maintenance and breeding of wild type BAC transgenic, *sidewinder*, *hesitant*, and *jittery* mouse lines.

Materials and methods

Mice – The *sidewinder* (*Atcay*^{swd}) line was generated from mice harboring the *ji*^{swd} allele, which arose at the Jackson Laboratory in 1999, on a C57BL/6J background, and were maintained in our laboratory on that background. The *hesitant* mice (C3H-*Atcay*^{ji}-*hes*/J, stock number 001904) were obtained from the Jackson Laboratory and bred in-house. *jittery* (B6.C(Cg)-*Atcay*^{ji}/BurJ, stock number 008140) were produced by our laboratory and donated to the Jackson Laboratory in 2007. The line was created by crossing inbred *jittery*/grizzled mice (JIGR/DnJ, stock number 000572) obtained from the Jackson Laboratory with C57BL/6J mice, pups from which were selected for the *ji* allele. *ji*-only heterozygotes were backcrossed with C57BL/6J over 15 generations. F2 crosses were performed as previously described [30], and mutant lines were maintained by heterozygote crosses. The *ATCAY*-containing BAC construct consisted of

Homo sapiens chromosome 19 clone CTB-171N13 (GenBank: AC011488.7) in vector pBeloBACII (Research Genetics, Huntsville, Alabama). The University of Michigan Transgenic Animal Model Core purified the BAC's and generated transgenic mice on a mixed (C57BL/6 X SJL)F2 background according to their protocols (http://www.med.umich.edu/tamc/tgoutline.html). The University of Michigan Unit for Laboratory Animals provided husbandry services for all mouse lines and the University of Michigan Committee on Use and Care of Animals approved all mouse experiments.

Copy number assay – A BAC copy number standard was generated based on the protocol provided by The University of Michigan Transgenic Animal Model Core (http://www.med.umich.edu/tamc/spike.html). Genomic DNA from BAC transgenic mice was spiked into 5µg of wt/wt *sidewinder* genomic DNA at concentrations equivalent to 1, 5, 10, 50, 100, 500, and 1000 copies. Concentrations were determined by calculating the mass of transgene DNA per microgram of wt/wt *sidewinder* genomic DNA with the assumption that the haploid content of the murine genome is $3x10^9$bp. Quantitative PCR was performed using GusB as a reference gene to determine dCt's. A standard curve was generated by plotting average dCt vs. Log_2(Copy Number) for each 1, 5, 10, 50, 100, 500, and 1000 copy number reference.

CNhAtcayfwd 5'-ttgatggacatgggttgcttccac-3'

CNhAtcayrev 5'-actaacctgggtgcaaggatggat-3'

Cell culture – SH-SY5Y cells were obtained from Dr. Stephen K. Fisher at the University of Michigan and maintained in complete growth medium (1:1 mixture of DMEM and F12 medium, with 10% FBS) in 5% CO_2 at 37°C. Cells were sub-cultured using the recommended ATCC protocol, with some modifications. Briefly, non-adherent cells were recovered from the media, adherent cells were rinsed with HBSS (Fisher Scientific, Cat. No. SH3058801) and incubated in HBSS containing 0.25% trypsin (Life Technologies, Cat. No 15090-046) and 0.53mM EDTA until detached. Adherent cells were combined with recovered non-adherent cells and sub-cultivated at a ratio of 1:50. Growth medium was renewed every 4-7 days.

Cell pellets harvested for Western blots using: AtT20 (mouse corticotroph pituitary tumor) at $2x10^6$ cells; PC12 (rat pheochromocytoma) at $1x10^6$ cells; C6 (rat astrocytoma) at $2x10^6$ cells; 132-1N1 (human glioma) at $10x10^6$ cells; A172 (human glioma) at $1x10^6$ cells; N2A (mouse neuroblastoma) at $1x10^6$ cells; SH-SY5Y (human neuroblastoma) at $1x10^6$ cells.

Cell line sources: SH-SY5Y (ATCC®: CRL-2266™) AtT20 (ATCC®: CRL-1795™), PC12 (ATCC®: CRL-1721™), C6 (ATCC®: CCL-107™), 132-1N1 (Sigma-Aldrich® Cat. No. 86030402), A172 (ATCC®: CRL-1620™), N2A (ATCC®: CCL-131™).

Genotyping – Mouse tail biopsies were performed between post-natal day 14-16 and genomic DNA was extracted using the PUREGENE® DNA Purification Kit

according to the manufacturer's protocol (Gentra, Cat. No. 158222 or 158267). Genomic PCR's for all strains were performed by amplifying a target region from 25ng of genomic DNA with the following buffer conditions: Expand Long Template System for *sidewinder* (Roche, Cat. No. 11681834001); PCR Buffer Set (Roche, Cat. No. 11699121001) for *jittery*; PCR Buffer set (Invitrogen, $MgCl_2$ Cat. No. Y02016 and 10x PCR buffer Cat. No. Y02028) for *hesitant*. Following the *sidewinder* genomic PCR, a subsequent restriction digest with enzyme *Msl* I (New England Biolabs, Cat. No. R0571S) was performed at 37^{o}C for 9 hours, followed by heat inactivation of the enzyme for 20 minutes at 65^{o}C. Agarose gel electrophoresis was performed using a 2% (*hesitant, jittery*) or 3% (*sidewinder*) sodium-borate agarose gels. *sidewinder* and *jittery* transgenic BAC lines were genotyped for mutant alleles (described above) and the presence of the BAC transgene using primers for both exons 2 and 6 of *ATCAY*.

sidewinder primers:	5'-atcataggggagcaagagcatc-3',
	5'-gatggactgacagcacactgg-3'
jittery primers:	5'-ccctgaccacaccctcaat-3',
	5'-tttggtccagggagatgttg-3',
	5'-ctggctgtcctggaactcac-3'
hesitant primers:	5'-cctccctgcacagacacaatag-3',
	5'-gggatgttagggtttaccacca-3',
	5'-tacaacagaattccagggtcca-3'
ATCAY exon 2 primers:	5'-catggggtagacgattgtcatt-3',
	5'-acagagaagactcgcacacagg-3'
ATCAY exon 6 primers:	5'-aggactctgacgttgccgat-3',

5’-tagggccacaatgcaatcct-3’

Antibodies – A construct to create a GST-human Caytaxin fusion protein was generated by excising a 1.3kb fragment from human *ATCAY* cDNA clone 4153341 (Life Technologies) with *Sal* I and *Eco* RI restriction enzymes, and cloning it into the pGEX vector (GE Healthcare Life Sciences). The GST-human Caytaxin fusion protein was created by expressing this vector in bacteria and purifying it by preparative SDS-PAGE. The purified human Caytaxin fusion protein was used as an immunogen in mice and spleen cells from an immunized mouse were fused with myeloma cells for generating anti-Caytaxin secreting hybridoma cell lines according to the University of Michigan Hybridoma Core Facility protocols:

(http://www.med.umich.edu/mdrtc/cores/hybridomaCore/services.htm).

Hybridoma supernatants were screened by Western blot analysis on total wild type mouse brain protein extracts and selected for specific reactivity compared with positive and negative control antibodies (Fig 2.1). Three hybridoma lines 1E2, 4E3, and 8F4 were selected, sub-cloned and used for ascites production by The University of Michigan Hybridoma Core Facility:

(http://www.med.umich.edu/mdrtc/cores/hybridomaCore/index.html).

Except where indicated, all anti-Caytaxin monoclonal antibodies were used at a dilution of 1:500. The anti-actin antibody was used for Western blotting according to the manufacturer’s protocol (monoclonal mouse anti-beta-actin from Sigma, Cat. No. A1978). Mouse-anti-beta tubulin E7 antibody was donated by Dr. Diane Fingar, Department of Cell and Developmental Biology, University of Michigan

and used at 1:1000 or 1:2000. Peroxidase-conjugated AffiniPure Goat anti-mouse IgG antibodies were used per manufacturer's protocol (Jackson ImmunoResearch Laboratories, Inc. Cat. No. 115-035-062).

Tissue lysate preparation – All protein extractions were performed on ice with pre-chilled reagents and materials. Tissues were homogenized in a glass dounce homogenizer in 1-2 mL of homogenization buffer (50mM Tris, 500mM NaCl, 1mM EDTA, 0.5% NP40, 1x Protease Inhibitor Cocktail (Thermo Scientific), 1x PMSF, 0.1% SDS or 2% SDS). Homogenization was performed for 1-2 minutes (approximately 50 strokes). Homogenate was centrifuged at 4^{o}C in a pre-cooled microcentrifuge at 15,000 x g for 10-15 minutes to clear large debris. Supernatant was used immediately or flash-frozen with liquid nitrogen and stored at -80^{o}C. Protein concentrations were measured using a commercial Bradford Assay (Bio-Rad, Cat. No. 500-0006).

SDS-PAGE – All Western blot SDS-PAGE gels were large (separating gel 25ml volume, ~10 inches in length, 1mm thick), and prepared to 10% polyacrylamide except where indicated. Samples were heated at 100^{O}C for 5-10 minutes in 2X Laemmli buffer with β-mercaptoethanol. Gels were run in 1X Tris-Glycine-SDS running buffer at a constant current of 15-30 milliamps and electrophoretically transferred at a constant current of 100 milliamps overnight at room temperature in 0.5X Tris-Glycine buffer onto a nitrocellulose membrane (Pall Life Sciences, BioTrace™ NT, Cat. No. 66485). Ponceau S staining of nitrocellulose membranes was performed according to the manufacturer's protocol (USB, Cat.

No. 32819, prepared as directed) to confirm transfer of proteins onto the membrane.

Immunoblotting – ECL*:* Membranes were incubated in blocking buffer (5% wt/vol non-fat dry milk powder in TBST) for at least 1 hour. Primary and secondary antibodies were diluted in blocking buffer and subsequently incubated with intermediate washes for 1 hour at room temperature. All washes were performed 3 times, 10 minutes each, in TBST. ECL (GE/Amersham, Cat. No. RPN2106 or Fisher Scientific/Pierce, Cat. No. PI32106), autoradiography blue film (Fisher Scientific, Cat. No. NC9469626 or AF5700). DAB*:* Performed as described by Hortsch *et al* [76]. Briefly, membranes were incubated in blocking buffer (1x PBS, 10% FCS, 0.05% TX100). Primary and secondary antibodies were diluted in blocking buffer to 1:1000 and 1:2000 respectively. Membranes were washed in blocking buffer after primary antibody incubation and in wash buffer (1xPBS and 0.05% TX100) after secondary antibody incubation followed by 1xPBS. Membranes were briefly rinsed with 50mM Tris-HCl before development with DAB (50mM Tris-HCl pH7.5, 0.05% diaminobenzidine, 30% H_2O_2). Reactions were stopped by rinsing membrane in dH_2O.

cDNA *c*onstructs and sequence alignment –

Human *ATCAY* cDNA – Open Biosystems (Cat. No. MHS1010-7429547, Clone ID 4153341

Mouse *Atcay* cDNA – Open Biosystems Cat. No. MMM1013-9200338, Clone ID 6491141

Site-directed mutagenesis – Mutagenic primer pairs were designed using Agilent Technologies web-based QuikChange® Primer Design Program (http://www.genomics.agilent.com).

Met1Thr	Sense 5'-ctctttccagctctcacgggaaccacagaagc-3'
	Anti 5'-gcttctgtggttcccgtgagagctggaaagag-3'
Met10Thr	Sense 5'-gaagctacactaaggacggaaaatgtggacgtgaggg-3'
	Anti 5'-ccctcacgtccacattttccgtccttagtgtagcttc-3'
Met1+10Thr	Sense 5'-gctctcacgggaaccacagaagctacactaaggacggaaaatg-3'
	Anti 5'-cattttccgtccttagtgtagcttctgtggttcccgtgagagc-3'

Reaction setup and PCR cycling parameters were followed according to the manufacturer's protocol with 25ng template DNA, 125ng primers, and an 8 minute PCR extension (QuikChange II Site Directed Mutagenesis Kit, Agilent Technologies, Cat. No. 200519). Mutagenesis reactions were transfected into XL1-Blue Competent Cells (Agilent Technologies, Cat. No. 200249) and plated on nutrient agar with 100µg/ml ampicillin. Positive clones were identified via miniprep (Qiagen, according to manufacturer's protocol) followed by sequencing using primer T7 (5'-taatacgactcactataggg-3').

***In vitro t*ranslation –** Coupled transcription/translation reactions were set up according to manufacturer's protocol using the TnT® T7/SP6 Coupled Reticulocyte Lysate System (Promega, Cat. No. L5020). 7µL of a 25µL reaction was loaded on 10% SDS-PAGE gels. Additional reagents included EasyTag™ L-[^{35}S]-Methionine, 500µCi (18.5MBq) (PerkinElmer, NEG709A500UC) and RNasin® Ribonuclease Inhibitor (Promega, Cat. No. N2111). Gels were fixed

overnight in 50% MeOH and 10% acetic acid, and then treated with EN^{3}HANCE™ Autoradiography Enhancer according to the manufacturer's protocol (PerkinElmer, Cat. No. 6NE9701). Gels were dried on a slab gel dryer for 2 hours at 80^{o}C and exposed to autoradiography blue film (Fisher Scientific, Cat. No. NC9469626 or AF5700) for 1-7 days at room temperature. *Atcay/ATCAY* cDNA inserts were correctly oriented from the SP6 promoter. Reactions with T7 RNA polymerase served as negative controls.

Rotarod – Animals were required to perch on a stationary rod for approximately 30-60 seconds to accustom themselves to the environment. The animals that were comfortable staying on the rod were allowed to run with a constant speed of 5 rpm for approximately 60 seconds. Animals that fell after three trials with constant low speed rotation (2 rpm) were removed from the experiment. When test animals were able to stay on the rod for approximately 30 seconds, they were allowed to return to their home cage. Animals were trained again after at least 2 hours of rest or the following day. During the third training session, the rod was allowed to accelerate until the animal fell. Those mice that passed initial testing requirements underwent testing with 3 trials per day over 3 days, for a total of 9 runs. 7 wt/*swd* BAC$^-$ and 10 *swd*/*swd* wtBAC$^+$ mice were tested, ages 3-5 months with mixed gender, and time on the rod for each test animal was recorded.

Graphs and statistics – All graphs were created using Microsoft Excel and p-values were calculated using Student's t-test. Error bars were calculated based

on standard deviation from the mean (SEM) of the corresponding group. Protein quantification was performed after scanning sub-saturationally-exposed films by analysis with ImageJ (http://rsbweb.nih.gov/ij/) and relative ratios were calculated based on density.

***In silico* analyses –** Sequence alignments, Caytaxin protein translation start site predictions, and Caytaxin molecular weight calculations were analyzed using sequences obtained from the NCBI database:

mRNA: Human (*ATCAY*): NM_033064.4; Mouse (*Atcay*): NM_178662.3

Protein: Human Caytaxin: NP_149053.1; Mouse Caytaxin: NP_848777.1

Clone CTB-171N13: AC011477.7

Potential translation start codons were analyzed using the NetStart 1.0 Prediction Server (http://www.cbs.dtu.dk/services/NetStart/). Met1 and Met10 were identified as the top two candidates with scores of 0.806 and 0.744 respectively [56]. The ATGpr prediction program (http://atgpr.dbcls.jp/) also identified Met1 and Met10 as the top two candidates with 0.70 and 0.31 reliability [77]. Mouse and human Caytaxin protein molecular weight was calculated using the SIB Swiss Institute of Bioinformatics "Compute pI/Mw" online tool (http://web.expasy.org/compute_pi/) [15, 77]. Sequence similarity calculations were performed by alignment using NCBI's BLAST®.

Preparation of chamber slides for primary cerebellar cultures – Poly-D-lysine was prepared according to the manufacturer's protocol (Sigma, Cat. No. P0899, 5mg) and stored at -20°C. Before preparing slides, 1 part poly-D-lysine

was mixed with 2 parts sterile culture PBS and added to each chamber of an 8-well chambered slide until covered. Slides were incubated at room temperature for 1 hour and rinsed thoroughly with sterile tissue culture grade H_2O. Slides were allowed to dry completely (about two hours) before immediately plating cells (described below).

Primary cerebellar cell culture – Protocol from Dr. Hisashi Umemori, Department of Biological Chemistry, University of Michigan. Cerebella were extracted from P3 mice and placed in DMEM + 0.25% glucose where meninges were removed, before transfer into a 15 ml tube with DMEM + 0.25% glucose. Cerebellum was washed once with HBSS and incubated in 1ml HBSS with 1% trypsin and 0.05% DNase I at room temperature for 13 min. Cerebellum was then washed three times with HBSS. Cerebellar cells were dissociated in 1ml HBSS + 12mM $MgSO_4$ +0.05% DNase I with a Pasteur pipet. Large particles were allowed to fall before the supernatant was transferred to a 1.5ml tube and centrifuged at 3,000xg for 5min. The pellet was resuspended in 200µl serum-free media and divided into a prepared 8-well chambered slide (prepared as described above). After 1 hour of incubation at 37^oC in a CO_2 incubator, 200µl serum free media was added to each well. Partial media changes were performed once per week

Immunostaining – Primary neurons were prepared from *swd*/*swd* and wt/wt littermates from the *sidewinder* lines (described above). 2% PFA was diluted in 1xPBS and used for fixation at 37^oC for 15 minutes. Cells were washed with

once with TBS + TX100 for 10 minutes at room temperature, and then blocked with TBSTS for 30 minutes at room temperature. Primary antibodies were diluted in TBSTS at the following dilutions: anti-Caytaxin mAb 4E3 at 1:300 and anti-synaptophysin at 1:100, and incubated overnight at +4^{o}C. Cells were washed 5x for 5 minutes each in TBST. Secondary antibodies were diluted in TBSTS at the following dilutions: FITC at 1:1000 (Caytaxin), C3 at 1:1000 (synaptophysin), and incubated for 1.5 hours at room temperature. Five final washes were performed: 4 times with TBST, and once with TBS. Cover slides were mounted with ProLong® Gold reagent (Life Technologies, Cat. No. P36930) and allowed to set before visualization via fluorescence microscopy.

Chapter III.

Generating transgenic mice as models for human disease

Introduction

Two single-nucleotide point mutations in *ATCAY* were found in all individuals with Cayman ataxia [18] (described in Chapter I). However, the relative importance of each mutation in disease pathogenesis has not been determined. Based on the nature of these mutations and the known nucleotide and amino acid sequences of *ATCAY* mRNA and Caytaxin, only the intron 9 mutation is expected to affect Caytaxin expression. Due to the abnormal splicing across exon 9, this aberrant transcript is expected to encode a protein truncation from the end of exon 9 [18]. Overall, the intron 9 mutation was hypothesized to be the causative mutation of the Cayman ataxia disease [18]. Since the proposed effects of these mutations on protein expression have not been further investigated, this study aimed to determine how these mutations affect Caytaxin function to cause the motor and cognitive defects observed in Cayman ataxia patients.

We have characterized Caytaxin protein expression in spontaneously occurring ataxic mouse models that harbor mutations in the 5' region of *Atcay* (discussed in Chapter II). The mutations in *Atcay* exon 5 and exon 4 of the severely affected

sidewinder and *jittery* mice, respectively, cause a lack of Caytaxin protein expression. Additionally, small amounts of protein which might be produced are predicted to be severely truncated. The *Atcay* intron 1 mutation in the mildly affected *hesitant* mice limits levels of normal *Atcay* transcript, and results in extremely low levels of Caytaxin expression (Fig 2.2 and summarized in Table 2.1). These data support the hypothesis that mutations which are deleterious to protein structure cause a more severe phenotype than those that reduce expression of the wild type protein. Since rodent models with mutations in the 3' region of *Atcay* have not been identified, there is no evidence to suggest how the human *ATCAY* mutations affect Caytaxin expression and whether this hypothesis will hold true in the representative mouse model.

In the study described here, we utilized a BAC complementation assay to produce a humanized mouse model for Cayman ataxia by generating mice expressing an *ATCAY* transgene harboring both Cayman ataxia mutations. Additionally, we also sought to examine each mutation individually by creating mice expressing transgenes carrying either the intron 9 or exon 9 variant. This method has proven successful in functionally rescuing ataxia in *sidewinder* mutant mice through the expression of human Caytaxin from a full-length human *ATCAY* transgene (described in Chapter II). Tests to examine the phenotype of these transgenic mice were designed to assess three significant symptoms displayed by patients with Cayman ataxia: muscle control, motor coordination, and mental retardation [15].

The experiments described below represent a novel approach to examining the effect of *ATCAY* mutations on Caytaxin protein expression, and contribute data regarding regions and expression levels of Caytaxin required for normal function. While this study is incomplete due to technical problems described in detail in Chapter IV, it suggests that both Cayman ataxia *ATCAY* mutations may act synergistically to cause disease. These data and the models described provide insight into the understanding of nervous system pathways dependent on Caytaxin, and may also aid in characterizing the etiology of other neurological disorders in the future.

Results

Transgenic mice were developed to express *ATCAY* harboring the Cayman ataxia mutations

Three separate BACs were created by mutagenesis from a parent BAC that we provided by the UC Davis Mouse Biology Program, which contain a transgene comprised of the full-length human *ATCAY* gene with either the Cayman ataxia *ATCAY* exon 9 mutation (BAC^{E9}), the intron 9 mutation (BAC^{I9}), or both mutations (BAC^{EI9}) (Fig 3.1). A PCR screen for BAC integration into the genome was developed and designed to detect the presence of *ATCAY* from the genomic DNA of potential founder mouse pups.

Primers were designed to amplify fragments within exons 2, 6, and 9 in an effort to detect the presence of a full length *ATCAY* gene. To ensure that mice which

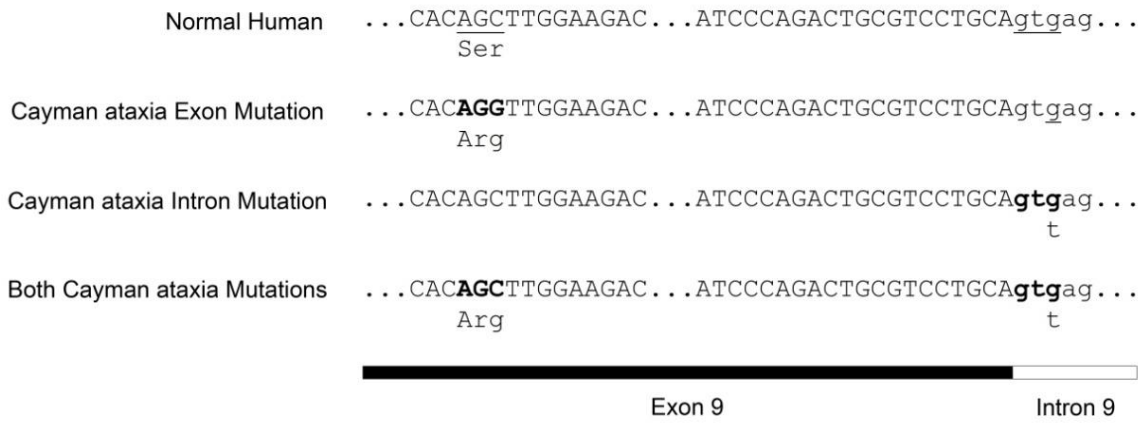

Figure 3.1. Generation of BAC transgenic mice with human *ATCAY* mutations.
Transgenic mice expressing the full-length human *ATCAY* transgene, without either mutation, were described in Chapter II. The *ATCAY* exon 9 mutation (AGC to AGG, bold) results in a serine (Ser) to arginine (Arg) amino acid conversion. The *ATCAY* intron 9 mutation is located near the exon 9-intron 9 junction (gtg to gtt, bold) and affects normal splicing around intron 9. A double *ATCAY* mutant was generated harboring both mutations (AGC and gtg, bold). Nucleotides spanning exon 9 are marked by the black bar, and those of intron 9 are marked by the white bar.

had integrated the BAC would not be lost as false negatives, the PCR assay was optimized to detect ratios of 1/3, 1, and 3 copies of the BAC against 1 equivalent mouse genome (Fig 3.2). With this level of sensitivity, BACs can be detected at a presence at less than 1:1 equivalence, ensuring that low levels of BAC integration will not go undetected. Each founder that tested positive for the BAC was bred onto the *sidewinder* background and maintained as a separate line.

Heterozygote mating within each line followed by PCR genotyping ultimately produced homozygous *swd*/*swd* mice which express the BAC (*swd*/*swd* BAC^{EI9+}, BAC^{I9+}, or BAC^{E9+}) as well as ataxic (*swd*/*swd* BAC^{EI9-}, BAC^{I9-}, and BAC^{E9-}) and non-ataxic (*swd*/wt BAC^{EI9+}, BAC^{I9+}, BAC^{E9+} and *swd*/wt BAC^{EI9-}, BAC^{I9-}, BAC^{E9-}) controls. BAC line nomenclature and gross phenotypes are summarized in Table 3.1. Since BAC mice were generated on a mixed background, ataxic and non-ataxic controls had to be generated within the same line as the experimental complementation mice. In total, 10 transgenic founders were identified as positive for the *ATCAY* transgene (4 for BAC^{EI9}, 3 for BAC^{I9}, and 3 for BAC^{E9}) and were subsequently bred with heterozygous *sidewinder* (wt/*swd*) mates, producing 10 different transgenic lines. Over multiple generations, six of the lines began to produce inconclusive results during the PCR screening assay, appearing to no longer possess the transgene (data not shown). However, four lines continued to show transgene transmission. Two lines contained the *ATCAY* transgene with both exon 9 and intron 9 mutations (lines BAC^{EI9}A and BAC^{EI9}B) and two lines contained the *ATCAY* transgene with only the intron 9 mutation

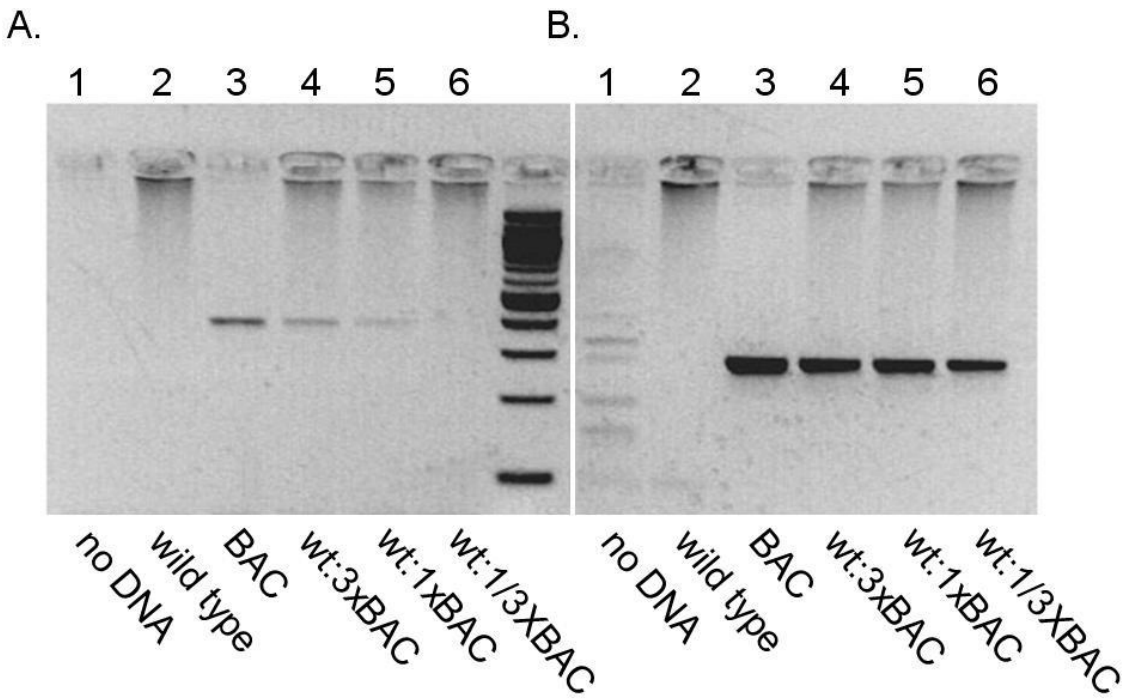

Figure 3.2. Developing a PCR screen for *ATCAY* transgenic founders.
Genomic PCRs were optimized to detect exons 2 **(A)** and 9 **(B)** of *ATCAY*, representing the 5' and 3' regions of the transgene, respectively. PCR conditions were optimized to detect the purified BAC spiked into wild type mouse genomic DNA at copy numbers equivalent to 3 (**lane 4**), 1 (**lane 5**) or 1/3 (**lanes 6**) copies against 1 equivalent of mouse genomic background (indicated as wild type or wt). Positive control purified BAC DNA used for injection (lane 3) and mouse genomic DNA (**lane 2**). Negative PCR control (**lane 1**) substituted DNA with H_20.

(lines BAC^{I9}A and BAC^{I9}B). No founders were confirmed as positive for the *ATCAY* transgene with only the exon 9 mutation. Hence, no data is available for the BAC^{E9} line (discussed further below and in Chapter IV).

Primary phenotypic assessment of transgenic mouse lines

Typically, transgenic mouse lines differ from one another in the number of transgene copies integrated as well as the transgene integration sites [78-80]. As a result, mice may display unusual behavioral and/or physical phenotype that could be mistakenly included in the assessment for disease rescue [70, 81]. Therefore, within these four transgenic lines, comparisons were made between BAC-positive progeny (BAC^{I9+}, BAC^{EI9+}) and BAC-negative littermates (BAC^{I9-}, BAC^{EI9-}), against non-transgenic *sidewinder* mice. Behaviors such as social interactions, feeding, grooming, mating, and general movement were monitored for any aberrant phenotype differences [70, 82].

Upon investigation of physical characteristics, mice between and within each line differed only in coat color, which appeared black, agouti, or white, a result of producing the transgenic founders in the mixed-background [15, 83]. Behavioral observation revealed hyperactivity among a number of founder BAC^{EI9+} mice and their BAC^{EI9+} progeny (both BAC^{EI9+}A and B) that manifested as circling or back-flipping (unpublished observations). Since this behavior was rare among progeny (<1%, data not shown), it was considered an artifact caused by the mixed background, and mice displaying these behaviors were not mated or included in

phenotype assessment. Similar behaviors were not observed in lines BAC^{I9+}A and B, or their BAC^{I9-} littermates.

Initial examination for ataxia and other obvious motor defects in each line confirmed that *swd*/*swd* BAC^{I9-} (A and B) and *swd/swd* BAC^{EI9-} (A and B) mice are severely ataxic consistent with their mutant background. These mice displayed symptoms similar to *sidewinder* mutants (described in Chapter II). No visible signs of ataxia or other motor defects were observed in *swd*/*swd* BAC^{EI9+}A mice. *swd*/*swd* BAC^{EI9+} (A and B) and BAC^{I9+}B mice also displayed an ataxic phenotype; however, their ataxia appeared slightly less severe than the matched BAC^{EI9-} and BAC^{I9-} controls. These mice seemed to harbor the ability to adapt to their condition over time and developed methods of moving around their cage without falling into uncontrollable ataxic episodes, a behavior rarely observed in *sidewinder* mutant mice. These modifications often involved remaining crouched near the base of the cage and 'creeping' forward with small movements of their limbs, similar to the moderately ataxic hesitant mutant mice. BAC line nomenclature and gross phenotypes are summarized in Table 3.1.

Coding regions in mutant *ATCAY* are incomplete or harbor unintended insertions

While testing for the presence of the BAC transgene via genomic PCR proved to be a quick assay for determining transgene integration, it was unreliable in determining whether the transgene was intact and would express Caytaxin protein. To examine the coding region of the *ATCAY* transgene, cDNA was

Mutation	Line	Background	-BAC (control)	-BAC phenotype	+BAC (rescue)	+BAC phenotype
None	wtBAC	*swd*/*swd*	wtBAC^{-}	Severe	wtBAC^{+}	None
		swd/wt	wtBAC^{-}	None	wtBAC^{+}	None
Intron 9	BAC^{I9}A	*swd*/*swd*	BAC$^{I9\text{-}}$A	Severe	BAC^{I9+}A	None
		swd/wt	BAC$^{I9\text{-}}$A	None	BAC^{I9+}A	None
Intron 9	BAC^{I9}B	*swd*/*swd*	BAC$^{I9\text{-}}$B	Severe	BAC^{I9+}B	Moderate/ Severe
		swd/wt	BAC$^{I9\text{-}}$B	None	BAC^{I9+}B	None
Both	BAC^{EI9}A	*swd*/*swd*	BAC$^{EI9\text{-}}$A	Severe	BAC^{EI9+}A	Moderate/ Severe
		swd/wt	BAC$^{EI9\text{-}}$A	None	BAC^{EI9+}A	None
Both	BAC^{EI9}B	*swd*/*swd*	BAC$^{EI9\text{-}}$B	Severe	BAC^{EI9+}B	Moderate/ Severe
		swd/wt	BAC$^{EI9\text{-}}$B	None	BAC^{EI9+}B	None

Table 3.1. Transgenic BAC line nomenclature and phenotypes.
Five transgenic BAC lines were examined, one with full-length *ATCAY* (Chapter II), and two each for the *ATCAY* intron mutation and both *ATCAY* mutations (**column 1**). **Column 2** lists the transgenic line names with the mutation indicated in superscript as I9 (intron mutation) or EI9 (both mutations), and A or B to denote separate founders. **Column 3** describes the *sidewinder* genotype of the corresponding mouse and **columns 5 and 7** describe ataxic phenotypes resulting from absence (**column 4**) or presence (**column 6**) of the BAC. Video recordings of phenotypes of all lines described above are available upon request to the author or the Burmeister laboratory, University of Michigan.

prepared from all four transgenic BAC lines. PCR was performed with three different primer sets designed to span human *ATCAY* cDNA exons 2-5 (Fig 3.3A), exons 5-8 (Fig 3.3B), and exons 8-12 (Fig 3.3C). Results were analyzed via agarose gel electrophoresis and examined for the presence and expected size of the amplicons. cDNA samples from full-length wild type BAC control mice (wtBAC^{+}, described in Chapter II) were included as a positive control.

Results from these PCRs (summarized in Fig 3.3E) reveal that exons 2-5 are present in transgenic mice from lines BAC^{EI9+}B and BAC^{I9+}A (Fig 3.3A, lanes 2 & 4) but absent from lines BAC^{EI9+}A and BAC^{I9+}B (Fig 3.3A, lanes 1 & 3). While the expected 475bp amplicon was detected in line BAC^{EI9+}B, additional PCR products were also evident and not observed in other samples (Fig 3.3A, lane 2). PCR for exons 5-8 from lines BAC^{EI9+}B, BAC^{I9+}A, and BAC^{I9+}B produced amplicons of approximately the expected size of 486bp (FIG 3.3B, lanes 2-4), with no amplification seen in line BAC^{EI9+}A (Fig 3.3B, lane 1). PCR for the region spanning exons 8-12 only produced an amplicon in line BAC^{EI9+}B (Fig 3.3C, lane 2) and failed to amplify this region in lines BAC^{EI9+}A, BAC^{I9+}A, and BAC^{I9+}B (Fig 3.3C, lanes 1, 3 & 4). This amplicon from BACE^{I9+}B appeared to be larger than the expected size of 293bp. Sequencing of this region in line BAC^{EI9+}B revealed that the 99bp exon 9 of the *ATCAY* transgene had been replaced with 207bp of plasmid DNA (not shown), resulting in a 401bp amplicon (Fig 3.3 E). The plasmid sequence was confirmed by the UC Davis Mouse Biology Program to be from a vector used during mutagenesis, and hence the insertion likely occurred during the construction of the BAC transgene [15, 83]. While line BAC^{I9+}A tested

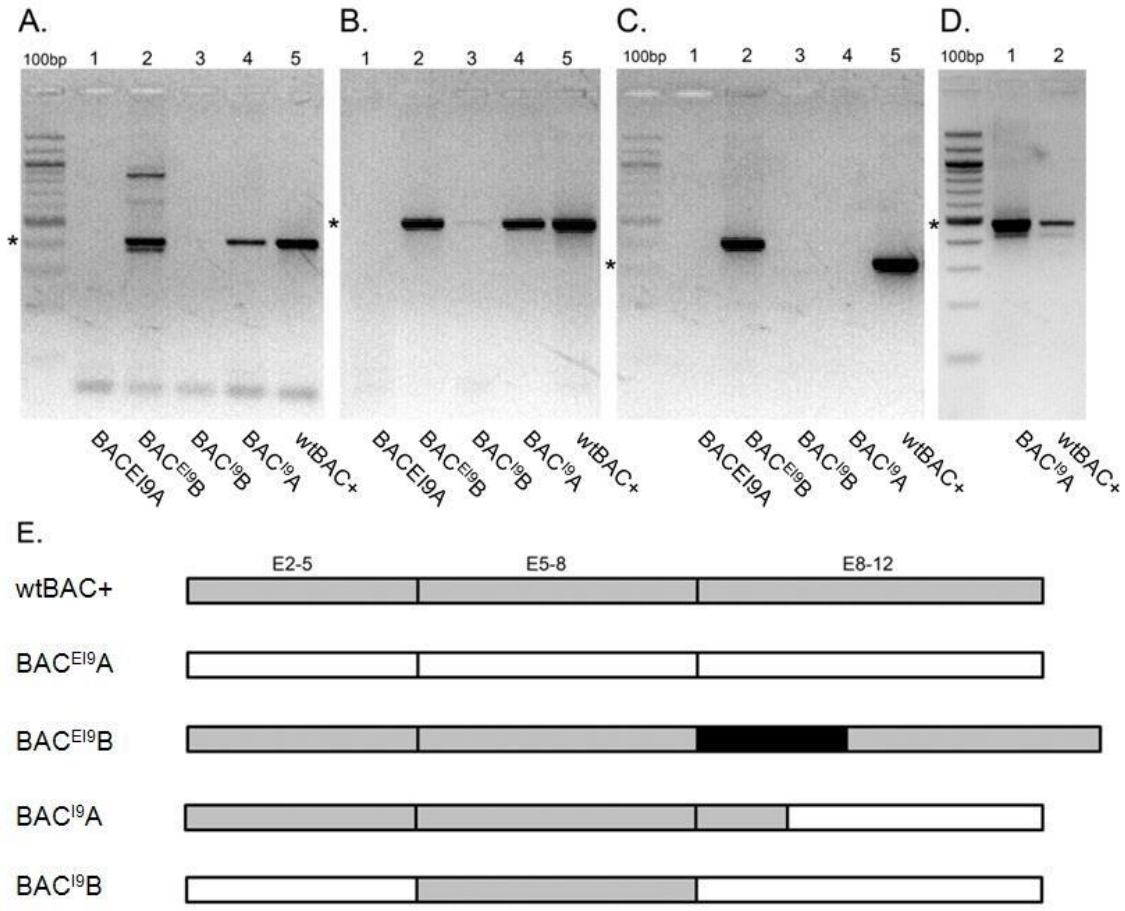

Figure 3.3. Transgene expression in *ATCAY* BAC mouse lines.
PCRs from brain cDNA of transgenic mouse lines with the double *ATCAY* mutations (BAC^{EI9}A and B), and the intron 9 *ATCAY* mutation (BAC^{I9}A and B) amplifying regions spanning *ATCAY* exons 2-5 **(A)**, 5-8 **(B)**, and 8-12 **(C)**. Expected size indicated by appropriate size marker (*****). **(D)** shows a confirmation of the presence exon 9 in the transgene of line BAC^{I9}A. **(E)** summarizes the results observed from cDNA PCRs in A-D. Presence of exonic regions indicated in grey, lack of exonic regions indicated in white, and the exon 9 replacement with plasmid sequence indicated in black (BAC^{EI9}B).

positive for *ATCAY* cDNA regions spanning exons 2-8, no amplification was observed for the region spanning exons 8-12. Further PCR and sequencing analysis revealed that this *ATCAY* transgene was complete through exon 9 (Fig 3.3D, lane 2), however these methods alone were insufficient in providing insight into why PCR amplification beyond exon 9 in line BAC^{I9+}A was not possible.

These results provided a rationale for the exclusion of lines BAC^{EI9+}A and B, and BAC^{I9+}B from subsequent quantitative phenotype assays. Although phenotypic observation suggested partial complementation, PCR from cDNA for *ATCAY* exons in these lines failed to provide evidence for an intact transgene (Fig 3.3E). Additionally, Western blots for Caytaxin in these lines failed to detect any Caytaxin expression (data not shown, data for line BAC^{I9}A shown below).

Analysis of Caytaxin protein expression in BAC^{I9} mutant mice detect a shorter human Caytaxin protein

Based on the data described in Figure 3.3, mice from line BAC^{I9+}A appeared to express a truncated *Atcay* cDNA, however these mice displayed no obvious signs of ataxia, in contrast to their BAC^{I9-}A littermates. We hypothesized that BAC^{I9+}A mice express the mutant transgene and produce a mutant form of the Caytaxin protein that is able to functionally rescue the ataxic phenotype. As only this transgenic line will be discussed in analyses below, mice with and without the transgene will be referred to as BAC^{I9+} and BAC^{I9-}, respectively. Additionally, specific *sidewinder* genotypes will be indicated as necessary.

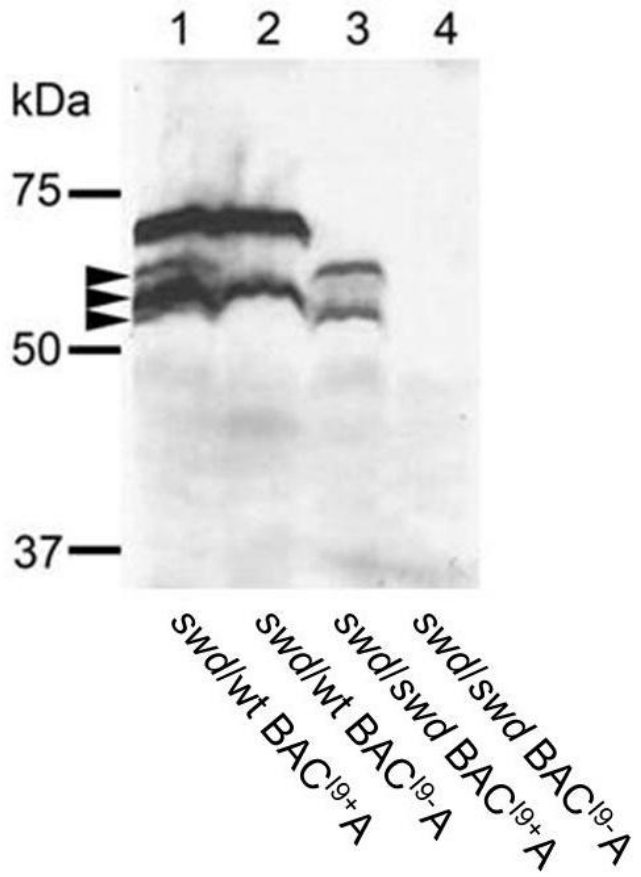

Figure 3.4. Caytaxin protein expression in BAC^{I9}A mouse line.
Western blots of approximately 30µg whole brain lysate from mice of different genotypes from the BAC^{I9}A transgenic line (intron 9 *ATCAY* mutant). **Lane 1**, BAC^{I9}A transgene on *sidewinder* heterozygote background; **lane 2**, same background as lane 1 without the BAC^{I9}A transgene; **lane 3**, BAC^{I9}A transgene on *sidewinder* homozygote background (not ataxic); **lane 4**, same background as lane 3 without the BAC^{I9}A transgene (ataxic). Arrows indicate location of smaller human Caytaxin. See Table 3.1 for nomenclature and phenotype summary.

To test this hypothesis, Western blot analysis was used to examine Caytaxin protein expressed by the mutant BAC^{I9+} line. Analysis of samples from *swd*/wt BAC^{I9+} and *swd*/wt BAC^{I9-} littermate controls (carrying one wild type copy of mouse *Atcay*) detected wild type mouse Caytaxin at the expected molecular weights (Fig 3.4, lanes 1 & 2). Additional lower molecular weight isoforms, in a protein pattern similar to human Caytaxin, were evident in the *swd*/wt BAC^{I9+} sample (Fig 3.4, closed arrowheads). Only these lower isoforms were detected in *swd*/*swd* BAC^{I9+}, and no Caytaxin was detected in *swd*/*swd* BAC^{I9-} littermates (Fig 3.4, lanes 3 & 4). The smallest isoform in this lower weight set runs at the same molecular weight as the smallest wild type Caytaxin isoform (~50kDa), but the largest isoform in the set is detected at approximately 60kDa, significantly smaller than the large wild type mouse or human isoforms.

Analysis of grip strength and fine motor control in BAC^{I9+} mice reveals functional but incomplete rescue of ataxic phenotype

We next sought to examine BAC^{I9+} mice and quantify phenotypes pertaining to symptoms displayed by individuals with Cayman ataxia, such as motor control, coordination, and learning capacity [15]. Mice were first tested via wire hang to examine muscle coordination and strength [84]. During this test, each mouse was placed on the face of a silicone-coated wire platform suspended above an empty cage, which was slowly rotated 180^{o} until the mouse was suspended. The time elapsed between the start of the rotation until the mouse fell to the bottom of the cage below was recorded. Generally, the test is performed with a cutoff time of 1 minute if the mouse has not released its grip from the platform by this time

[85]. However, in an effort to determine average potential performance for each test group, this cutoff time was not enforced and mice were allowed to remain hanging from the platform past 1 minute without intervention.

To gain a baseline for wild type and mutant performance, we first tested non-transgenic *swd*/wt and *swd*/*swd* mice and found that *swd*/wt mice are able to remain suspended for 60±8.4 seconds (Fig 3.5A, column 1). Homozygous mutant mice are only able to remain on the platform for an average of 4 seconds (Fig 3.5A, column 2). Most mutant mice experienced an ataxic episode as the platform began to move, which appeared as an uncoordinated attempt to maintain balance. As a result, these mice were unable to effectively grasp the wire platform in a way that would sustain their weight, and quickly fell to the bottom of the cage as the platform reached a 90^{o} angle. Since any additional movement often resulted in uncontrolled muscle spasms, those mutant mice that were able to remain stationary achieved a hang time of as long as 10 seconds.

Next, transgenic mouse line BAC^{I9+} was examined. Littermate groups of *swd*/wt BAC^{I9+}, *swd*/*swd* BAC^{I9+} and *swd*/*swd* BAC^{I9-} were compared to non-transgenic *swd*/wt mice (as a normal control) (Fig 3.5B). *swd*/*swd* BAC^{I9+} performed significantly better than *swd*/*swd* BAC^{I9-} littermates ($p<0.001$) (Fig 3.5B, column 3 vs. 4); not only were these mice able to remain suspended for an average of 52±4.2 seconds, they were also able to travel the wire platform while suspended. However, despite the apparent phenotype rescue, these mice did not perform as well as non-transgenic *swd*/wt mice or *swd*/wt BAC^{I9+} littermate controls (Fig3.5B,

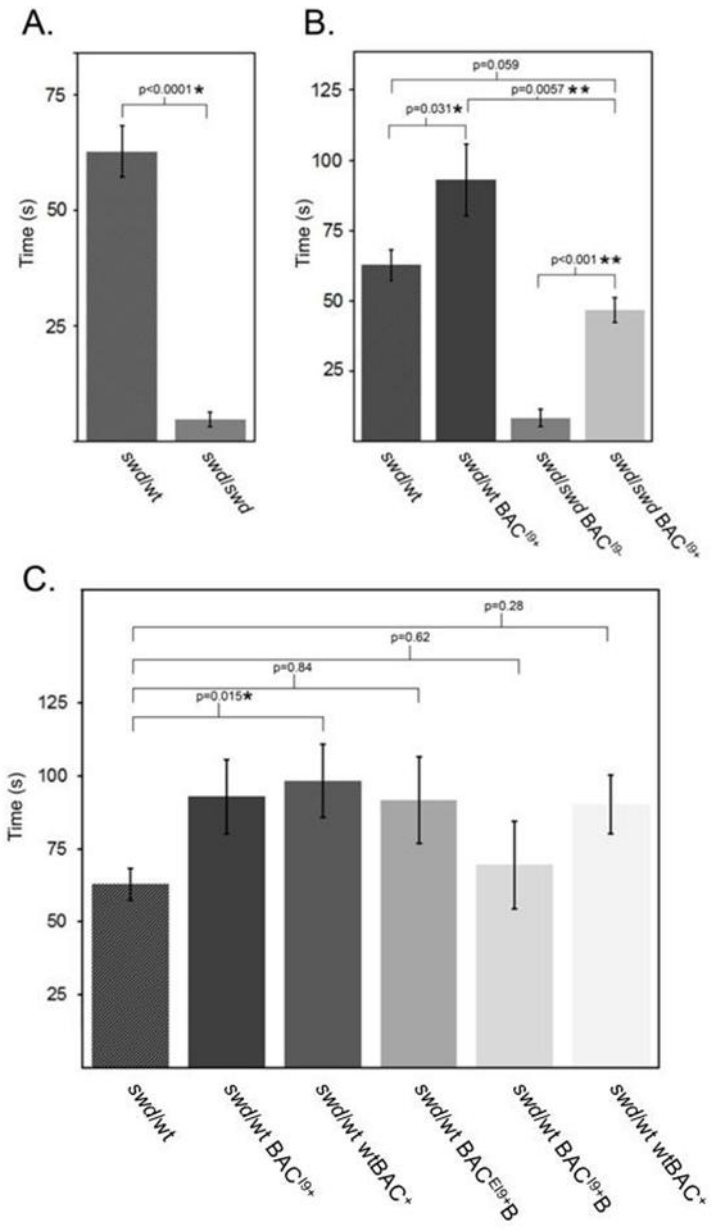

Figure 3.5. Wire hang test in transgenic *ATCAY* BAC mouse lines.
(A) Wild type (**column 1**) and ataxic (**column 2**) *sidewinder* littermates were compared. **(B)** Non-transgenic *sidewinder* wild types (**lane 1**), transgenic wild types positive for the BAC (**lane 2**), transgenic mutants without the BAC (**lane 3**), and transgenic mutants positive for the BAC (**lane 4**). Nominally significant (*), significant after correction for multiple testing (**) **(C)** Comparing BAC expression and performance. Non-transgenic wild type *sidewinder* (**column 1**) represented non-transgenic controls and transgenic *swd*/*swd* wtBAC^{+} represented BAC-expressing controls (**column 6**). Nominally significant, but not significant after correction for multiple testing (*). In all groups, n=3 mice. Averages were plotted with error bars representing ± SEM.

lanes 1 & 2 vs. lane 4). Interestingly, wild type *swd*/wt BAC^{I9+} littermates performed significantly better than the non-transgenic *swd*/wt control (p=0.031, not significant after multiple testing correction), with an average time of 93±9.2 seconds compared to 60±8.4 seconds (Fig 3.5B, columns 1 vs. 2).

To determine if this trend was typical of BAC^{+} mice from all transgenic lines, the analysis was expanded to include BAC-expressing mice from the wtBAC line (*swd*/wt wtBAC^{+} and *swd*/*swd* wtBAC^{+}) and from two of the excluded lines BAC^{EI9+}B and BAC^{I9+}B. Although not all differences were statistically significant, BAC-expressing mice showed an increased average hang time compared to non-transgenic *swd*/wt mice (Fig 3.5C, columns 2-5). Therefore, wild type control groups used in further phenotype testing of line BAC^{I9} consisted of either *swd*/wt BAC^{I9+} littermates or *swd*/*swd* wtBAC^{+} rescue mice (Chapter II).

Quantification of motor coordination and cognitive ability in BAC^{I9} mice confirms functional rescue of ataxia and indicates lack of learning or memory defects

BAC^{I9+} mice were assessed for learning and memory using a scent recognition test, which was chosen as a method to test mental capacity and normal social behavior without requiring fine motor control and coordination [84]. The experimental group consisted of mature female *swd*/*swd* BAC^{I9+} mice and the control group consisted of mature female *swd*/*swd* wtBAC^{+} mice. Females were exposed to a novel object (juvenile male mouse) for a period of 4 minutes, during which, total time of interaction (sniffing) was recorded. Mice were separated for inter-exposure times of 60 minutes and 5 days to test both short term and long

term memory, respectively, before a 4-minute re-introduction period. Total investigation time of mice with no defects in learning or memory will decrease upon reintroduction, whereas those with memory defects may investigate the novel object for a similar length of time as the initial introduction [86, 87].

We first compared total introduction and re-introduction interaction times for both experimental and control groups at each time point. Upon introduction of the novel object, BAC^{I9+} mice display a somewhat lower average investigation time of 84±6.7 seconds compared to $wtBAC^{+}$ investigation time of 96±4.1 seconds (Fig 3.6, columns 1 & 2); however, this difference was not significant (p=0.08). No significant differences between *swd*/*swd* BAC^{I9+} and $wtBAC^{+}$ controls were found after inter-exposure times of 60 minutes and 5 days (p=0.9 and p=0.2, respectively) (Fig 3.6, columns 3 & 4, 5 & 6). We next assessed learning and memory by comparing investigation time between the introduction and 5-day re-introduction and found that the decrease in investigation time between the initial introduction and the 5-day time point was significant for both lines ($p<0.05$, for each).

We next examined line BAC^{I9+} via rotarod testing, which generally tests motor coordination and balance over a few trials [85, 88, 89]. These trials were expanded to also test for learning by extending the test period over multiple days. Mice were placed on a rod which was then rotated at accelerating speeds until they failed to maintain balance and fell to the bottom of the testing platform. The time between the start of rod rotation until the mice fall onto the platform is

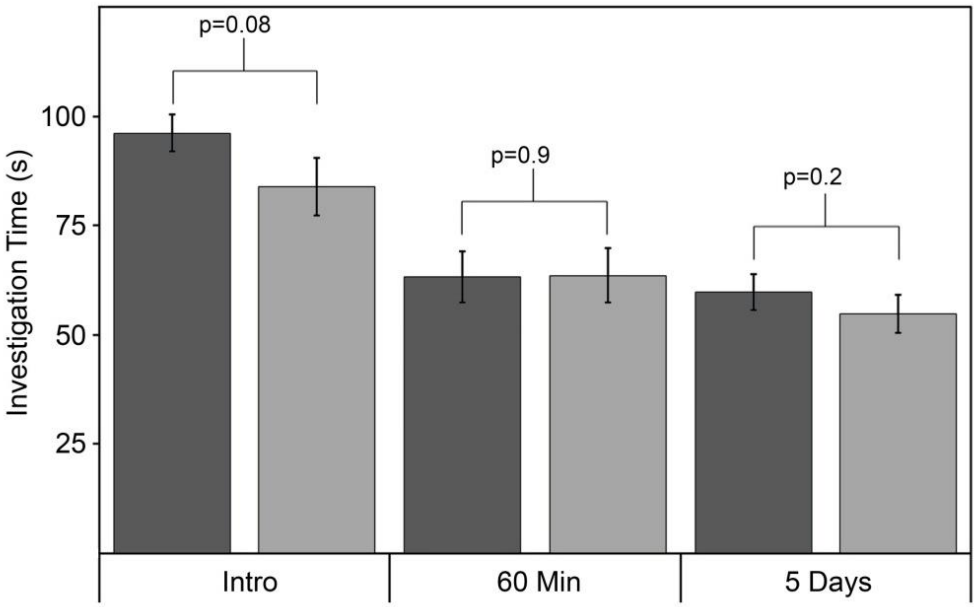

Figure 3.6. Scent recognition test in *ATCAY* BAC transgenic lines.
Bars represent total interaction time over 4 minutes recorded between female transgenic BAC mice (n=10 per group) and juvenile males (n=2 males). Interaction times for *swd*/*swd* wtBAC^{+} females (dark bars) and *swd*/*swd* BAC^{l9+} (light bars) were compared after initial introduction, and interexposure times of 60 minutes and 5 days. Average time was plotted with error bars representing ± SEM.

recorded. By repeating these trials over several days, normal mice learn how to balance themselves on the rotating accelerating rod and remain on the rod for longer times with each successive trial [85, 89]. The experimental group included *swd*/*swd* BAC^{I9+} mice and two control groups, consisting of *swd*/wt BAC^{I9-} littermates and *swd*/wt wtBAC^{-} mice from the wtBAC rescue line (both control lines are phenotypically wild type).

Total average time on the rod was compared between all three groups of mice per trial day (Fig 3.7). Though *swd*/wt BAC^{I9-} mice had the highest average time per day (Fig 3.7, columns 2, 5 & 8), average hang time was equivalent across all groups tested. Learning and memory was assessed in these groups of mice by comparing performances on the first and last testing days. Compared to Day 1, a significant increase in time on the rod was seen in the *swd*/*swd* BAC^{I9+} experimental group ($p<0.0001$) by Day 3 (Fig 3.7, columns 3 vs. 9). This trend was consistent with control groups, which also showed significant increases in performance on the rod between the first and last test days (Fig 3.7, columns 2 vs. 8). Overall, data obtained from behavior and motor analysis indicates that Caytaxin function is retained despite the intron 9 mutation.

Mutant *ATCAY* mRNA from BAC^{I9+} mice includes intron 9 and the presence of a premature stop sequence

We confirmed that *ATCAY* cDNA from BAC^{I9+}A contains coding exons 2-9 (Fig 3.3), but we were unable to account for the absence of the 3' region spanning exons 10-13 in cDNA. However, genomic DNA PCR using primer sets located

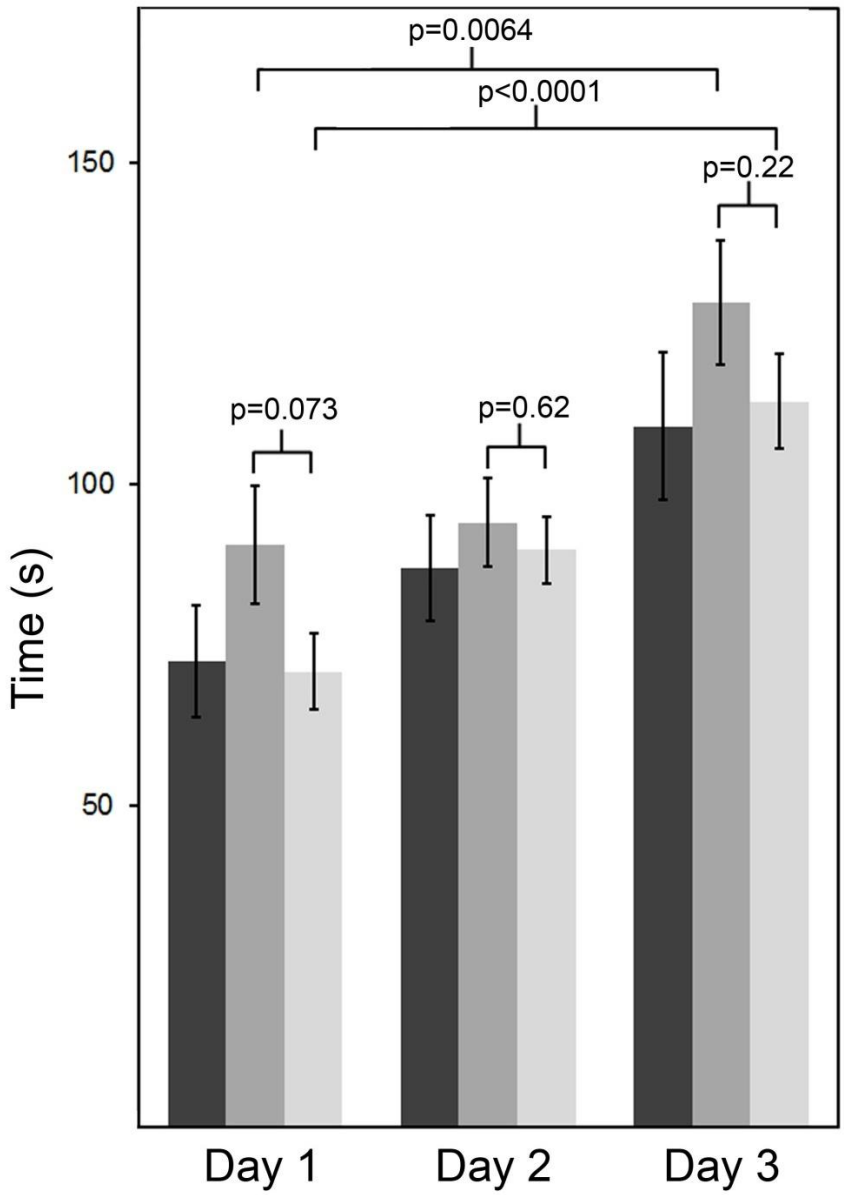

Figure 3.7. Rotarod test in *ATCAY* BAC transgenic lines.
Bars indicate average time on a rotating rod per day, over 3 days with 10 mice per group; error bars represent ± SEM. wt/*swd* wtBAC^{-} mice (dark grey, columns 1, 4, 7, n=7), wt/*swd* BAC^{I9-} mice (grey, columns 2, 5, 8, n=10), and *swd*/*swd* BAC^{I9+} mice (light grey, columns 3, 6, 9, n=10).

within introns flanking each *ATCAY* exon were able to amplify exons spanning the entire gene, including exons 9, 10, and 11 (Appendix VI), providing evidence that the transgene is in fact intact in BAC^{I9+} mice. Initial Western blot analysis examining Caytaxin expression in BAC^{I9+} mice detected a protein product with a pattern similar to human Caytaxin, but smaller in size by approximately 5 kDa (Fig 3.4). Since this protein was not detected in BAC^{I9-} mice, we hypothesized that this mutant Caytaxin protein results from splicing defects caused by the intron 9 mutation in *ATCAY*.

To test this hypothesis, we utilized 3' Rapid Amplification of cDNA Ends (3' RACE) to determine the 3' nucleotide sequence of *ATCAY* mRNA downstream of exon 9 in BAC^{I9+} mice. Gene-specific primer (GSP) pairs were designed to amplify fragments spanning small regions between exon 9 through the 3' UTR, using either primary PCRs or secondary "nested" PCRs with an internal GSP. Upon analysis of the resulting amplicons via gel electrophoresis, two unexpected fragments were observed about 550bp and 400bp in size (Fig 3.8A). DNA sequencing of these two amplicons provided inconclusive results as polymerase slippage prevented a full sequence reconstruction.

However, two adenine-rich (polyA) regions in intron 9 located 550bp and 395bp downstream of the original forward primer were evident upon further sequence analysis (Fig 3.8B, bold & underlined). Based on these data, we hypothesized that the BAC^{I9+} transgene affects splicing by preventing the proper excision of intron 9. Inclusion of intron 9 introduces a premature translation stop sequence

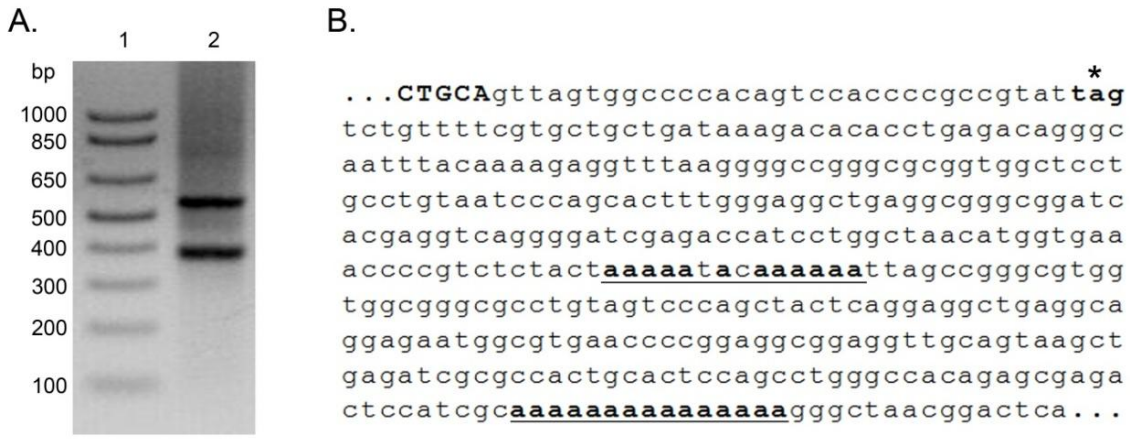

Figure 3.8. 3'RACE provides evidence for inclusion of intron 9 in *ATCAY* cDNA of BAC^{I9+}mice.
(A) RT-PCR with exon 8 GSP primers and 3'RACE AUAP primers produces two bands. **(B)** Sequence analysis of intron 9 (lower case) with 3' of exon 9 (capitalized, bold), the introduced stop codon (*), and two putative poly-A priming sites for 3'RACE oligo-dt AP primers (bold, underlined).

31 nucleotides after exon 9 (Fig 3.8B, bold & starred). This is predicted to result in the translation of a truncated Caytaxin protein of 332aa (37.5kDa) instead of the expected 371aa (42.12kDa) – a difference of 4.62kDa. The observed difference in apparent molecular weight observed on the Western blot between the wild type and mutant Caytaxin proteins of approximately 5kDa (Fig 3.4) is consistent with this hypothesis.

To confirm the inclusion of intron 9 in the coding sequence of BAC^{I9+} *ATCAY* mRNA, we performed a series of PCRs to examine BAC^{I9+} *ATCAY* genomic DNA and cDNA. Genomic PCRs were designed to amplify a region spanning from *ATCAY* exon 9 into intron 9 to reconfirm that these two regions are indeed adjacent in the BAC^{I9+} transgene. The amplicon produced from BAC^{I9+} is consistent with the expected size of 317bp, which was detected in the $wtBAC^{+}$ genomic DNA positive control (Fig 3.9A, lanes 1 & 2). Next, PCR primers for *ATCAY* cDNA were designed to amplify a 251bp region from exon 8 into intron 9, which would only produce an amplicon if intron 9 is included in the cDNA sequence. Amplification of this region is indeed observed in cDNA from BAC^{I9+} mice, with low levels of amplification also detected in the $wtBAC^{+}$ control cDNA (Fig 3.9A, lanes 5 & 6). Quantitative real-time PCR (qRT-PCR) was used to more sensitively detect and quantify the levels of mutant transcript, and found strong expression of this aberrant transcript in BAC^{I9+} mice (Fig 3.9B & C, column 3). Similar to the non-quantitative PCR, the mutant transcript is also detected in $wtBAC^{+}$ mice (Fig 3.9B & C, column 2), but at significantly lower levels (2,500-fold vs. BAC^{I9+}, $p<0.05$).

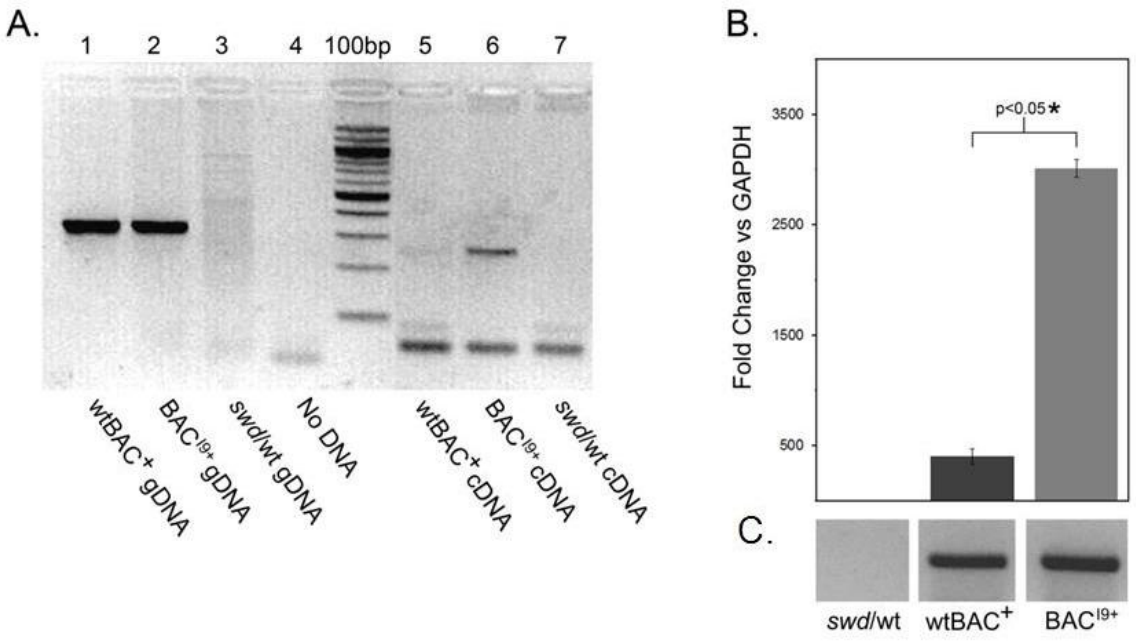

Figure 3.9. Confirmation for presence of intron 9 in BAC^{I9} mutant transcript. **(A)** PCR to confirm intact exon9-intron 9 boundary in genomic DNA of wtBAC^{+} (**lane 1**), BAC^{I9+} (**lane 2**), and non-transgenic wild type *sidewinder* control (**lane 3**). **Lane 4** contains control PCR with no DNA. PCR for presence of intron 9 in brain cDNA from wtBAC^{+} (**lane 5**), BAC^{I9+} (**lane 6**), and non-transgenic wild type *sidewinder* control (**lane 7**). **(B)** qRT-PCR to quantify level of mutant transcript from brain in control non-transgenic wild type *sidewinder* mice (**column 1**), transgenic wtBAC^{+} (**column 2**), and transgenic BAC^{I9+} (**column 3**). Fold change vs. GAPDH averaged for biological triplicates are plotted with error bars representing ± SEM. **(C)** Resulting PCR amplicon visualized on a single agarose gel.

Transgenic BAC^{I9+} mice only express mutant *ATCAY* mRNA transcript

Though these data suggest that the *ATCAY* intron 9 mutation causes aberrant splicing and inclusion of intron 9 in the coding region, we examined whether full-length *ATCAY* cDNA was also expressed from the BAC^{I9+} transgene. To examine levels of full-length versus truncated *ATCAY* RNA, primers were designed to test unique 3' regions in each of these transcripts. Primers located in the 5' region were chosen to detect both total (truncated and full-length) *ATCAY* mRNA. Results from these experiments reveal that total full length *ATCAY* levels in wtBAC^{+} controls are ~16,000-fold higher than in BAC^{I9+} mice (Fig 3.10A & B, column 2 vs. 3).

In creating transgenic mice, it is common for multiple copies of the transgene to integrate within the mouse genome [90, 91]. This often results in over-expression of the gene. It was next examined whether the difference in *ATCAY* expression between wtBAC^{+} and BAC^{I9+} mice is due to a difference in transgene copy numbers. qRT-PCR on genomic DNA suggest only 3 BAC copies integrated in line BAC^{I9+} versus 12 copies in the wtBAC^{+} line (Fig 3.11, column 2 vs. 3). PCR for transcripts containing the 3' region of *ATCAY* revealed that BAC^{I9+} mice do not express full-length transcripts containing the 3' region of *ATCAY* (Fig 3.12A & B, column 3).

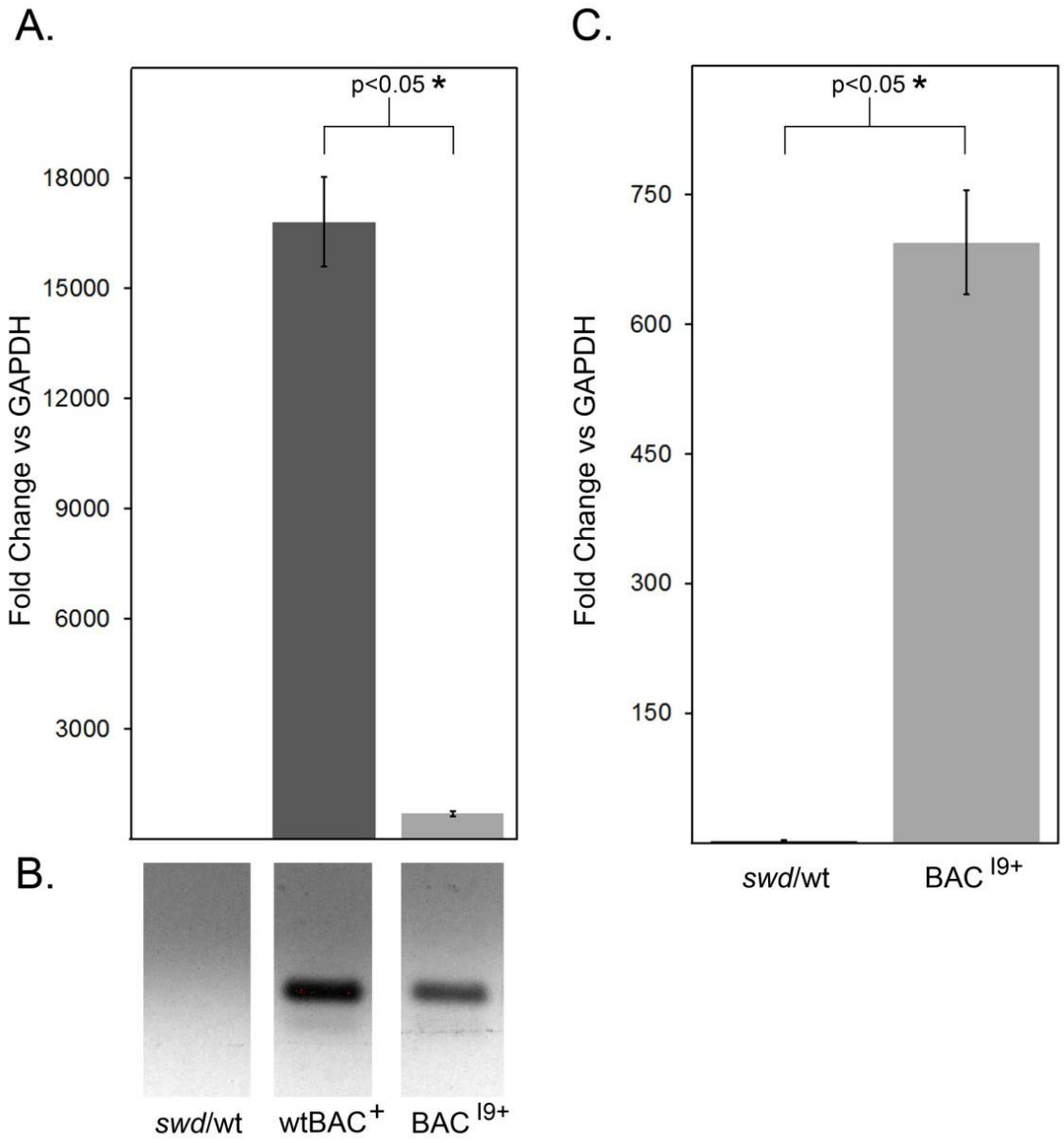

Figure 3.10. qRT-PCR for 5' region of *ATCAY* in transgenic line BAC^{I9}.
(A) qRT-PCR to quantify total levels of *ATCAY* transcript from brain in control non-transgenic wild type *sidewinder* mice (**column 1**), transgenic wtBAC^{+} (**column 2**), and transgenic BAC^{I9+} (**column 3**). **(B)** Resulting PCR amplicon visualized on a single agarose gel (lower panels). **(C)** Results from (A) re-plotted with smaller y-axis values for comparison between wild type *sidewinder* controls (**column 1**) and intron 9 mutant BAC (**column 2**). Fold change vs. GAPDH averaged for biological triplicates are plotted with error bars representing ± SEM.

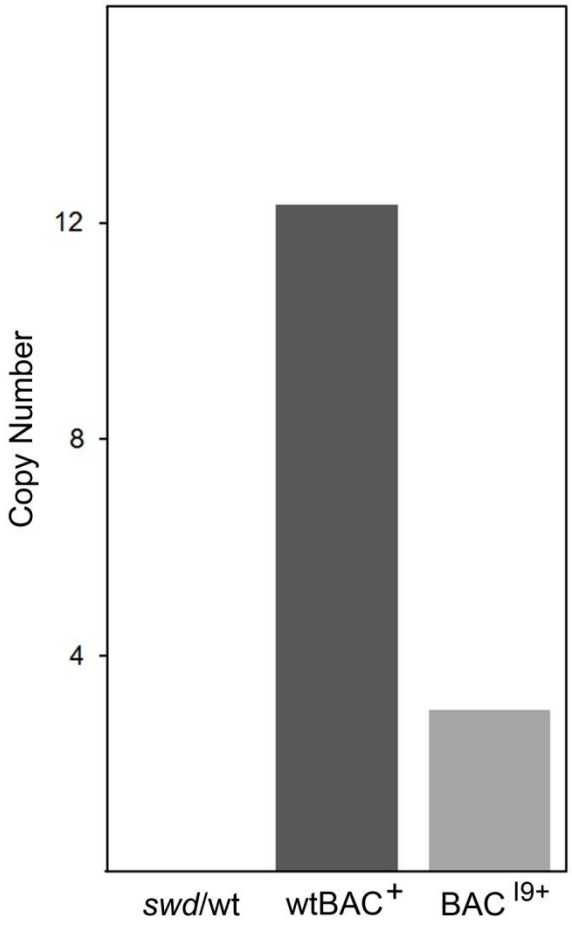

Figure 3.11. BAC copy number analysis in transgenic line BAC^{I9}.
qRT-PCR was used to detect human *ATCAY* as described in Materials and methods. Genomic DNA from non-transgenic *swd*/wt mice (**column 1**), wtBAC^{+} mice (**column 2**), or BAC^{I9+} mice was amplified. Average copy number calculated from triplicate measurements. Total copies of the *ATCAY* transgene on the y-axis.

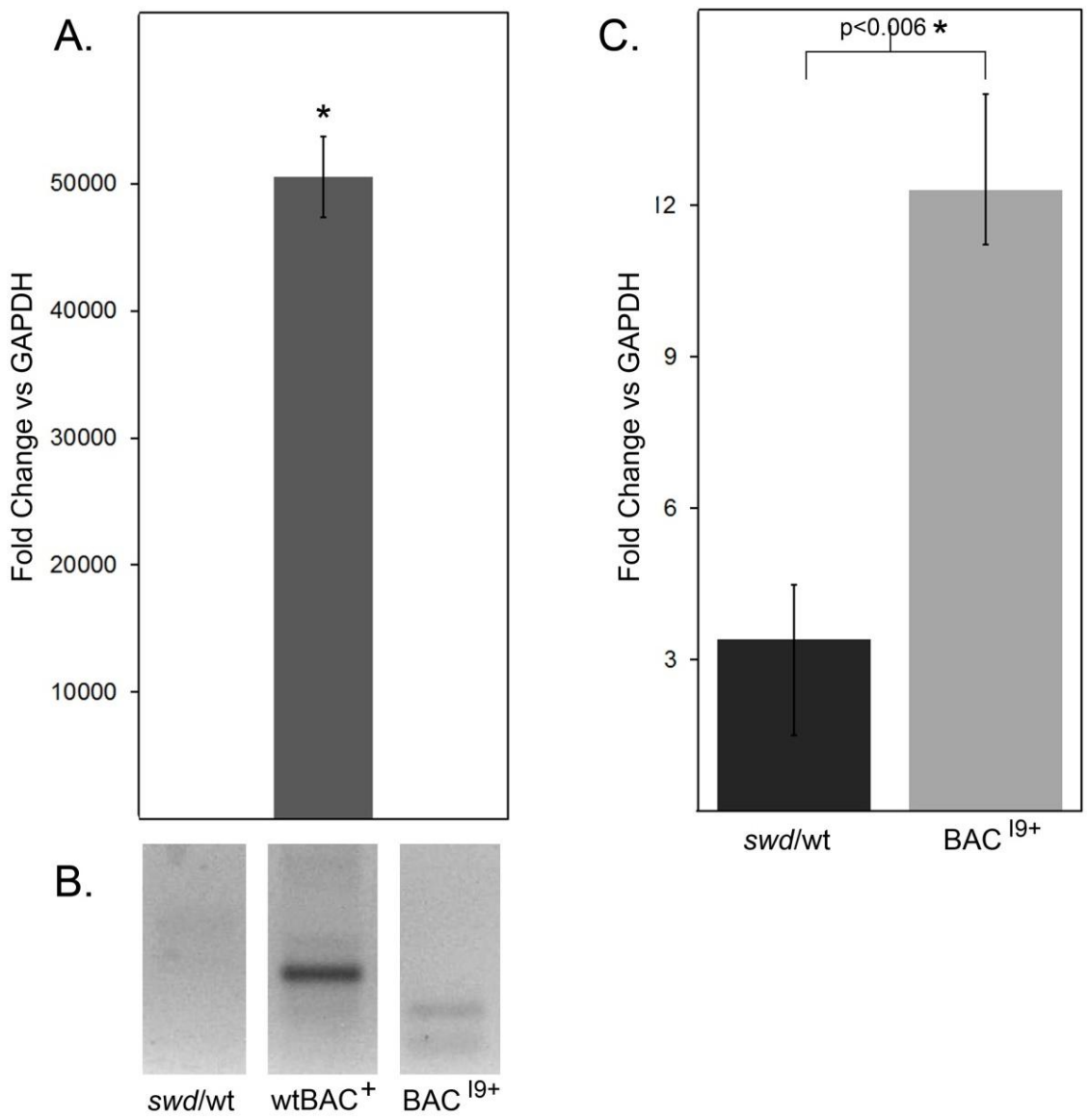

Figure 3.12. qRT-PCR for 3' region of *ATCAY* in transgenic line BAC^{I9}.
(A) qRT-PCR to quantify levels of *ATCAY* transcript containing exon 10 (3' end) from brain in control non-transgenic wild type *sidewinder* mice (**column 1**), wtBAC^{+} (**column 2**), and wtBAC^{I9+} (**column 3**). **(B)** Resulting PCR amplicon visualized on a single agarose gel (lower panels). **(C)** Results from (A) re-plotted with smaller y-axis values for comparison between non-transgenic controls (**column 1**) and wtBAC^{I9+} (**column 2**). Fold change vs. GAPDH averaged for biological triplicates are plotted with error bars representing ± SEM.

Discussion

Mutations in the *Atcay*/*ATCAY* gene have been shown to cause varying levels of motor and cognitive defects in a number of rodent models, as well as in individuals with Cayman ataxia [18, 27, 32]. In Chapter II, we correlate mouse *Atcay* mutations with protein expression, however the two human *ATCAY* mutations have not been characterized and their effect on protein expression is unknown. Utilizing a BAC complementation assay, the study described here determined that the intron 9 mutation results in C-terminal truncation of Caytaxin. Surprisingly, we also found that this mutation is not sufficient to disrupt Caytaxin function, indicating that both Cayman ataxia *ATCAY* mutations may be required to fully recapitulate the human disease.

While we were successful in creating a transgenic mouse to represent the intron 9 variant in human *ATCAY*, technical difficulties in retaining and expressing a complete transgene prevented the generation of the exon variant or double mutant. Introducing mutations into the *ATCAY* gene involved extensive manipulation of the BAC constructs, which are already prone to degradation, rearrangement, and fragmentation [83, 91, 92]. When transgenes are microinjected into pronuclei, they integrate randomly into the genome. As a result, each founder may differ in transgene integration site, number of transgene copies [83], and transmission efficiency [93]. The integration of multiple gene copies is not uncommon in transgenic BACs as previous groups have found between 5-1,000 copies integrated into a single chromosomal site [78]. This can

result in gene silencing due to methylation caused by multiple transgenes inserted as head-to-tail concatemers [94]. Additionally, the chromosomal environment at the transgene integration site can have a significant impact on transgene expression [95]. Expression can be silenced if integration occurs in or if large sequences are recognized as foreign and targeted for transcriptional inactivation [96]. Conversely, inclusion of heterologous introns or insulator sequences can enhance expression.

Initial analysis of gene expression utilized Western blots to examine protein products from transgenic mice, and detected three isoforms with a pattern similar to human Caytaxin (Fig 3.4), but at a lower molecular weight than observed in controls; consistent with a protein truncation corresponding to a loss of exons 10-13 in *ATCAY* mRNA. Additionally, Caytaxin was expressed from BAC^{I9+} at lower levels than endogenous mouse Caytaxin (Fig 3.4, lane 1), which may be attributed to either transgene integration site effects or nonsense mediated decay (NMD). qRT-PCR specific to the 3' region of human *ATCAY* mRNA did not detect *ATCAY* expression in BAC^{I9+} mice (Fig 3.12). Consistent with this, wild type Caytaxin could not be detected by Western blot in these mice upon blot over-exposure (Fig 3.4). This suggests that the phenotype rescue observed in the BAC^{I9+}A mice is indeed due to the low-level expression of the truncated form of Caytaxin, and not from undetectable low levels of full-length protein. Upon quantification of gene expression and copy number of BAC^{I9+}, it was found that gene and protein expression levels do not correlate with number of BAC^{I9} copies which had integrated (Figs 3.4, 3.10 & 3.11). The $wtBAC^{+}$ transgene was

expressed at levels 16,000-fold over BAC^{I9+}, but only harbors 9 more copies of the BAC. While this may explain potential differences in protein expression between the two transgenic lines, these data do not provide insight into level of transgene expression per BAC copy.

We observed no correlation between DNA in terms of integrated copies, mRNA levels and protein levels. While there are 3 and 9 copies of the BAC, it is unknown how many of them are complete, hence there may be no difference (1, 2 or 3 copies active in both strains) or up to a 9 fold difference. We observed a 16,000 fold difference in mRNA level. In addition to some effect that may be due to BAC copy numbers, mRNA levels are likely influenced by the site of integration and, in this case, mRNA may be degraded due to nonsense-mediated decay. Compared to that mRNA difference, the reduction in protein level is less drastic at approximately 2-10 fold (see Fig 3.4) compared to wild type. This may be due to protein stability (see Chapter II), and possibly selection of cells that express more protein. Hence, before making final conclusions, it will be necessary to investigate more than one line with a BAC with this mutation.

In assessing severity of ataxia and quantifying disease phenotype in BAC^{I9} transgenic mice, a panel of phenotype tests was designed. The wire hang test, the rotarod test, and the scent recognition test were chosen to broadly represent the major symptoms display by patients with Cayman ataxia, namely mental retardation and motor control deficits [15]. A number of potential confounding factors were taken into account during the experimental design, such as age,

weight, and sex, which can affect testing performance. Specifically, in some tests, females tend to perform better than males, and with increasing age and weight, movement becomes restricted [89]. For these reasons, when possible, mice chosen for phenotype testing were between 3-5 months of age, and were either primarily female or an equal mixture of both male and female when appropriate. Importantly, test groups consisted of mice of the same line, when possible, to maintain similar background strain and BAC expression levels.

Specific confounding factors within each test were also taken into account. Performance in the scent recognition test depends on a mouse's natural social instincts [97], however wide variation exists within transgenic and non-transgenic wild type mouse lines [85, 98, 99]. Additionally, the initial inter-exposure time of 60 minutes was chosen based on conventional protocols [100], but additional inter-exposure time of 5 days was utilized to test long term memory retention. As mice have been demonstrated to retain scent memory for up to one week [89], a 5 day separation period would be within memory limitations but long enough to reveal long-term memory defects. Since the same juvenile males need to be used for subsequent reintroductions, inter-exposure times longer than one week would begin to push the line between juvenile to adult. The existence of potential subtle defects was also considered, and is evidenced by the wire hang test, where extending the allowed hang time beyond 60 seconds revealed that *swd*/wt BAC^{l9+} and *swd*/wt $wtBAC^{+}$ generally performed better than the non-transgenic *swd*/wt mice. Evaluating average hang times with a 60sec cut-off, as is common in the literature, minimizes this difference in performance between lines

(Appendix VII). This disparity could be caused by a number of confounding factors such as differences in grip strength, susceptibility to muscle fatigue, or motivation (apathy) [84, 87].

A variety of additional tests could complement the battery described above to further examine subtle differences between BAC^{I9+} rescue and wild type BAC^{I9} littermates, especially since our data demonstrate that BAC^{I9+} mice perform similarly to wild type mice in all but one test. Apathy is often displayed by individuals with mental retardation or other cognitive defects [101], and can be examined via the forced swim test [102], open field test [66], or the sucrose consumption test [102]. To test muscle strength, mice could undergo a grip test using a dynamometer [103], or the more invasive test for physical muscle fiber strength [104].

Ultimately, these tests provide the first investigation into the human *ATCAY* mutations and indicate that despite the intron 9 mutation, Caytaxin retains partial function, as evidenced in functional complementation of the BAC^{I9} *ATCAY* mice. This mouse line represents the only model carrying a defect in the 3' region of the gene. As described in Chapter I, mutations in rodent *Atcay* have all been found between exons 1-5 (Figure 1.1 & Table 2.1), out of the total 13 exon gene. Since a more subtle defect may be present in the human disease, this model represents an important system for investigation of Caytaxin function.

Though we were unsuccessful in generating a complete set of mutant *ATCAY* transgenic mice to more definitively answer the question as to which mutation is the most likely cause of human Cayman ataxia, analysis of the intron 9 *ATCAY* mutation provides insight into Caytaxin expression and function.

First, we demonstrate that the intron 9 mutation causes a defect in normal mRNA splicing and results in a truncation of Caytaxin protein. No full length *ATCAY* cDNA was detected in BAC^{I9+} mice (Fig 3.4 lane 3), and only smaller molecular weight forms of Caytaxin could be detected by Western blot (Fig 3.4, lane 3), indicating complete suppression of normal splicing by the intron mutation. Second, results from phenotype assessment indicate that the expression of the mutant form of Caytaxin, even at somewhat lower levels, is sufficient to rescue the ataxic phenotype of *swd*/*swd* mice. From these two observations, we can conclude that a truncated form of Caytaxin, missing the C-terminal region after the BCH domain, is functional, and hence the last 10 amino acids of Caytaxin are dispensable for the functions we could observe.

Acknowledgements

ATCAY BAC constructs were generated via mutagenesis by the UC Davis Mouse Biology Program. BACs were purified and injected by the University of Michigan Transgenic Animal Core. Rotarod testing was performed by Steven Whitesall, University of Michigan Physiology and Phenotyping Core.

Materials and methods

Mice – Described in Chapter II, Materials and Methods.

Transgenic founder assay – All transgenic founder mice from each injection were screened for the presence of the *ATCAY* transgene using methods described by the University of Michigan Transgenic Animal Core (http://www.med.umich.edu/tamc/spike.html). Copy standards were prepared by mixing wild type mouse genomic DNA with concentrations of transgene DNA corresponding to 1, 3, or 1/3 copies. These values were calculated with the assumption that the transgene DNA would be spiked into 2µg of wild type genomic DNA, that the haploid content of the mammalian genome is $3x10^9$bp, and that the transgenic founder mice are hemizygous for the transgene. Upon confirmation of assay efficiency, founders were screened using PCR to detect *ATCAY* exons 2, 6, and 9. PCR conditions were optimized for each primer pair (synthesized by Integrated DNA Technologies, Inc., Coralville, IA):

ATCAY Exon 2: 5'-catggggtagacgattgtcatt-3', 5'-acagagaagactcgcacacagg-3'

Buffer 2, ELT PCR System (Roche, Cat. No. 11681834001)

ATCAY Exon 6: 5'-aggactctgacgttgccgat-3', 5'-tagggccacaatgcaatcctt-3'

Buffer 3, ELT PCR System (Roche, Cat. No. 11681834001)

ATCAY Exon 9: 5'-gaggtgtcgtcgtctgcact-3', 5'-actaatacggcggggtgga-3'

Buffer 2, ELT PCR System (Roche, Cat. No. 11681834001)

Annealing temperature of 61^oC for all reactions.

Genotyping – Described in Chapter II, Materials and methods.

Antibodies – Production of anti-Caytaxin monoclonal antibodies is described in Chapter II, Materials and methods. Antibodies were used at a 1:500 dilution. Peroxidase-conjugated AffiniPure Goat anti-mouse IgG antibodies were used per manufacturers' protocol (Jackson ImmunoResearch Laboratories, Inc. Cat. No. 115035062).

Tissue lysate preparation – Described in Chapter II, Materials and methods.

SDS-PAGE - Described in Chapter II, Materials and methods.

Immunoblotting – Described in Chapter II, Materials and methods, with the some changes. Membranes were incubated in blocking buffer (5% wt/vol non-fat dry milk powder in TBST) with gentle agitation for at least 2 hours at room temperature. Primary antibodies were diluted in blocking buffer and incubated for at least 2 hours at room temperature. Proteins were detected via ECL (Fisher Scientific/Pierce, Cat. No. PI32106) on autoradiography blue film (Fisher Scientific, Cat. No. AF5700).

Rotarod – Animals were required to perch on a stationary rod for approximately 30-60 seconds to accustom themselves to the environment. The animals that were comfortable staying on the rod were allowed to run with a constant speed of 5 rpm for approximately 60 seconds. Animals that fell after three trials with

constant low speed rotation (2 rpm) were removed from the experiment. When test animals were able to stay on the rod for approximately 30 seconds they were allowed to return to their home cage. Animals were trained again after at least 2 hours of rest or the following day. During the third training session, the rod was allowed to accelerate until the animal fell. Those mice that passed initial testing requirements underwent testing with 3 trials per day over 3 days, for a total of 9 runs. 7 *swd*/wt wtBAC^{-}, 10 *swd*/wt BAC^{I9-}, and 10 *swd*/*swd* BAC^{I9+} mice were tested, ages 3-5 months with mixed gender, and time on the rod for each test animal was recorded.

Wire hang test – Each mouse was placed on a rubber silicone-coated wire platform, which was gently shaken three times to encourage the mouse to grip the wire. The platform was then slowly rotated 180^{o} until the mouse was suspended up-side-down approximately 30cm above an empty cage floor. The time it took each mouse to fall from the platform to the cage floor below was recorded, with the start of timing from the start of platform rotation. A major adaptation to the common protocol [105] involved allowing mice still gripping the cage top after 60 seconds to remain suspended on the platform. The aim of this was to tease out potentially slight differences in performance between each group of mice by gauging total potential. Test was performed with biological and experimental triplicates.

Scent recognition test – The scent recognition test was performed according to protocol [106] with some adaptions. Briefly, 10 adult (3-5mo) females for each

test group (*swd*/*swd* wtBAC^{+} or BAC^{I9+}) were introduced to a juvenile (P18-21) male (stimulus). On the first day, each female was placed in a clean holding cage with food and allowed to acclimate for 30 minutes. Stimulus was placed in each cage along the wall furthest from the test subject, and total interaction time was recorded over 4 minutes. After an inter-exposure time of 60 minutes, stimulus was reintroduced to each test subject for 4 minutes and total interaction time was recorded. Mice were returned to their home cages, and testing was repeated after a 5 Day inter-exposure time, beginning with the 30 minute acclimation. Testing was performed with two different juvenile male stimuli, and total interaction time was averaged for all trials.

Rapid amplification of cDNA ends (RACE) – Fragments representing the 3' end of *ATCAY* cDNA were amplified and analyzed using the Life Technologies' 3' RACE System according to their protocol (Life Technologies, Cat. No. 18373-019). In summary, cDNA was generated from 1µg total RNA and primed using the AP to introduce a specific sequence downstream of the polyA tail, which was utilized as a priming site by the AUAP in subsequent PCR reactions.

Adapter Primer (AP): 5'-ggccacgcgtcgactagtacttttttttttttttt-3'

Abridged Universal Amplification Primer (AUAP): 5'-ggccacgcgtcgactagtac-3'

RT-PCR – Whole mouse brains were extracted and either stored or processed immediately for total RNA using TRIzol® according to their protocols (Life Technologies, Cat. No. 15596). Briefly, 50-100mg of brain tissue was macerated with a scalpel and vortexed in 1ml of TRIzol®. Samples were either flash frozen

in liquid nitrogen and stored at -80^{o}C or processed for total RNA extraction with the addition of chloroform. RNA was precipitated using isopropanol, washed with 75% ethanol, and rehydrated in 100µL of RNase-free H_2O. RNA concentrations were measured using spectrophotometric analysis and flash frozen in liquid nitrogen for storage at -80^{o}C or immediately processed for cDNA production. cDNA was synthesized using the SuperScript™II Reverse Transcriptase kit according to their protocols (Life Technologies, Cat. No. 18064022). 1ng of total RNA was included in the 20µL reaction, which was primed using Oligo(dT)$_{12\text{-}18}$. RNaseOUT™ was not included in the reaction. 2 units of RNaseH were added to synthesized cDNA to remove unprocessed RNA according to their protocols (Life Technologies, Cat. No. 18021-071). Short term storage for the cDNA was at +4^{o}C, and -20^{o}C for long term storage.

cDNA PCR – 2µL cDNA was used from the first-strand RT-PCR reaction (RT-PCR, described above) in a 50µL total reaction volume, which also included: 10uM each primer (sequences below, synthesized by Integrated DNA Technologies, Inc., Coralville, IA), 50mM $MgCl_2$ in 10X PCR buffer (Life Technologies, Cat. No. 18067-017), 10mM dNTP mix (Life Technologies, Cat. No. 10297-018), and *Taq* polymerase (from Dr. David Burke, Department of Human Genetics, University of Michigan). Reactions performed as described by the SuperScript™II Reverse Transcriptase kit (Life Technologies, Cat. No. 18064022).

Exons 2-5: 5’-aaggaggaatggcaggacgaaga-3’,

5’-aaggccggatcatgtgcaggtct-3’

Exons 5-8: 5’-gccaccgccaagaacatgcc-3’,

5’-agggcgagagatggccagca-3’

Exons 8-12: 5’-gaagtccttgatcatcgtccaccc-3’,

5’-agaccagagcagacctgttttcca-3’

Exon 9 fwd: 5'-gccctttcatcagcgtcaagttc-3'

Intron 9 rev: 5’-aattgccctgtctcaggtgtgtct-3’

Quantitative RT-PCR – Quantitative real-time PCR assay to measure *ATCAY* mRNA expression utilized the SYBR® Green detection system in the Bio-Rad iQ™SYBR® Green supermix according to their protocol (Bio-Rad, Cat. No. 170-8882). Briefly, regions from synthesized cDNA (described above) were amplified in a 20µl reaction containing iQ™ SYBR® Green supermix, 250nM of each primer (below, synthesized by Integrated DNA Technologies, Inc., Coralville, IA), and cDNA diluted 1:100 from original RT-PCR reaction (above). Reactions were performed using the MyiQ™ single-wavelength thermal Cycler (Bio-Rad Laboratories, Inc., Hercules, CA). The typical 3-step real-time PCR program was used and included a melt curve from 55^{o}C-95^{o}C in 0.5^{o}C increments to evaluate the quality of real-time PCR product. All experiments included biological and experimental triplicates for each primer pair.

E8-I9 (splice form) 5’-gaagtccttgatcatcgtccaccc-3’,

5’-aattgccctgtctcaggtgtgtct-3’

Exons 2-4 5’-aaggaggaatggcaggacgaagat-3’,

5’-atttagcgtgttgggaggagagga-3’

Exons 10-12 5’-agaggaaagactgaaggccagga-3’,

5’-tctgagaccagagcagacctgttt-3’

Transgene copy number assay – Described in Chapter II, Materials and methods.

Graphs and statistics – All graphs were created using Microsoft Excel and p-values were calculated using students t-test. Error bars were calculated based on standard deviation from the mean (SEM) of the corresponding mouse line. Analysis of qRT-PCR data for relative expression was determined using a $\Delta\Delta C_T$ method with GAPDH as the reference gene [56]. Average ΔC_T for each sample were calculated to include each biological and experimental triplicate, which were plotted for fold-change analysis.

In silico **analyses** – All sequences were obtained from the NCBI database:

mRNA: Human (*ATCAY*): NM_033064.4; Mouse (*Atcay*): NM_178662.3

Protein: Human Caytaxin: NP_149053.1; Mouse Caytaxin: NP_848777.1

Clone CTB-171N13: AC011477.7

PCR and qRT-PCR primers were designed using Integrated DNA Technologies’ PrimerQuest^{TM} online tool [56]. Nucleotide to amino acid sequence translation was performed using the SIB Swiss Institute of Bioinformatics’ “Translate” online tool (http://web.expasy.org/translate/) [38, 40, 45, 46, 52, 53, 107]. Protein molecular weights were calculated based on sequence using the SIB Swiss Institute of Bioinformatics’ “Compute pI/Mw” online tool (http://web.expasy.org/compute_pi/) [68].

Chapter IV.

Atcay/ATCAY mutations and implications for Caytaxin protein function – Conclusions and future directions

Summary

Within the past 70 years, mutations in the gene encoding Caytaxin have been identified in both rodents and humans [15, 18, 26, 31, 36]. These mutations are consistently associated with severe defects in motor coordination and cerebellar function, classified as ataxia or dystonia [5, 9, 11]. This suggests that Caytaxin is critical for normal nervous system function, however the exact functional mechanism remains poorly understood.

Thus far, characterization of the *Atcay/ATCAY* gene and its encoded protein Caytaxin has utilized immortalized neuronal cell lines and *in vitro* systems [38, 40, 44, 46, 52], as well as a single study in the dystonic rat (*dystonic*) [53]. Information gathered from biochemical methods are based on protein binding assays using recombinant Caytaxin protein or purified protein extracts, which often fail to account for all components of large protein complexes and co-factors. Antibodies and constructs which were designed to detect and represent the Caytaxin protein in these systems did not consider the potential importance of the complete coding region and full-length protein. To date, there has been no

thorough characterization of endogenous Caytaxin expression within mouse models that naturally express mutant forms of Caytaxin due to mutations in *Atcay*. Observation of *Atcay* mutant mice led us to hypothesize that establishing a direct link between genotype and phenotype is necessary to determine how the protein functions within the brain. To address this hypothesis, we sought to establish reliable mouse models in which to study Caytaxin protein and the ataxic phenotype generated by abrogated Caytaxin function.

In the previous chapters, we described the generation and use of novel monoclonal anti-Caytaxin antibodies and find that Caytaxin is consistently expressed as three isoforms (Chapter II). Previous reports alluded to the presence of one or two bands on Western blots, which have been mistakenly attributed to post-translational modifications and alternative splicing without further investigation [67, 69]. Our study is not only the first to identify the production of three isoform, but we also find that they all originate from a single *Atcay*/*ATCAY* mRNA transcript, with the two larger isoforms translated from two different start methionines (discussed in Chapter II and below). Transgenic mice were generated which are null for mouse Caytaxin but instead over-express human Caytaxin, demonstrating conservation of function between human and mouse Caytaxin. Additionally, investigation into the effect of the two Cayman ataxia *ATCAY* mutations on Caytaxin expression and function suggest that the intron 9 mutation is not sufficient to completely abrogate Caytaxin function, despite a C-terminal truncation.

There are many open questions remaining. From out work, the following questions remain to be addressed:

1. What is the physiological significance of the multiple Caytaxin isoforms?
2. Are both human *ATCAY* mutations required to abrogate Caytaxin function?
3. What role does Caytaxin play in synaptic transmission?

Exploring the significance of the multiple Caytaxin isoforms

As a neuronal protein, the potential multi-functionality of Caytaxin imparted by its multiple isoforms would prove to be a unique characteristic. Currently, it's unknown if all three protein isoforms harbor functionality or if they are simply a byproduct of protein regulation. Identification of the origin for the smallest Caytaxin isoform will allow a thorough and accurate assessment of how these isoforms contribute to Caytaxin function.

As described in Chapter II, additional efforts are under way to identify the source of the third Caytaxin isoform through purification and subsequent amino-terminal sequencing (Appendix XI). Once the sequence around the origin of the third isoform is obtained, comparison with published amino acid sequences can be performed to elucidate whether the protein is produced from an alternative translation start site or by protease cleavage. Subsequent experiments can then be performed to determine which isoforms are required for Caytaxin function and localization.

Upon complete identification of the origin of all three Caytaxin isoforms, experiments aimed at examining Caytaxin binding partners could determine whether binding is restricted to certain isoforms or if it involves all three. Similar to the methionine point mutations described in Chapter II, three different constructs can be created to individually represent each protein isoform. Caytaxin translated in cell culture or *in vitro* could then be examined in binding assays with key interaction factors such as KGA and KLC to assess binding capabilities. Additionally, utilizing expression vectors harboring a GFP tag would enable investigation into the cellular localization of each isoform. Preliminary Western blot experiments in rat synaptosomes did not indicate differential localization of the three isoforms (data not shown), suggesting that all isoforms may have the same function.

Further analysis of whether both human *ATCAY* mutations are required to abrogate Caytaxin function

Genetic analyses of *ATCAY* mutations in patients with Cayman ataxia find that patients are homozygous for two variants in *ATCAY*, a rare occurrence. Neither of these variants have been identified in population samples (data not shown), suggesting that both mutations are associated with the disease. However, since most mutation analysis to date has been performed in Caucasians, mutation occurrence may be in part a reflection of the enormous diversity of the African gene pool. Determining the etiology of the disease with respect to required mutations will not only aid in elucidating the overall mechanism of Caytaxin, but would provide insight into this unique disease. Due to limitations in BAC

transfection and transgene expression *in vitro* or in cell lines, transgenic mice were instead generated. Due to the sequence variability between human and mice surrounding each variant, techniques involving BAC recombineering were utilized. The mutated transgene was built using homologous recombination to insert regions containing either mutation or both mutations.

While we were unsuccessful in generating mouse lines with the exon variant and the double mutation, information gathered from a single transgenic line carrying the intron 9 variant proved to be informative. Our analysis of the BAC^{I9} transgenic mouse demonstrates that this *ATCAY* mutation completely prevents normal splicing, may cause reduced protein expression, and leads to a C-terminal truncation of Caytaxin. Additionally, most protein function is preserved. Based on known interactions and conserved Caytaxin protein domains, the removal of 39 amino acids from the C-terminal end of the protein results in an elimination of downstream binding sites for both KGA and Pin1, but retains the interaction regions for CHIP, KLC, and caspase-3, and the nuclear export signal (Fig 1.1F). Maintenance of these regions may explain the lack of apparent phenotypic deficit in mice expressing this mutant protein. Not only can these mice successfully breed, but there is no decrease in life span, and no development of ataxic symptoms with advanced age (data not shown).

As it remains unknown whether the exon mutation also affects Caytaxin expression, we cannot dismiss the following possibilities:

First, the splice mutation may actually cause Cayman ataxia due to truncation of Caytaxin, but the disease phenotype manifests differently in mice and is not as apparent as that seen in individuals with Cayman ataxia. Alternatively, the ataxic phenotype may be masked in mice due to variation in Caytaxin levels. We detect that the BAC^{I9} mice harbor multiple copies of the transgene but express mutant Caytaxin at similar levels as endogenous mouse Caytaxin (Chapter III). This may be due to nonsense-mediated mRNA decay (NMD), which is the predominant consequence of nonsense mutations [108-110]. The variation in NMD efficiency between cells allows for low levels of protein translation from mutant transcripts that escape degradation [111-114]. In the BAC^{I9} mouse brain, enough truncated transcript may escape NMD to produce a truncated Caytaxin protein that significantly rescues the ataxic phenotype. Alternatively, the missing C-terminal region of Caytaxin may contain a modification site critical for optimal protein stability [115]. Disruptions of regions which could affect protein modifications or folding may result in the activation of a protective cellular mechanism, leading to the elimination or reduction of Caytaxin protein levels.

Second, rather than the intron 9 variant, the amino acid variant may be responsible for causing the disease. While it's unlikely that a protein truncation has less of an effect on function than a single amino acid conversion, alterations in peptide sequence may affect protein folding or more complex protein dynamics. Third, it's possible that both mutations are required to cause a significant defect in Caytaxin function. Despite the rarity of two different mutations in the same gene necessary to cause a phenotype, the combination of

a protein truncation and a change in peptide charge within the exon 9 region of Caytaxin may act synergistically to affect protein stability. While valuable insight into characteristics of the disease protein could be provided by examining Caytaxin from Cayman ataxia brain tissue, formalin-fixation of existing samples prevents further protein analysis.

In considering how the human *ATCAY* mutations could affect the properties of the conserved BCH domain and the folding of Caytaxin, *in silico* protein fold prediction analysis was performed (Appendix XIV). The most significant changes to high order protein folding appear to result from the intron 9 mutation (Appendix XIV, A right panel), causing the region encoded by exons 10-13 to be labile and extended. However truncation of this region eliminates the unfolded domain and the new C-terminal region is instead predicted to become highly folded. The exon 9 mutation is not predicted to have a significant effect on protein folding dynamics, even with the introduction of a charged residue (Appendix XIV, A bottom left panel). Narrowing the region to focus on the BCH domain, which is only partially truncated by the intron 9 mutation, reveals a considerable change in charge and hydrophobicity (Appendix XIV, B). The 3' end of the BCH domain, which is predicted to normally undergo a low level of folding with a slight increase in charge, is instead predicted to remain highly folded with little to no charge (Appendix XIV, B bottom panel).

In order to more accurately examine the potential contributions of each mutation on protein function, transgenic mouse lines should be re-created with specific

techniques to achieve a single-copy insertion of the transgene in a targeted region of the genome and more than one line analyzed to account for the effect of different integration sites – 3 lines is standard protocol [83]. In addition, to eliminate potential strain and integration site variation, mutations in *ATCAY* should instead be introduced into the germline of the strain (C57Bl/6) on which the *sidewinder* mutation is maintained, thus becoming a “knock-in”. Additional techniques and how they will overcome potential technical issues will be discussed below.

While transgenic animals have proven effective in the identification of new genes through the complementation and transgene rescue of mutant phenotypes [116], the task of generating a transgenic mouse is not without its difficulties. A major limitation to BAC transgenesis is their extreme sensitivity to pre-injection manipulation, such as those involved in creating point mutations or deletions as required for our studies. It is common for mistakes to occur during construction [117], as evidenced in our transgenic lines where *ATCAY* exon 9 was replaced by plasmid sequence and where *ATCAY* exon 10 was duplicated (Chapter II). The variability of transgenesis efficiency, integration, and expression was discussed in Chapter III, however another potentially confounding factor is choice of mouse strain used for transgenesis. The hybrid mouse strain B6SJLF1/J is the preferred mouse line for creating transgenics at the University of Michigan since the females consistently generate large numbers of injectable embryos, and fewer mice are needed for each microinjection [118]. Since this mouse contains genetic material from both C57BL/6 and SJL mice, transgenic founders contain

variation in their genetic identity due to meiotic recombination [83]. While use of the mixed-background mouse strain generates large numbers of transgenic founders, the variation in genetic background of engineered mice appeared to have an effect on their phenotype.

Methods utilizing targeted transgenesis can be employed to re-create the desired transgenic lines while addressing the issues described above. However, these protocols are newly-established and are expensive. In targeted transgenesis, a single transgene can be inserted into the genome via homologous recombination into a specific locus (such as the Rosa26 locus on mouse chromosome 6), thus eliminating the risk of interrupting important genetic regions [119]. Beginning with the generation of a single-copy full-length ATCAY transgene, techniques utilizing Zinc Finger Nucleases (ZFNs) can be employed to create each Cayman ataxia mutation from within this line. This is achieved via co-transfection of ZFN and a template containing the desired mutation into embryos from the full-length *ATCAY* transgenic females. With these new techniques, transgenesis protocols can now be designed to prevent issues of BAC instability, multiple transgene copies, random integration sites, and inconsistent strain backgrounds.

Examining the role for Caytaxin in synaptic transmission

Through a collaborative effort with Drs. Vikram Shakkottai and Katiuska Molina-Luna (Department of Neurology, University of Michigan), electrophysiology assays of *hesitant* and *sidewinder* cerebellar signaling have identified

quantifiable differences between mutant (*swd*/*swd* or *hes*/*hes*) and wild type (wt/wt) mice. Preliminary experiments have been performed by Drs. Shakkottai and Molina-Luna examining cerebellar signaling in the *hesitant* and *sidewinder* mouse lines (Appendix XII). Analysis of the *sidewinder* mouse demonstrated a defect in the spontaneous firing of their Purkinje neurons as well as relative insensitivity to application of electrical current. Interestingly, the *swd*/*swd* firing defect is identical to that observed in FGF14-/- mice who display decreased expression in sodium channel, voltage gated, type VIII, alpha subunit (Scn8A or Nav1.6) [120]. Additionally, preliminary immunohistochemical staining in wild type and *swd*/*swd* cerebellar slices for NaV1.1 and NaV1.6 reveals a decrease in expression within Purkinje cells and the granule cell layer (Appendix XIII, A & B).

Preliminary results from Western blotting for total NaV1.6 in cerebellar membrane preparations which sought to confirm the IHC findings indicate no difference in expression in *hes/hes* or *swd/swd* mice versus wild type littermates (Appendix XIII, C). While it is unknown whether the signaling defect in these mice involves sodium channel expression, these data suggest a requirement for Caytaxin in neuronal signaling. It is possible that in the absence of Caytaxin, signaling from granule cells to Purkinje cells is absent or decreased, and inhibitory signals from the Purkinje cells cannot be relayed onto the deep cerebellar nuclei. This could result in hyper-excitability which can manifest as ataxia or dystonia [6].

Based on phenotypic and biochemical data presented in previous chapters,

Atcay mutant and transgenic mice may aid in elucidating in which signaling pathways Caytaxin participates. Brain extracts and primary cerebellar cultures from *Atcay* mutant mouse lines could be used in binding and cleavage assays as well as in immunofluorescence for protein localization. Caytaxin cellular localization is mediated by the nuclear export signal and by KLC, which transports Caytaxin toward neurites [45, 46]. Investigation of cellular localization of mutant proteins lacking these conserved regions would provide insight into how Caytaxin localization contributes to its function. This would require construction of a representative GFP-tagged cDNA construct with subsequent transfection into and induced differentiation of a neuronal cell culture system. Since the interaction sites for KLC and CHIP are eliminated together, accumulation within the cytosol may occur due to a lack of protein degradation. Combining binding assays with additional staining of co-localizing factors such as mitochondria would also provide information regarding its ability to maintain function at the synapse. Since Pin1 and caspase are expected to play a larger role in cellular function [40, 46], consequences from elimination of these interaction sites can be determined based on an overall readout of cellular growth and survival. These interaction partners can be examined in the context of the whole organism where Caytaxin expression has been characterized. Narrowing the list of known neuronal interaction factors to those absolutely required for protein function may reveal the defective signaling pathway.

Conclusion

Such as in the case of Cayman ataxia, rare diseases are difficult human conditions to study. There is very little data that can be gathered from small populations, a feat made even more difficult in cases where the disease is being rapidly eradicated [15]. Inherited rare disorders can provide unique information regarding normal physiology if disease inheritance can be accurately mapped. Records for the prevalence of Cayman ataxia were transmitted via word-of-mouth or through cryptic public reports, which are subject to bias and personal interpretation. Even upon obtaining reliable historical documentation, no clinical trials or large scale studies can be organized that could generate a large enough dataset for a thorough study. Additionally, since the defect lies within the brain, obtaining fresh human Cayman ataxia tissue samples is nearly impossible, and can only be achieved post-mortem, which also poses a new set of problems regarding proper extraction, preparation, and storage. It is because of these issues that establishing and characterizing a non-human model for a rare disease is invaluable.

Disorders which only affect a small number of people are not only rare in their occurrence, but also rare in the amount of research devoted to their study. Diseases with a higher prevalence often garner the most attention; however, information gathered from rare disease research has proven informative regarding normal bodily processes. The studies described in this dissertation contribute towards the characterization of ataxic mouse models and introduce novel methods for studying a neuronal protein required for normal nervous system function. Together, this work demonstrates the importance of easily

overlooked details in developing reliable methods and models for studying human diseases, particularly for rare human conditions where recapitulation of disease symptoms requires a well-characterized non-human animal model.

This information is especially valuable when elucidating mechanisms within complex organs such as the brain. Advancing our understanding of this major organ and its intricate processes is met with difficulty due to its complex and fragile architecture. Opportunities which bring attention to previously unidentified neuronal mechanisms should be embraced, as they provide a window into the body – shining light on aspects of basic functions which are so poorly understood.

Appendices

Appendix I. Caytaxin protein isoforms are not due to phosphorylation.

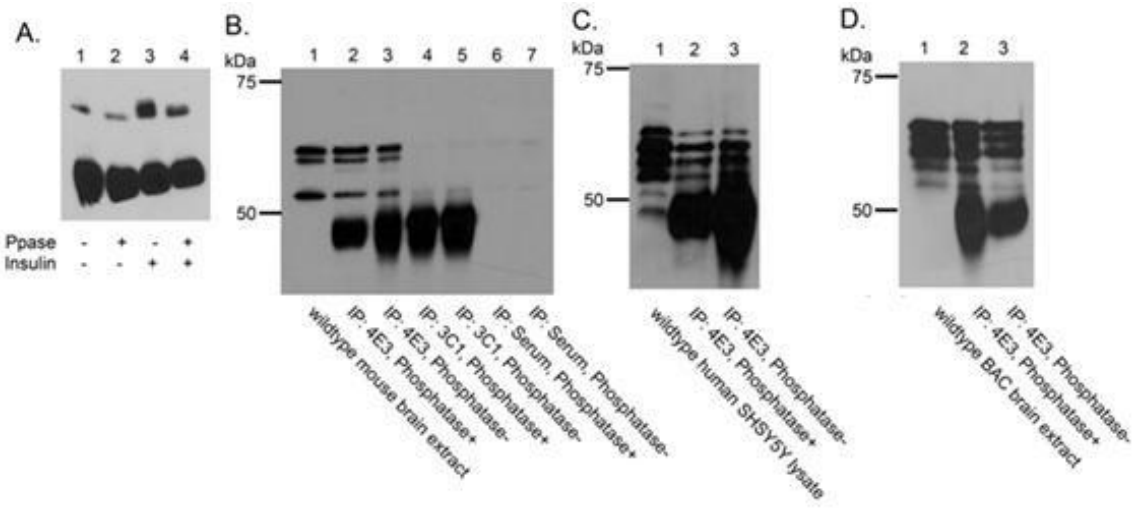

Appendix I. Caytaxin protein isoforms are not due to phosphorylation.
(A) Positive control HEK-293T cells untreated (**lane 1**) or phosphatase treated (**lane 2**). HEK-293T cells un-stimulated (**lane 3**) or insulin-stimulated before phosphatase treatment (**lane 4**). **(B)** Caytaxin from wild type mouse brain (**lane 1**) immunoprecipitated with anti-Caytaxin 4E3 (**lanes 2 & 3**), control *Drosophila* antibody 3C1 (**lanes 4 & 5**), or control serum (**lanes 6 & 7**, to detect cross-reactivity). 4E3 IP'ed Caytaxin treated with phosphatase (**lane 2**). Caytaxin from human SH-SY5Y cells **(C)** and wtBAC^{+} **(D)** IP'ed and phosphatase treated (**lane 1**). Western blot in (A) (generated by Hugo Acosta-Jaquez of Dr. Diane Fingar's Laboratory) probed with antiS6K, B-D probed with anti-Caytaxin mAb 8F4, all were developed with ECL. Methods described in Appendix XVIII.

Summary. Caytaxin protein was immunoprecipitated from brain lysates prepared from mice or SH-SY5Y cells, and phosphatase treated to eliminate bands which are caused by phosphorylation. All three protein isoforms remain, indicating that none of the larger isoforms are created by phosphorylation of a smaller species.

Appendix II. Smallest Caytaxin isoform is not translated from downstream non-ATG site.

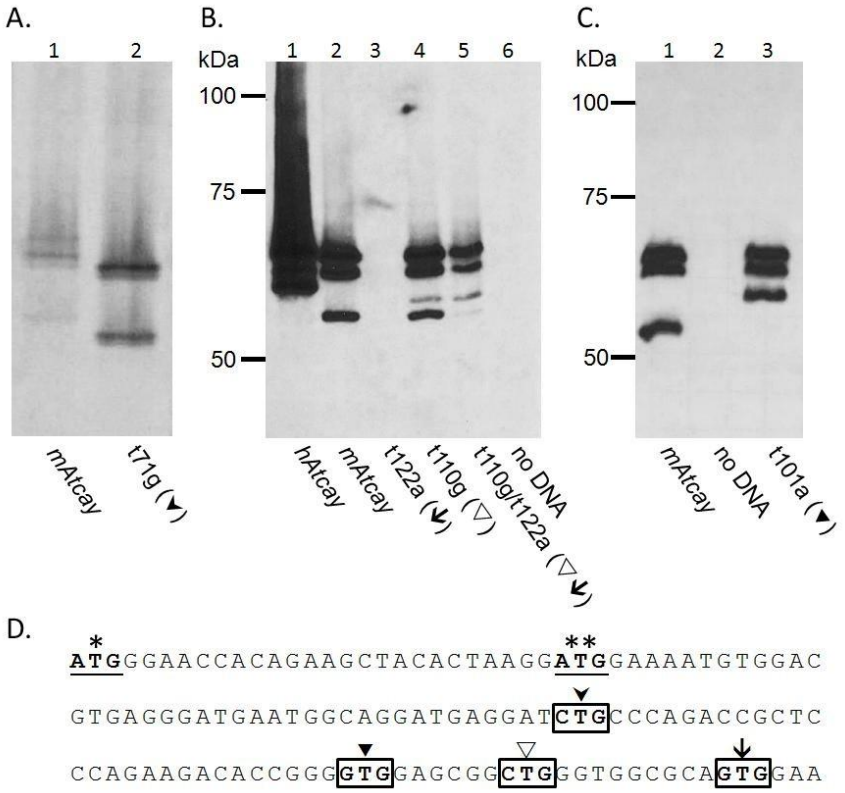

Appendix II. Smallest Caytaxin isoform is not translated from downstream non-ATG site.

Mouse *Atcay* non-ATG sites (CTG and GTG) were mutated via site-directed mutagenesis and translated *in vitro*. **(A)** Wild type *Atcay* (**lane 1**), CTG to CGG mutation (**lane 2**). **(B)** Human (**lane 1**) and mouse (**lane 2**) *Atcay*/*ATCAY*, GTG to GAG mutation (**lane 3**), CTG to CGG mutation (**lane 4**), double mutant combining previous mutants from lanes 3 and 4 (**lane 5**), and no DNA control (**lane 6**). **(C)** Mouse *Atcay* (**lane 1**), no DNA control (**lane 2**), and GTG to GAG mutation. **(D)** Met1 (*, bold & underlined) and Met10 (**, bold & underlined) are indicated. t71g (arrowhead), t101a (filled triangle), t110g (open triangle), and t122a (arrow). Mutagenesis in vitro translation protocols described in Chapter II. Mutagenesis primers are listed in Appendix XVIII.

Summary. Common non-methionine start sites were identified downstream of the second conserved ATG as potential translation origins based on high Kozak sequence consensus. Despite elimination of these sites, the smallest isoform remained, however at different molecular weights. Thus it cannot be concluded whether or not the third isoform is translated from a non-methionine start site.

Appendix III. Non-specific protease degradation does not explain the production of multiple Caytaxin isoforms.

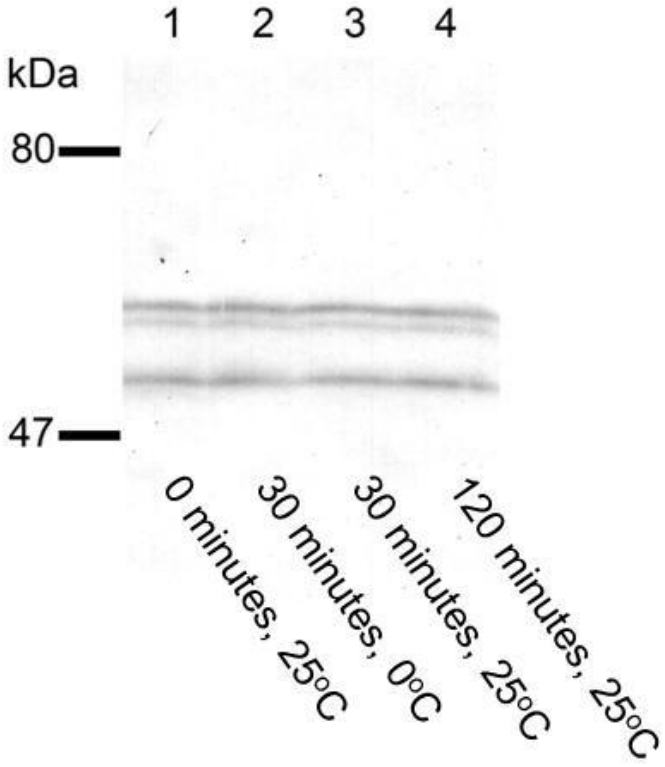

Appendix III. Non-specific protease degradation does not explain the production of multiple Caytaxin isoforms.

Four wild type mouse brains were extracted and treated as follows: immediately homogenized at 25^{o}C (**lane 1**), left on ice for 30 minutes before homogenization (**lane 2**), left at 25^{o}C for 30 minutes before homogenization (**lane 3**), or left for 120 minutes at 25^{o}C before homogenization (**lane 4)**. 30µg homogenate was loaded on gel for Western blot analysis with anti-Caytaxin mAb 8F4, developed with DAB. Figure generated by Michael Tysor of Dr. Michael Hortsch's Laboratory, Department of Cell and Developmental Biology, University of Michigan.

Summary. Whole brains from wild type mice were allowed to undergo varying degrees of degradation to determine whether protease activity affects the production of the Caytaxin isoforms. It was determined that all isoforms are stable and are not affected by non-specific protease degradation.

Appendix IV. All three Caytaxin isoforms originate from the N-terminus of the protein.

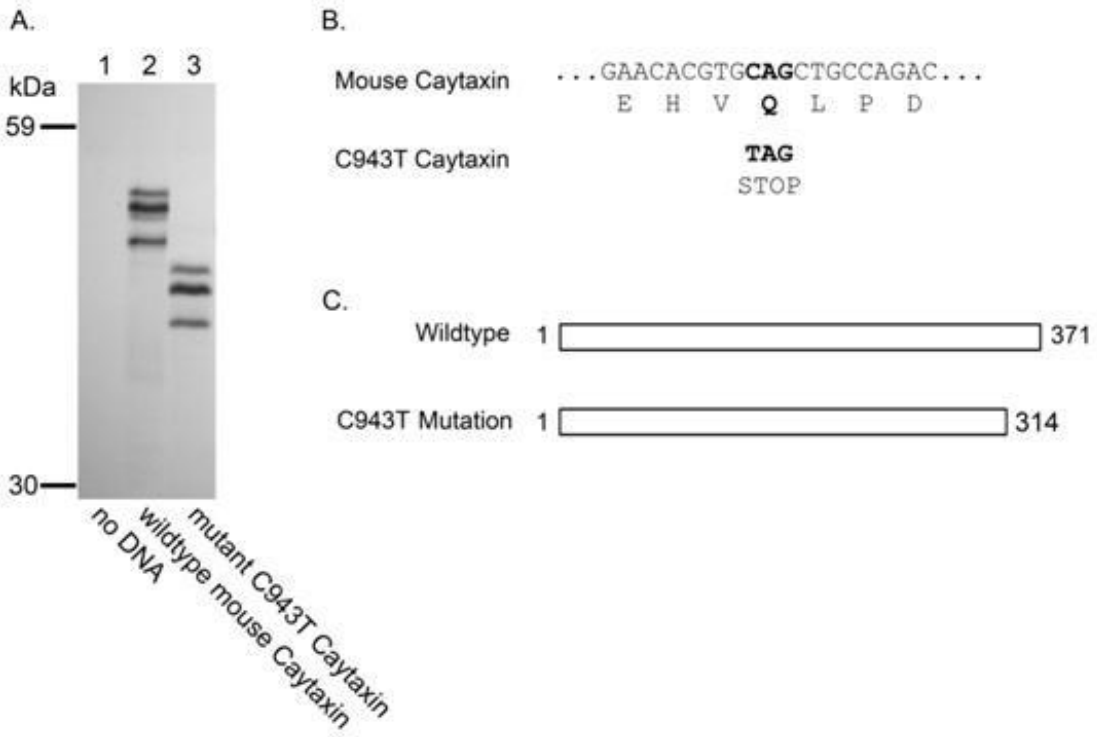

Appendix IV. All three Caytaxin isoforms originate from the N-terminus of the protein.

A point mutation was introduced in the 3' region of *Atcay* via site-directed mutagenesis and translated *in vitro* **(A)**. Mutant Caytaxin (lane 3) was compared to positive control wild type mouse *Atcay* (lane 2) and no DNA control (lane 1). **(B)** The point mutation introduced a stop codon at nucleotide 943 (CAG to TAG). **(C)** The Caytaxin truncation results in a protein missing 57 amino acids from the C-terminal.

Summary. C-terminal truncation of Caytaxin was induced via the introduction of a premature stop codon to determine if the smallest Caytaxin isoform is generated by specific C-terminal protease cleavage of a larger species. Upon *in vitro* translation, all three isoforms are retained, but at a reduced size corresponding to the lack of 57 residues. This indicates that the origin of all isoforms is located at the N-terminus of the protein.

Appendix V. *in vitro* translation of Caytaxin in wheat germ produces the two largest isoforms and low levels of the smallest isoform.

Appendix V. *in vitro* translation of Caytaxin in wheat germ produces the two largest isoforms and low levels of the smallest isoform.
Human **(lane 2)** and mouse **(lane 3)** *Atcay*/*ATCAY* cDNA translated in the in vitro wheat germ lysate system. No DNA control in **(lane 1)**. Methods described in Appendix XVIII.

Summary. Translation of Caytaxin in the plant-based wheat germ lysate system produces the two largest mouse isoforms and the largest human isoform, with faint translation of the smaller species. This suggest the presence of lysate-specific mechanisms which either result in the production or elimination of the smaller isoforms. These include specific protease cleavage and leaky ribosomal scanning.

Appendix VI. Genomic PCR demonstrates that all human *ATCAY* exons are present in wtBAC and BAC^{I9} mouse lines.

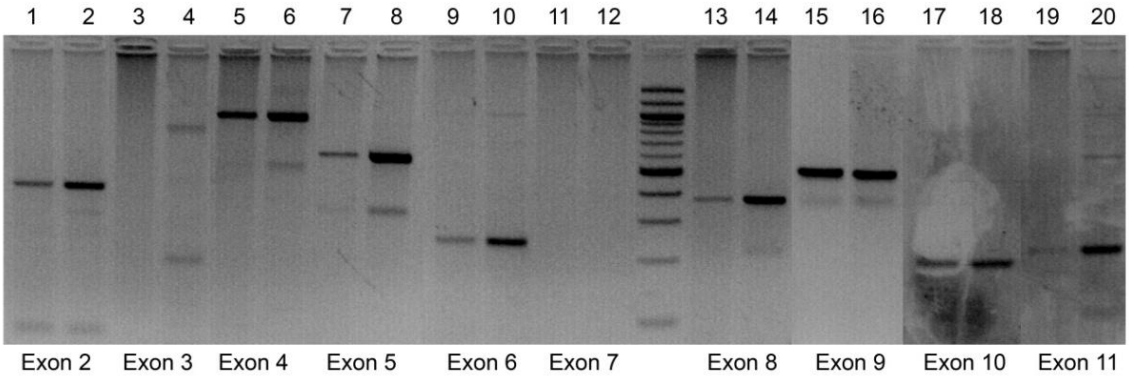

Appendix VI. Genomic PCR demonstrates that all human *ATCAY* exons are present in wtBAC and BAC^{I9} mouse lines.

Genomic PCR for individual exons in human *ATCAY* genomic DNA purified from wtBAC^{+} and BAC^{I9+} mice. Exons 2-11 were examined out of 13 total exons. For each exon, wtBAC precedes BAC^{I9+} for size comparison of each amplicon. Primer pairs and PCR parameters are listed in Appendix XVIII.

Summary. Genomic PCR's were performed on DNA extracted from tail samples from each wtBAC and BAC^{I9} lines using primers designed to flank exons 1 through 11. Differences in required reaction conditions prevented the production of amplicons for exons 3 and 7, however signals are present for the remaining exons in both mouse lines. This indicates that the *ATCAY* transgene in both of these lines is intact and not re-arranged.

Appendix VII. Extending the wire hang time cut-off beyond 1 minute reveals pronounced differences between transgenic lines.

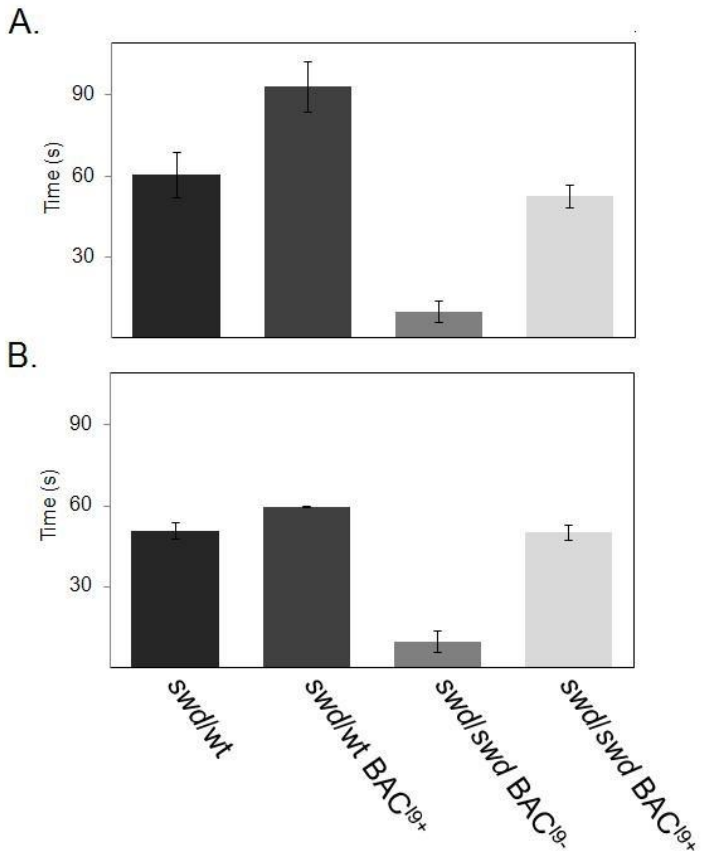

Appendix VII. Extending the wire hang time cut-off beyond 1 minute reveals pronounced differences between transgenic lines.
In each line, hang times exceeding 60 seconds were adjusted to reflect a 60 second cut-off for each mouse. Data was re-analyzed as described in Chapter III materials and methods. **(A)** Original graph with total hang time, **(B)** adjusted times with a 60-second cut-off. Average times for each group (n=3 mice) plotted with error bars representing ± SEM.

Summary. Established wire hang protocols utilize a 1 minute cut-off for allowed hang time per trial. In our analysis, mice were allowed to hang up to 2 minutes in an effort to tease out potential subtleties in phenotype. At a 1 minute cut-off, differences in performance between mouse lines are subtle compared to the extended cut-off. This suggests that phenotype differences between these lines may be more subtle than can be tested using traditional protocols.

Appendix VIII. Predicted *Atcay* RNA folding.

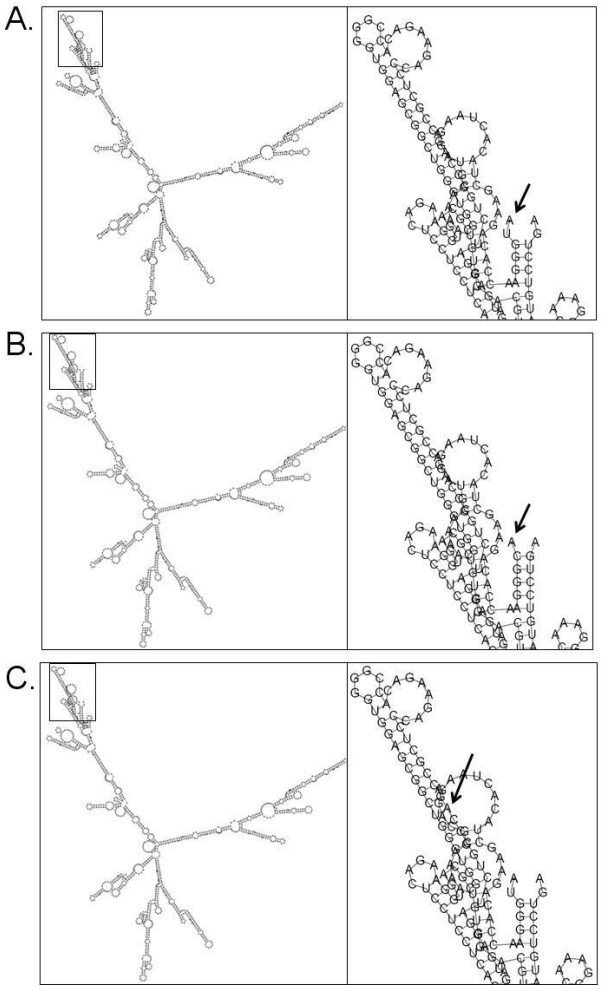

Appendix VIII. Predicted *Atcay* RNA folding.
mRNA folding was predicted based on mRNA sequence (NM_178662.3) using GeneBee RNA secondary structure online tool [121]. Left panels represent entire structure of coding sequence. Right panels are a magnified view of boxed regions in left panels. **(A)** Wild type *Atcay* mRNA with arrow indicating first methionine (Met1). **(B)** *Atcay* with Met1 mutation (arrow). **(C)** *Atcay* with Met10 mutation (arrow).

Summary. Mutation of conserved methionines in mouse *Atcay* affects the translation of the third isoform. It was hypothesized that these mutations created a more complex RNA structure, thus preventing downstream translation. *In silico* analysis indicates that RNA structure is not greatly affected by the methionine mutations, and is therefore an unlikely explanation.

Appendix IX. Lysate-specific protease cleavage does not explain the difference in Caytaxin translated from wheat germ or rabbit reticulocytes.

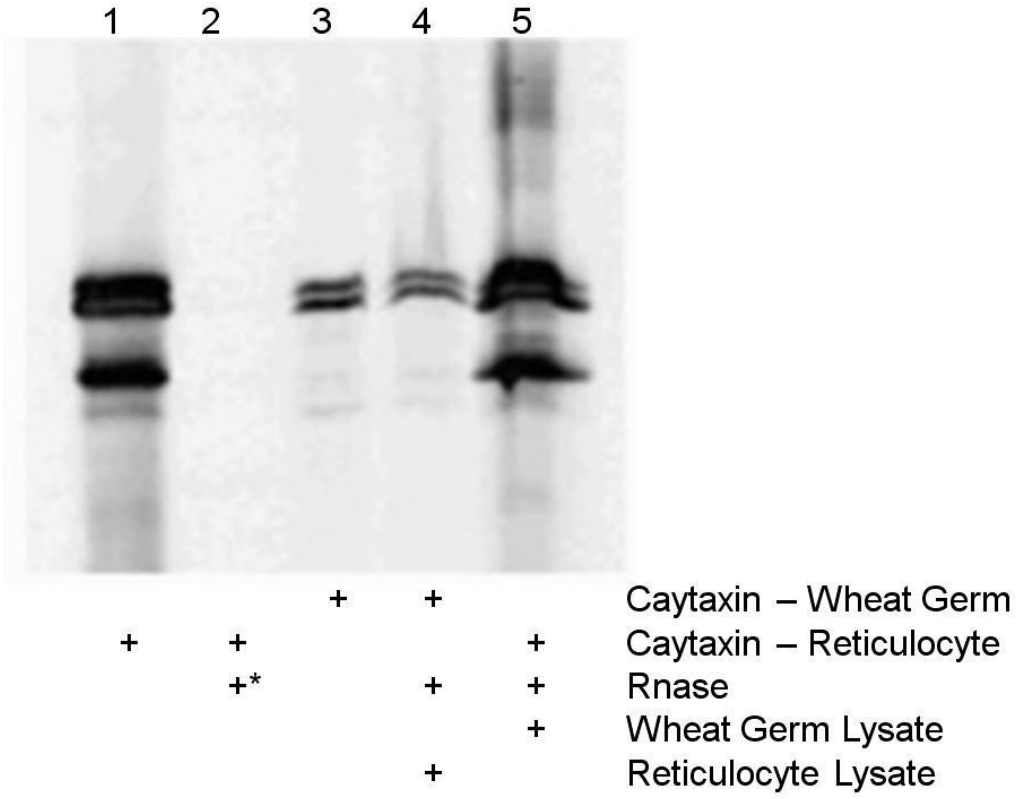

Appendix IX. Lysate-specific protease cleavage does not explain the difference in Caytaxin translated from wheat germ or rabbit reticulocytes.
Wild type mouse Caytaxin translated in rabbit reticulocyte (**lane 1**) and wheat germ lysate (**lane 3**) were treated with RNase and incubated with wheat germ (**lane 5**) or reticulocyte lysate (**lane 4**), respectively. RNase was added to reticulocyte reaction (**lane 2**) to control for RNase efficiency. Materials and methods are described in Appendix XVIII.

Summary. The smallest mouse Caytaxin isoform is not produced in the wheat germ lysate system, but is robustly translated in rabbit reticulocyte lysates. To determine if this result is due to lysate-specific proteases, protein produced from reticulocyte or wheat germ was post-translationally incubated with wheat germ or reticulocyte lysates, respectively. No difference in isoform pattern was observed, indicating that the difference in Caytaxin pattern produced by either system is not due to the presence of either plant or mammalian proteases.

Appendix X. The production of the smallest mouse Caytaxin isoform is not due to protease cleavage.

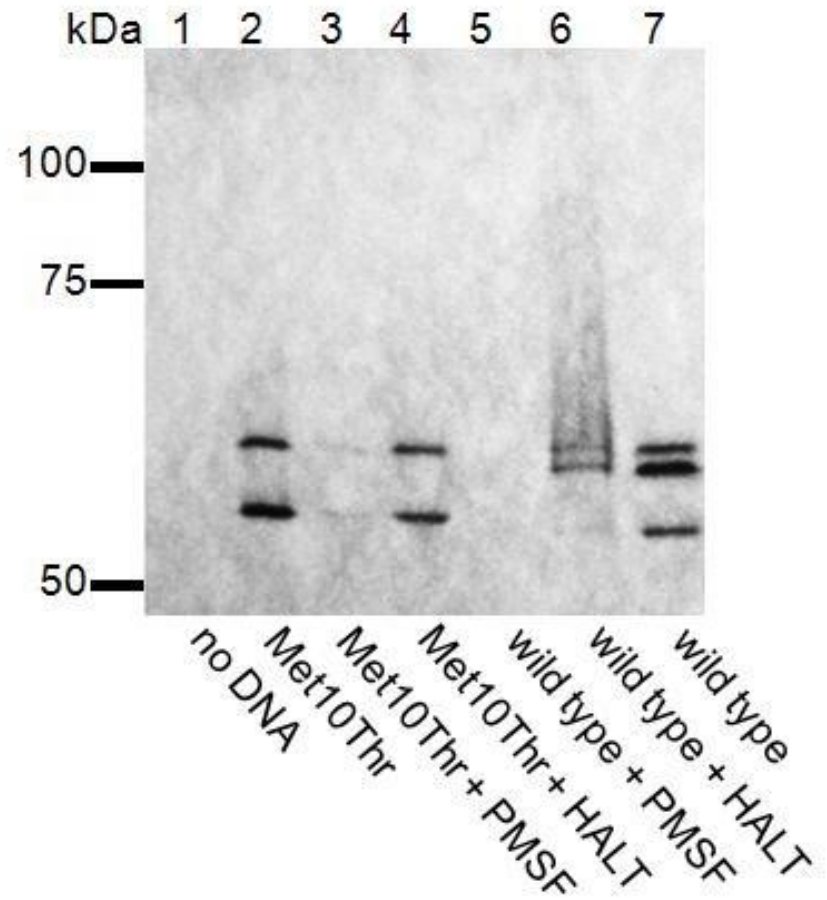

Appendix X. The production of the smallest mouse Caytaxin isoform is not due to protease cleavage.
Mouse *Atcay* cDNA harboring the Met10Thr mutation (**lane 2**) was translated in the presence of protease inhibitor PMSF (**lane 3**) or the HALT protease inhibitor cocktail (**lane 4**). Wild type *Atcay* cDNA was similarly treated (**lanes 5 & 6**). Untreated wild type *Atcay* (**lane 7**) and no DNA (**lane 1**) controls were included. Materials and methods are described in Appendix XVIII.

Summary. Caytaxin was translated *in vitro* in the presence of protease inhibitors to determine if the smallest Caytaxin isoform is a product of co-translational protease cleavage. In some reactions, the presence of protease inhibitors affect translation efficiency, however there was no effect on the production of the third Caytaxin isoform. This suggests that the third isoform is not a product of cleavage by common proteases.

Appendix XI. The addition of a 6xHis tag at the 3' region of mouse *Atcay* enables the purification of low levels of mouse Caytaxin.

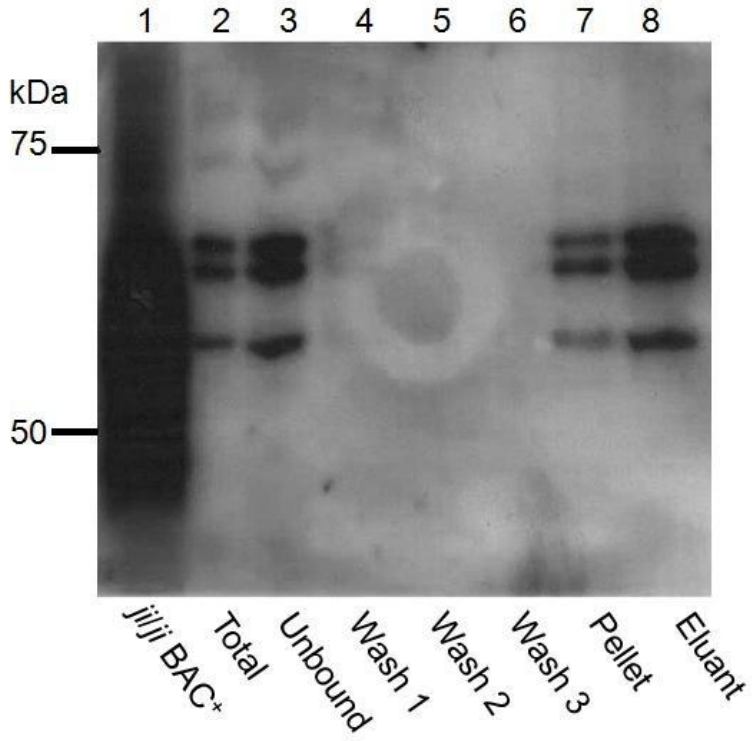

Appendix XI. Appendix XII. The addition of a 6xHis tag at the 3' region of mouse *Atcay* enables the purification of low levels of mouse Caytaxin.
Annealed oligos containing 6xHis flanked by sticky ends were cloned into the mouse *Atcay* cDNA construct. cDNA was transfected with FuGENE®6 (Roche, Cat# 11814443001) into COS-1 cells and processed according to the MagneHis™ Protein Purification System protocol (Promega, Cat# V8500). Lysates were run on a 10% SDS-PAGE gel and transferred onto PVDF membrane. Membranes were processed via Western blot with anti-Caytaxin mAb 8F4 or Coomassie stained (not shown). Positive control lysate from wtBAC^{+} (**lane 1**), total lysate from transfected cells (**lane 2**), unbound Caytaxin from MagneHis™ column (**lane 3**), 3 washes (**lanes 4-6**), boiled beads (**lane 7**) after elution (**lane 8**).

Summary. To identify the source of the third Caytaxin isoform, an *Atcay*-His cDNA construct was generated and expressed in COS-1 cells to enable purification of Caytaxin without the use of antibodies. Upon resolution on a Coomassie-stained membrane, the smallest protein band could be extracted and submitted for N-terminal sequencing. Here, low levels of Caytaxin were purified, but not at sufficient concentrations for N-terminal sequencing.

Appendix XIII. Highly abnormal cerebellar granule cell signaling in *sidewinder* mutant compared to control mice.

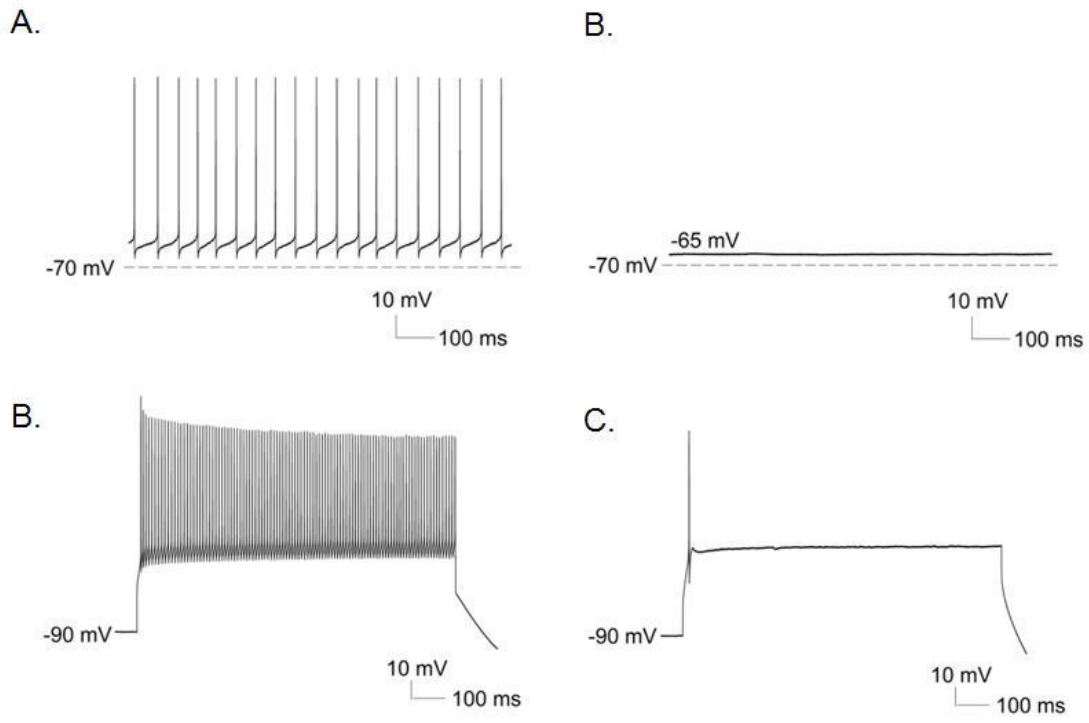

Appendix XII. Highly abnormal cerebellar granule cell signaling in *sidewinder* mutant compared to control mice.
Electrophysiology from cerebellar slices measuring granule cell signaling onto Purkinje cells via patch clamp. **(A)** Wild type spontanous firing, **(B)** absence of spontaneous firing in *swd*/*swd* mutant, **(C)** wild type increased firing in response to current injection, and **(D)** initial spike but inability to maintain firing upon current injection in *swd*/*swd* mutants. Results and figure generated by Dr. Vikram Shakkottai, Department of Neurology, University of Michigan.

Summary. Defects in signaling between granule cells and Purkinje cells were detected in *sidewinder* mutant mice. This was detected via electrophysiology on cerebellar slice preparations. This suggests a defect in the inhibitory effect of Purkinje cell signaling onto deep cerebellar nuclei. Without this inhibition, over stimulation of the DCN may occur and cause symptoms associated with dystonia or ataxia.

Appendix XIV. Sodium channel expression is reduced in *sidewinder* mutant cerebella compared to controls.

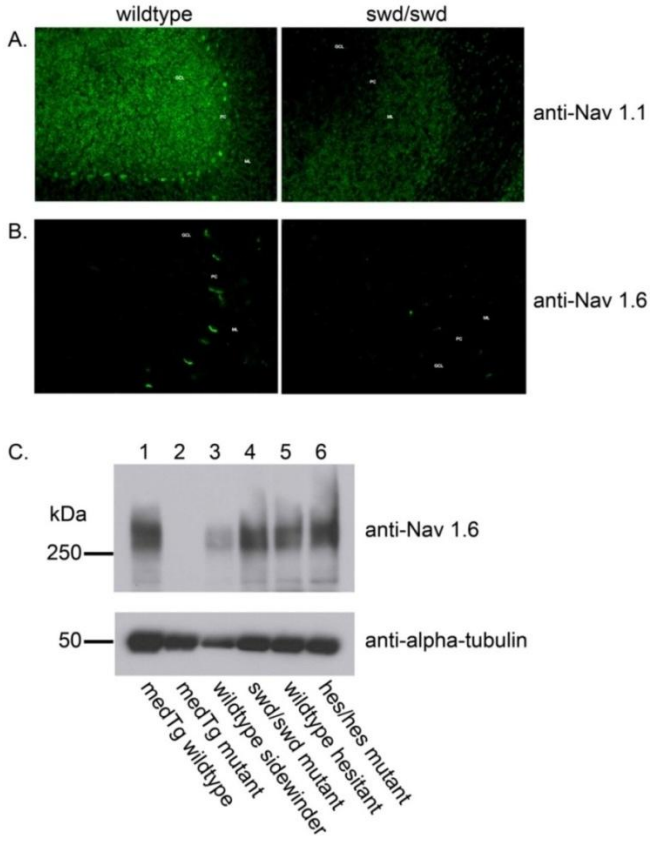

Appendix XIII. Sodium channel expression is reduced in *sidewinder* mutant cerebella compared to controls.
(A) Wild type (left panel) and *swd*/*swd* mutant (right panel) cerebellar section stained with anti-Nav1.1. (B) Wild type (left panel) and *swd*/*swd* mutant (right panel) cerebellar section stained with anti-Nav1.6. (C) Cerebellar membrane preps (protocol from Dr. Lori Isom's Laboratory, Department of Pharmacology, University of Michigan) probed via Western blot for anti-Nav1.6. Control samples from $Nav1.6^{+}$ (lane 1) and $Nav1.6^{-}$ (lane 2) mice. Wild type *sidewinder* (lane 3) vs. mutant *sidewinder* littermate (lane 4). Wild type *hesitant* (lane 5) vs. mutant *hesitant* littermate (lane 6). IHC figure generated by Dr. Katiuska Molina-Luna, Department of Neurology, University of Michigan. Western blot performed by Dr. Janelle O'Brien of Dr. Miriam Meisler's Laboratory, Department of Human Genetics, University of Michigan.

Summary. Cerebellar slices were prepared from wild type and sidewinder mutant mice and probed via immunohistochemistry using anti-Nav1.1 and 1.6 antibodies. Decreases in both sodium channels appeared reduced in IHC, but no reduction was detected on Western blot, indicating that sodium channel localization (not expression) may be affected.

Appendix XV. Cayman ataxia mutations are not predicted to greatly affect Caytaxin protein folding.

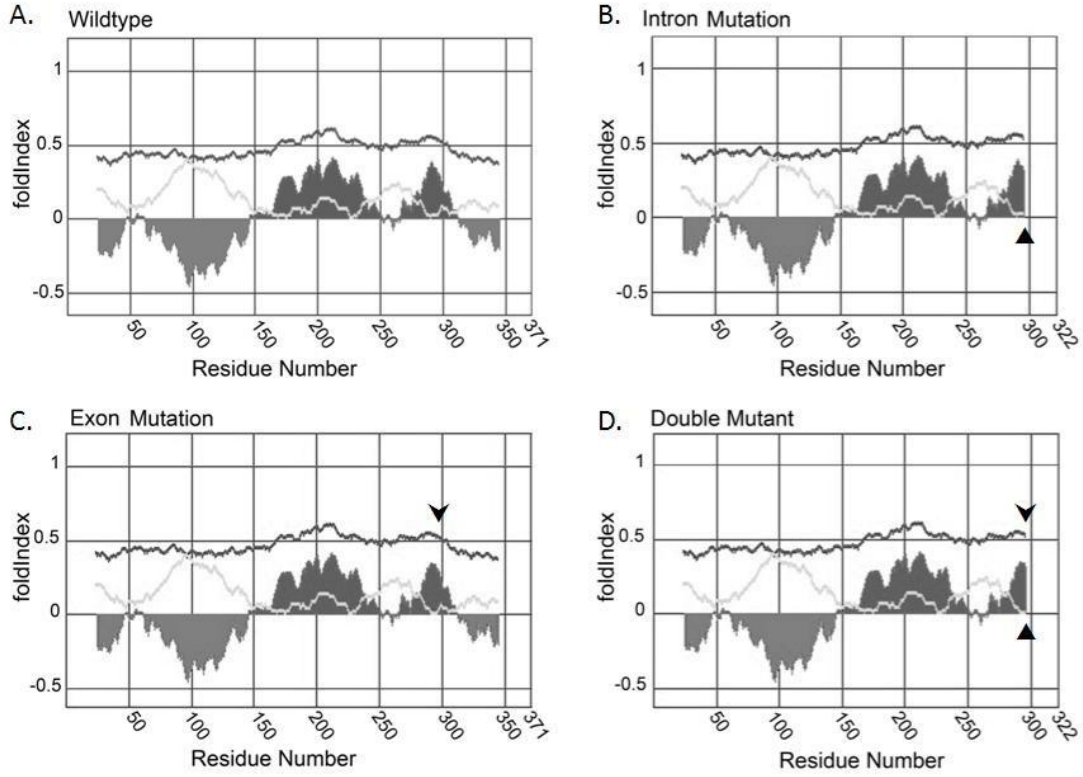

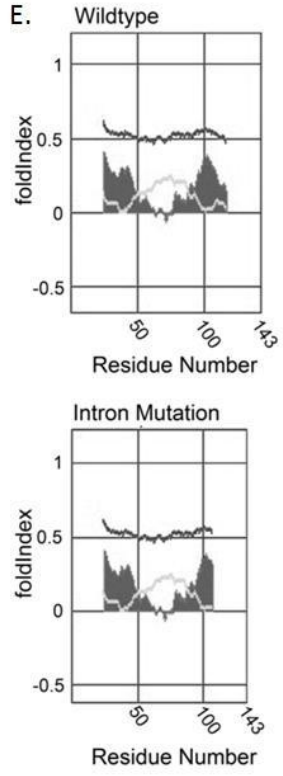

Appendix XIV. Cayman ataxia mutations are not predicted to greatly affect Caytaxin protein folding. Caytaxin protein folding was predicted based on amino acid sequence (NP_149053.1) using the FoldIndex online fold prediction tool [1]. Residues along the x-axis are plotted according to their foldindex value along the y-axis. **(A)** Wild type human Caytaxin; **(B)** human Caytaxin with Cayman ataxia intron 9 mutation, closed triangle indicates location of mutation; **(C)** human Caytaxin with Cayman ataxia exon 9 mutation (arrowhead); **(D)** human Caytaxin with both mutations (arrowhead and closed triangle). **(E)** displays only the BCH domain of wild type (top panel) vs. the intron 9 mutant (bottom panel).

Summary. In examining how the two Cayman ataxia mutations could act synergistically to cause disease, predicted Caytaxin protein folding was examined. The intron 9 mutation was found to create a C-terminal truncation, however the exon 9 mutations results in an amino acid conversion from a neutral to a charged residue. Based on the nature of this mutation, it's possible that the impartment of charge within this area affects protein folding. Combined with the intron 9-induced truncation, this could abrogate Caytaxin function by preventing critical interactions. Upon in silico analysis of how Caytaxin folds in the presence of either or both mutations, it was found that no large differences in protein folding occur.

Appendix XVI. Mass spectrometry of immunopurified Caytaxin indicates interaction with glutaminase and a mitochondrial factor.

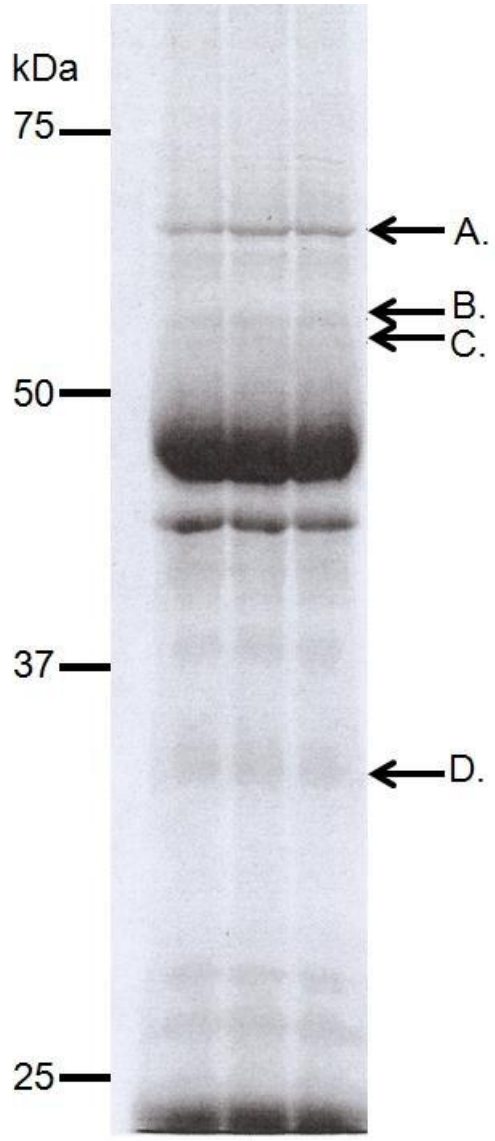

Appendix XV-1. Mass spectrometry of immunopurified Caytaxin indicates interaction with glutaminase and a mitochondrial factor.
Three fractions of eluted Caytaxin was run on a 10% SDS-PAGE gel and stained with Coomassie brilliant blue. Materials and methods are described in Appendix XVII. **(A)** was identified as KGA and Pyruvate dehydrogenase complex component E2. **(B)** and **(C)** were identified as Caytaxin. **(D)** was identified as keratin.

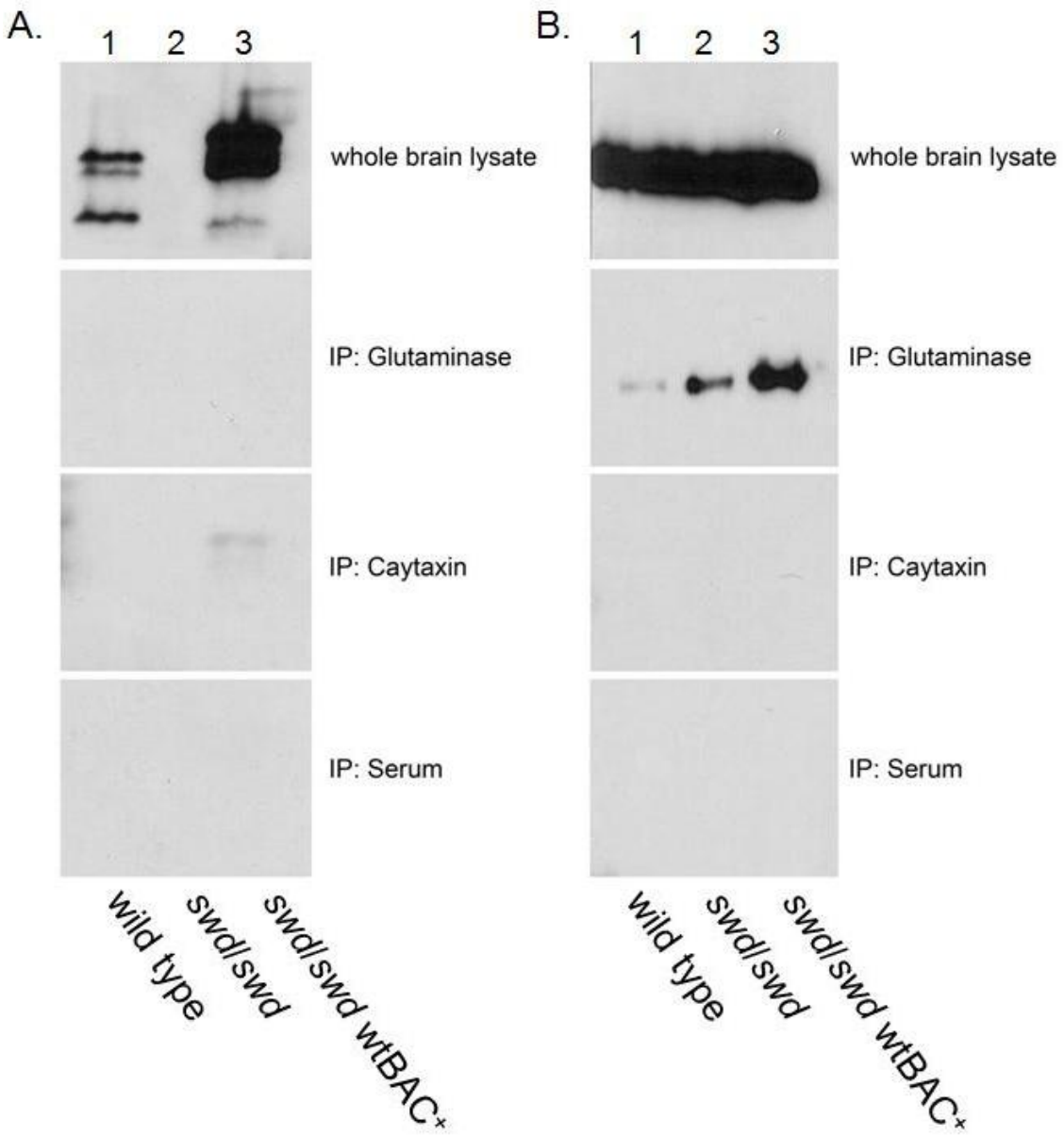

Appendix XV-2. No interaction between Caytaxin and glutaminase could be confirmed via co-immunoprecipitation. Immunoprecipitations from wild type mice (lane 1), *swd*/*swd* mutants (lane 2), and wtBAC^{+} transgenic mice (lane 3). (A) Western blot probed with anti-Caytaxin mAb 8F4; (B) Western blot probed with anti-glutaminase (donated by Dr. Norm Curthoys, Biochemistry & Molecular Biology, Colorado State University). Materials and methods described in Appendix XVII.

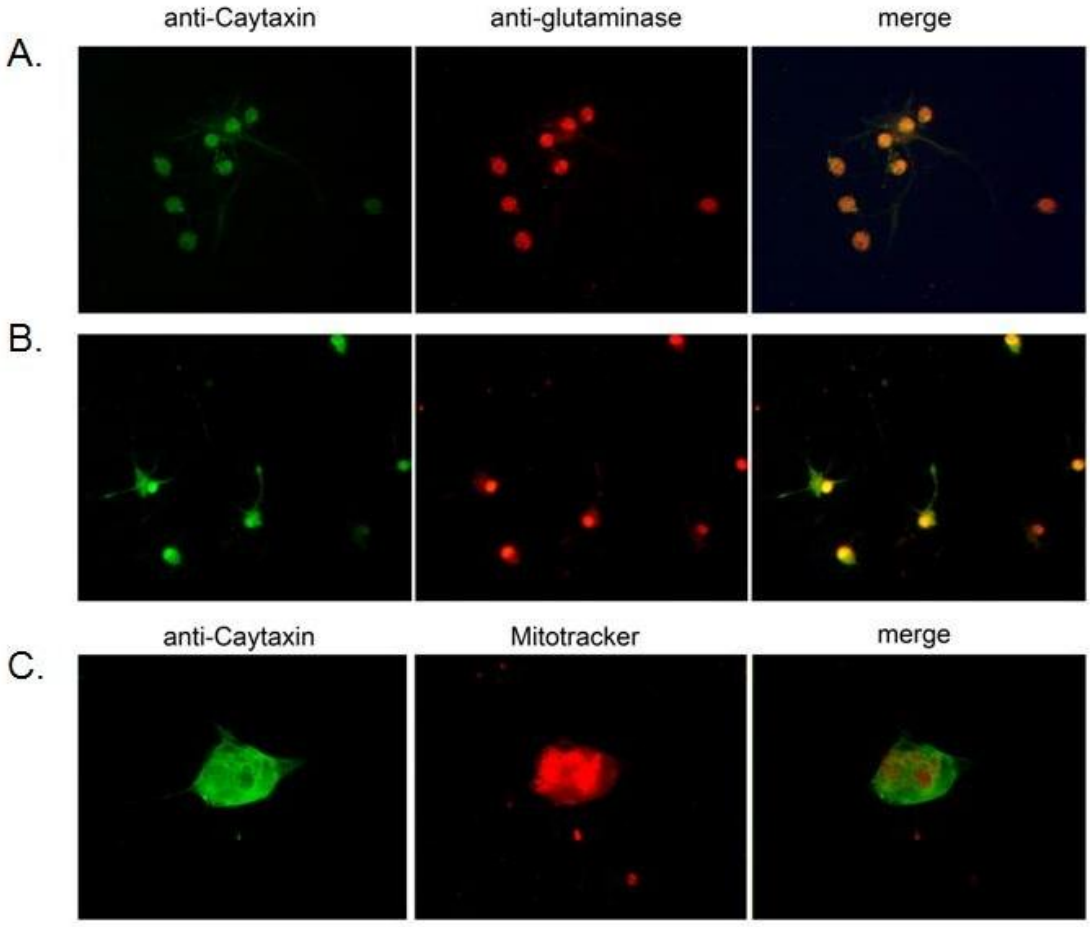

Appendix XV-3. No co-localization was detected between Caytaxin and mitochondria. Caytaxin co-localization with glutaminase was examined in primary granule cell cultures from wild type (A) or *swd*/*swd* mutant (B) mice. Signals for Caytaxin (green, left panels) and glutaminase (red, middle panels) were merged (right panels) to determine co-localization (yellow). (C) Caytaxin co-localization with mitochondria was examined in wild type mice by merging (right panel) signals for Caytaxin (green, left panel) and mitochondria (middle panel). Materials and methods described in Appendix XVII.

Appendix XVII. Discussion for Appendix XV: Mass spectrometry of immunopurified Caytaxin indicates interaction with glutaminase and a mitochondrial factor.

Monoclonal antibodies for Caytaxin were raised against the full length protein and recognized Caytaxin as three isoforms on Western blots (Fig 2.2). To examine protein binding partners for Caytaxin, mass spectrometry analysis was performed on Caytaxin affinity purified with anti-Caytaxin mAb 4E3. Purification strategies were optimized to maximize Caytaxin yield from whole wild type mouse brain lysates and obtain a Caytaxin-saturated sample for analysis. Efforts were made to crosslink the antibody to the protein G beads, however heavy chain contamination prevented adequate resolution of the smallest isoform around 50kDa (data not shown). Upon successful purification of Caytaxin, samples were analyzed via Coomassie-stained SDS-PAGE gel by the University of Michigan MLSC core.

Four bands were indicated for analysis (Appendix XV-1) and were identified as kidney-type glutaminase and pyruvate dehydrogenase complex component E2 (A), Caytaxin (B & C), and keratin (D). Mass spectrometry analysis confirms the identity of the two largest isoforms as Caytaxin, supporting the ability of our antibody to bind Caytaxin and validating the mass spectrometry technique. Keratin was likely identified due to a contamination of mouse fur in the purified sample. Importantly, band (A) was detected as both glutaminase and the mitochondrial pyruvate dehydrogenase complex, suggesting an interaction with both of these factors. Our results confirm previous reports by Buschdorf *et al* who

also detected KGA as a binding partner for Caytaxin, and provided evidence for its role in glutamate signaling [38]. The relationship between Caytaxin and mitochondria had been previously investigated by Hayakawa *et al*, who discuss the role of Caytaxin in the localization of mitochondria within neurites [52]. Aoyama *et al* also observe this localization and also the requirement of Caytaxin to transport mitochondria from the cell body toward the distal ends of neurites [45]. To confirm our mass spectrometry results, preliminary experiments were performed to assess Caytaxin's interaction with glutaminase and mitochondria using immunoprecipitation (IP) and immunocytochemistry (ICC). Materials and methods are described in Appendix XVII.

IP experiments were performed on lysates from wild type mice as well as Caytaxin-deficient (*swd*/*swd* mutant) mice and Caytaxin-overexpressing (wtBAC+) mice. If a direct correlation between Caytaxin and glutaminase expression exists, then we hypothesized that the overexpression or lack of Caytaxin would result in increased or decreased glutaminase levels, respectively. Caytaxin is robustly expressed in wild type and wtBAC lysates (Appendix XV-2, A, top panel), however no Caytaxin is detected upon IP with anti-glutaminase (Appendix XV-2, A, second panel). Additionally, Caytaxin is only detected from IP with anti-Caytaxin in wtBAC^{+} mice (Appendix XV-2, A, third panel). This suggests that optimization may be required to maximize binding within the IP system. A similar result is observed upon Western blotting with glutaminase where glutaminase is detected in IP with anti-glutaminase (Appendix XV-2, B, second panel), but not with anti-Caytaxin (Appendix XV-2, B, third panel). Interestingly,

glutaminase levels increase in Caytaxin-overexpressing lysate, suggesting a direct relationship between Caytaxin and glutaminase. Upon ICC analysis of glutaminase and Caytaxin co-localization, robust expression of both proteins is observed in primary neurons from both wild type (Appendix XV-3, A, left and middle panels) and in *swd*/*swd* mutant (Appendix XV-3, B, left and middle panels) mice. Additionally, investigation into the relationship between Caytaxin and mitochondria detects a lack of co-localization.

Given that anti-Caytaxin mAb is not specific for Caytaxin, no conclusions can be drawn from these data that either support or dispute the hypotheses that Caytaxin interacts with glutaminase and mitochondria. A more direct approach to analyzing this relationship is to utilize *Atcay* mouse mutants, whose varying Caytaxin expression is described in this dissertation. Similar Western blot and ICC analysis for glutaminase, without the use of the anti-Caytaxin mAb, could more thoroughly quantify levels of glutaminase in mice who over-express (wtBAC^{+}), do not express (swd/*swd*), or express low levels of Caytaxin (*hes*/*hes*). Similarly, localization of glutaminase and mitochondria could be further assessed via fluorescence recovery after photobleaching (FRAP) [122] techniques which would indicate whether Caytaxin deficiencies affect the transport and correct localization of these proteins.

With the characterization of the BAC^{I9+} mouse, these experiments could also be extended to examine whether the mutant form of Caytaxin is also able to affect glutaminase expression or localization. The truncation caused by the inclusion of

intron 9 in the mRNA coding sequence eliminates a portion of the second KGA binding site (Fig 1.1). Whether this is sufficient to abrogate the interaction between KGA and Caytaxin is unknown, but can be determined by assessing glutaminase expression in wtBAC^{+} mice versus BAC^{I9+} mutant mice.

Our initial analysis and confirmation of Caytaxin binding partners has optimized and established methods which could now be utilized to specifically examine whether Caytaxin plays a role in glutamate signaling through interactions with glutaminase. Thus far, glutaminase and Caytaxin co-localization has been observed in transfected cell lines, but no characterization of this enzyme has been performed in *Atcay* mouse models. Utilizing the Atcay mice and transgenic lines described herein can confirm the link between Caytaxin and glutaminase in a whole-organism model system.

Appendix XVIII. Materials and methods for Appendix XV.

Affinity purification of Caytaxin – A 1ml Protein G column was prepared with 1ml anti-Caytaxin mAb 4E3 by incubating rotating overnight at +4^{o}C. The column was washed twice with 10ml 0.2M TEA 7.8pH before crosslinking was performed with DMP diluted to 40mM in TEA. Beads were incubated rotating at room temperature for 45 minutes and then with 10ml 20mM ethanolamine for 1 hour at room temperature. wtBAC^{+} brain whole brain homogenate was prepared as described in Chapter II materials and methods. Lysate was incubated with prepared Protein G beads for 48 hours rotating at +4^{o}C. Beads were pre-eluted with 2% SDS, washed once with 1xPBS, and eluted in approximately 100ml 2%SDS by boiling for 10 minutes. Samples were processed on a 10% SDS-PAGE gel. The gel was stained for 2 hours with Coomassie Brilliant Blue before detaining and submission to the proteomics core.

Caytaxin-Glutaminase Immunoprecipitation – Whole brain lysates were prepared from wild type, wild type *ATCAY* BAC^{+}, and *swd*/*swd* mutant mice as described in Chapter II. 200µL of each lysate was diluted in 200µL buffer and incubated with 3µL monoclonal anti-Caytaxin 4E3 antibody, 3µL anti-glutaminase, or 3µL serum at +4^{o}C overnight. 25µL Protein G slurry was added to each mixture and incubated 1.5hrs rotating at room temperature. Beads were collected and washed three times with 1xPBS. Beads were eluted by boiling in 50µL 2X Laemmli buffer with β-mercaptoethanol. Samples were run on a 10% SDS-PAGE gel and blotted as described in Chapter II (materials and methods)

with 1:500 anti-Caytaxin mAb 8F4 or 1:1000 anti-glutaminase (from N. Curthoys [123]).

Immunostaining – Primary neurons were prepared from *swd*/*swd* and wt/wt littermates from the *sidewinder* lines (protocol described in Chapter II, Materials and methods). 2% PFA was diluted in 1xPBS and used for fixation at 37^{o}C for 15 minutes. Cells were washed with once with TBS + TX100 for 10 minutes at room temperature, and then blocked with TBSTS for 30 minutes at room temperature. Primary antibodies were diluted in TBSTS at the following dilutions: anti-Caytaxin mAb 4E3 at 1:300 and anti-glutaminase at 1:1000, and incubated overnight at +4^{o}C. Cells were washed 5x for 5 minutes each in TBST. Secondary antibodies were diluted in TBSTS at the following dilutions: FITC at 1:1000 (Caytaxin), C3 at 1:1000 (glutaminase), and incubated for 1.5 hours at room temperature. Five final washes were performed: 4 times with TBST, and once with TBS. Cover slides were mounted with ProLong® Gold reagent (Life Technologies, Cat. No. P36930) and allowed to set before visualization via fluorescence microscopy. Mitochondrial staining was performed according to the manufacturer's protocol (Life Technologies, MitoTracker® Red CMXRos, Cat# M7512).

Appendix XIX. Appendices materials and methods.

Examining Caytaxin PTM (Phosphorylation) – Lysates were prepared from wtBAC^{+} mice, SH-SY5Y cells, wild type mice and incubated with anti-Caytaxin mAb 4E3. Positive control cell lysates from HEK 293 +insulin (stimulation of S6K phosphorylation) and -insulin (no stimulation of S6K phosphorylation) were prepared by Hugo Acosta-Jaquez (Dr. Diane Finger's Laboratory, University of Michigan) and incubated with anti-S6K. Lysate+antibody incubations were performed overnight at +4^{o}C and immunoprecipitated with 25µL Protein A beads (S6K) or Protein G beads (Caytaxin) for 1.5hrs at room temperature. Beads were washed 3x with ST buffer (150mM NaCl + 50mM Tris pH7.4). 200u lambda protein phosphatase (λ-PPase) and 10X λ-PPase buffer were added to the beads and incubated at 30^{o}C for 30 minutes. Reaction was inactivated by the addition of 2x sample buffer with β-mercaptoethanol and boiling for 10min. Samples were processed on a 10% SDS-PAGE gel and blotted with 8F4 (Caytaxin) or anti-S6K1 and Phospho-S6K1 (S6K). Membranes were developed via ECL.

Mutagenesis of potential non-AUG start sites

t122a sense 5'-ctgggtggcgcagaggaagactcctcc-3'

anti 5'-ggaggagtcttcctctgcgccacccag-3'

t71g sense 5'-caggatgaggatcggcccagaccgctc-3'

anti 5'-gagcggtctgggccgatcctcatcctg-3'

t101a sense 5'-agacaccggggaggagcggctgg-3'

anti 5'-ctgcgccaccccgccgctccacc-3'

t110g sense 5’-ggtggagcggcggggtggcgcag-3’

anti 5’-ccactgcgccaccccgccgctccaccccg-3’

Wheat germ *in vitro* translation – Coupled transcription/translation reactions were set up according to manufacturer’s protocol using the TnT® Coupled Wheat Germ Extract System (Promega, Cat. No. L4130). 10µL of a 50µL reaction was loaded on 10% SDS-PAGE gels. Additional reagents included EasyTag™ L-[^{35}S]-Methionine, 500µCi (18.5MBq) (PerkinElmer, NEG709A500UC) and RNasin® Ribonuclease Inhibitor (Promega, Cat. No. N2111). Gels were fixed overnight in 50% MeOH and 10% acetic acid, and then treated with EN^{3}HANCE™ Autoradiography Enhancer according to the manufacturer’s protocol (PerkinElmer, Cat. No. 6NE9701). Gels were dried on a slab gel dryer for 2 hours at 80^{o}C and exposed to autoradiography blue film (Fisher Scientific, Cat. No. NC9469626 or AF5700) for 1-7 days at room temperature. *Atcay/ATCAY* cDNA inserts were correctly oriented from the SP6 promoter.

Genomic PCR – Genomic PCR reactions utilized primer sets located within introns flanking each *ATCAY* exon (synthesized by Integrated DNA Technologies, Inc., Coralville, IA).

Exon 2: 5’-catggggtagacgattgtcatt-3’, 5’-acagagaagactcgcacacagg-3’

Buffer 2 (Roche, Cat. No. 11681834001), Annealing Temp 61^{o}C

Exon 3: 5’-acctgtctgggccactcc-3’, 5’-ccttctgtggacgtggaaactt-3’

Buffer 3 (Roche, Cat. No. 11681834001), Annealing Temp 61^{o}C

Exon 4: 5’-aggtggcctgacatcgttaca-3’, 5’-ggaatccagagacggaaaggt-3’

Buffer 1 (Roche, Cat. No. 11681834001), Annealing Temp 60^{o}C

Exon 5: 5’-ctcgtggtttgatgaagcagat-3’, 5’-aagcgagttgacggcttaacat-3’

Optiprime™ Buffer 7 (Stratagene), Annealing Temp 61^{o}C

Exon 6: 5’-aggactctgacgttgccgat-3’, 5’-tagggccacaatgcaatcctt-3’

Buffer 3 (Roche, Cat. No. 11681834001), Annealing Temp 61^{o}C

Exon 7: 5’-caggtgtcctgaccctgga-3’, 5’-gtgattttcatgcccccact-3’

Buffer 3 (Roche, Cat. No. 11681834001), Annealing Temp 61^{o}C

Exon 8: 5’-ggaatgagcagagtgacgaatg-3’, 5’-gagaagctggaacatgcacatc-3’

Buffer 3 (Roche, Cat. No. 11681834001), Annealing Temp 61^{o}C

Exon 9: 5’-gaggtgtcgtcgtctgcact-3’, 5’-actaatacggcggggtgga-3’

Buffer 2 (Roche, Cat. No. 11681834001), Annealing Temp 61^{o}C

Exon 10: 5’-gaaagggatttccccaaaaagt-3’, 5’-gggttgccctaactgagagttc-3’

Buffer 3 (Roche, Cat. No. 11681834001), Annealing Temp 61^{o}C

Exon 11: 5’-tgggctagtcacccttgtcac-3’, 5’-ctgaacaaggacccatcttcct-3’

Buffer 3 (Roche, Cat. No. 11681834001), Annealing Temp 61^{o}C

Exon 12: 5’-aataacgcccagtctccgtct-3’, 5’-taagtcatggggcagttttcct-3’

Buffer 2 (Roche, Cat. No. 11681834001), Annealing Temp 61^{o}C

Protease Inhibitor – Coupled transcription/translation reactions were set up according to manufacturer’s protocol using the TnT® Coupled Wheat Germ Extract or Reticulocyte Lysate Systems (described previously) with the addition of protease inhibitors 1x HALT protease inhibitor cocktail (Thermo Scientific) and 40µg/mL PMSF. 7µL of a 25µL reaction was loaded on 10% SDS-PAGE gels.

Co-incubation of *in vitro* translated Caytaxin – 7µL Caytaxin produced in vitro by wheat germ or reticulocyte lysates (described previously) was incubated at 55^{o}C for 5 minutes to release any residual RNA secondary structure. 1µL RNase was added and incubated for 10 minutes at 30^{o}C to digest residual RNA. Reactions were then heated at 70^{o}C for 10 minutes to inactivate RNase. 7µL reticulocyte lysate or wheat germ lysates were added to reactions with Caytaxin from wheat germ or reticulocyte lysates, respectively. H_2O was added to each reaction to a final volume of 15µL. Reactions were heated at 30^{o}C for 1 hour. 15µL 2X Laemmli buffer with β-mercaptoethanol was added to each reaction and boiled for 2 minutes. Samples were cooled and run on a 10% SDS-PAGE gel and visualized according to *in vitro* protocols described in Chapter II.

References

1. Prilusky J, Felder CE, Zeev-Ben-Mordehai T, Rydberg EH, Man O, Beckmann JS, Silman I, Sussman JL: **FoldIndex: a simple tool to predict whether a given protein sequence is intrinsically unfolded**. *Bioinformatics* 2005, **21**(16):3435-3438.
2. Bartholow R, Clarke R, Co: **Progressive locomotor ataxia**: Robert Clarke & Co.; 1866.
3. Althaus J: **On epilepsy, hysteria and ataxy: three lectures**: Churchill; 1866.
4. Allbutt TC: **Remarks on the Phenomena of Locomotor Ataxy: With an Appendix Relative to Discussion Thereon**. *Br Med J* 1869, **1**(425):157-159.
5. Harding AE: **Classification of the hereditary ataxias and paraplegias**. *Lancet* 1983, **1**(8334):1151-1155.
6. Shakkottai VG, Chou CH, Oddo S, Sailer CA, Knaus HG, Gutman GA, Barish ME, LaFerla FM, Chandy KG: **Enhanced neuronal excitability in the absence of neurodegeneration induces cerebellar ataxia**. *J Clin Invest* 2004, **113**(4):582-590.
7. Zoghbi HY, Orr HT: **Glutamine repeats and neurodegeneration**. *Annu Rev Neurosci* 2000, **23**:217-247.
8. Zoghbi HY: **Spinocerebellar ataxias**. *Neurobiol Dis* 2000, **7**(5):523-527.
9. Palau F, Espinos C: **Autosomal recessive cerebellar ataxias**. *Orphanet J Rare Dis* 2006, **1**:47.
10. Koenig M: **Rare forms of autosomal recessive neurodegenerative ataxia**. *Semin Pediatr Neurol* 2003, **10**(3):183-192.
11. De Michele G, Coppola G, Cocozza S, Filla A: **A pathogenetic classification of hereditary ataxias: is the time ripe?** *J Neurol* 2004, **251**(8):913-922.
12. Bird TD: **Hereditary Ataxia Overview**. 1993.
13. Paulson HL: **The spinocerebellar ataxias**. *J Neuroophthalmol* 2009, **29**(3):227-237.
14. Anheim M, Tranchant C, Koenig M: **The Autosomal Recessive Cerebellar Ataxias**. *New England Journal of Medicine* 2012, **366**(7):636-646.
15. Kumar AK MJ, and Smith C: **Genetic Disorders in the Cayman Islands**. In: *Cayman Islands Country Conference http://wwwcavehilluwiedu/bnccde/cayman/conference/papers/merrenhtml*. 2004.
16. Thurtell MJ, Leigh RJ: **Nystagmus and saccadic intrusions**. *Handb Clin Neurol* 2011, **102**:333-378.

17. Bloom AD, Johnson WG, Murphy M, Murphy WI, Lindheim N, Smith P: **513 CAYMAN DISEASE AND A NEW STORAGE DISEASE IN A WEST INDIES ISOLATE**. *Pediatr Res* 1978, **12**(S4):449-449.
18. Bomar JM, Benke PJ, Slattery EL, Puttagunta R, Taylor LP, Seong E, Nystuen A, Chen W, Albin RL, Patel PD *et al*: **Mutations in a novel gene encoding a CRAL-TRIO domain cause human Cayman ataxia and ataxia/dystonia in the jittery mouse**. *Nat Genet* 2003, **35**(3):264-269.
19. Nystuen A BP, Merren J, Stone EM, and Sheffield VC: **A cerebellar ataxia locus identified by DNA pooling to search for linkage disequilibrium in an isolated population from the Cayman Islands**. *Human Molecular Genetics* 1996, **5**(4):535-531.
20. Sheffield VC, Weber JL, Buetow KH, Murray JC, Even DA, Wiles K, Gastier JM, Pulido JC, Yandava C, Sunden SL *et al*: **A collection of tri- and tetranucleotide repeat markers used to generate high quality, high resolution human genome-wide linkage maps**. *Hum Mol Genet* 1995, **4**(10):1837-1844.
21. Kapfhamer D, Sweet, HO, Sufalko, D, Warren, S, Johnson, KR and Burmeister, M: **The Neurological Mouse Mutations Jittery and Hesitant Are Allelic and Map to the Region of Mouse Chromosome 10 Homologous to 19p13.3**. *Genomics* 1996, **35**:533-538.
22. Seal RL, Gordon SM, Lush MJ, Wright MW, Bruford EA: **genenames.org: the HGNC resources in 2011**. *Nucleic Acids Res* 2011, **39**(Database issue):D514-519.
23. Saunders NJ: **The Peoples of the Caribbean: An Encyclopedia of Archeology and Traditional Culture**: ABC-CLIO; 2005.
24. (ESP) NESP: **Exome Variant Server. http://evs.gs.washington.edu/EVS/.** In.
25. Altschul SF, Gish W, Miller W, Myers EW, Lipman DJ: **Basic local alignment search tool**. *J Mol Biol* 1990, **215**(3):403-410.
26. Lorden JF, McKeon TW, Baker HJ, Cox N, Walkley SU: **Characterization of the rat mutant dystonic (dt): a new animal model of dystonia musculorum deformans**. *J Neurosci* 1984, **4**(8):1925-1932.
27. LeDoux MS: **Animal models of dystonia: Lessons from a mutant rat**. *Neurobiol Dis* 2011, **42**(2):152-161.
28. LeDoux MS, Lorden JF, Ervin JM: **Cerebellectomy eliminates the motor syndrome of the genetically dystonic rat**. *Exp Neurol* 1993, **120**(2):302-310.
29. Green M: **Grizzled (gr), jittery (ji) on same side of waltzer (v)**. *Mouse News Letter* 1968, **39**(28).
30. Kapfhamer D, Sweet HO, Sufalko D, Warren S, Johnson KR, Burmeister M: **The neurological mouse mutations jittery and hesitant are allelic and map to the region of mouse chromosome 10 homologous to 19p13.3**. *Genomics* 1996, **35**(3):533-538.
31. Snell G: **Linkage of Jittery and Waltzing in the Mouse**. *The Journal of Heredity* 1945, **36**(9):279-280.

32. Arnold C, Smart, NG, and Beutler, B: **Record for *wobbley***. In.: MUTAGENETIX(TM), B. Beutler and colleagues, Center for the Genetics of Host Defense, UT Southwestern, Dallas, TX; 2008.
33. DeOme K: **A new recessive lethal mutation in mice**. *University of California publications in zoology* 1945, **53**:41-65.
34. Sweet HaD, MT: **Hesitant (hes)**. *Mouse Genome* 1993(92):355.
35. Gilbert N, Bomar, JM, Burmeister, M, and Moran, JV: **Characterization of a Mutagenic B1 Retrotransposon Insertion in the Jittery Mouse**. *Human Mutation* 2004, **24**:9-14.
36. Sweet H: **Hesitant (hes)**. *Mouse Genome* 1991, **84**(4):844.
37. Lua BL, Low BC: **BPGAP1 interacts with cortactin and facilitates its translocation to cell periphery for enhanced cell migration**. *Mol Biol Cell* 2004, **15**(6):2873-2883.
38. Buschdorf JP, Li Chew L, Zhang B, Cao Q, Liang FY, Liou YC, Zhou YT, Low BC: **Brain-specific BNIP-2-homology protein Caytaxin relocalises glutaminase to neurite terminals and reduces glutamate levels**. *J Cell Sci* 2006, **119**(Pt 16):3337-3350.
39. Gupta AB, Wee LE, Zhou YT, Hortsch M, Low BC: **Cross-Species Analyses Identify the BNIP-2 and Cdc42GAP Homology (BCH) Domain as a Distinct Functional Subclass of the CRAL_TRIO/Sec14 Superfamily**. *PLoS One* 2012, **7**(3):e33863.
40. Buschdorf JP, Chew LL, Soh UJ, Liou YC, Low BC: **Nerve growth factor stimulates interaction of Cayman ataxia protein BNIP-H/Caytaxin with peptidyl-prolyl isomerase Pin1 in differentiating neurons**. *PLoS One* 2008, **3**(7):e2686.
41. Pan CQ, Low BC: **Functional plasticity of the BNIP-2 and Cdc42GAP Homology (BCH) domain in cell signaling and cell dynamics**. *FEBS Lett* 2012, **586**(17):2674-2691.
42. Zhou YT, Soh UJ, Shang X, Guy GR, Low BC: **The BNIP-2 and Cdc42GAP homology/Sec14p-like domain of BNIP-Salpha is a novel apoptosis-inducing sequence**. *J Biol Chem* 2002, **277**(9):7483-7492.
43. Kang JS, Bae GU, Yi MJ, Yang YJ, Oh JE, Takaesu G, Zhou YT, Low BC, Krauss RS: **A Cdo-Bnip-2-Cdc42 signaling pathway regulates p38alpha/beta MAPK activity and myogenic differentiation**. *J Cell Biol* 2008, **182**(3):497-507.
44. Grelle G, Kostka S, Otto A, Kersten B, Genser KF, Muller EC, Walter S, Boddrich A, Stelzl U, Hanig C *et al*: **Identification of VCP/p97, carboxyl terminus of Hsp70-interacting protein (CHIP), and amphiphysin II interaction partners using membrane-based human proteome arrays**. *Mol Cell Proteomics* 2006, **5**(2):234-244.
45. Aoyama T, Hata S, Nakao T, Tanigawa Y, Oka C, Kawaichi M: **Cayman ataxia protein caytaxin is transported by kinesin along neurites through binding to kinesin light chains**. *J Cell Sci* 2009, **122**(Pt 22):4177-4185.
46. Itoh M, Li S, Ohta K, Yamada A, Hayakawa-Yano Y, Ueda M, Hida Y, Suzuki Y, Ohta E, Mizuno A *et al*: **Cayman ataxia-related protein is a**

presynapse-specific caspase-3 substrate. *Neurochem Res* 2011, **36**(7):1304-1313.
47. Curthoys NP, Lowry OH: **Glutamate and glutamine distribution in the rat nephron in acidosis and alkalosis**. *Am J Physiol* 1973, **224**(4):884-889.
48. Liou YC, Sun A, Ryo A, Zhou XZ, Yu ZX, Huang HK, Uchida T, Bronson R, Bing G, Li X *et al*: **Role of the prolyl isomerase Pin1 in protecting against age-dependent neurodegeneration**. *Nature* 2003, **424**(6948):556-561.
49. Ryo A, Togo T, Nakai T, Hirai A, Nishi M, Yamaguchi A, Suzuki K, Hirayasu Y, Kobayashi H, Perrem K *et al*: **Prolyl-isomerase Pin1 accumulates in lewy bodies of parkinson disease and facilitates formation of alpha-synuclein inclusions**. *J Biol Chem* 2006, **281**(7):4117-4125.
50. Lu KP, Liou YC, Vincent I: **Proline-directed phosphorylation and isomerization in mitotic regulation and in Alzheimer's Disease**. *Bioessays* 2003, **25**(2):174-181.
51. Yi CH, Yuan J: **The Jekyll and Hyde functions of caspases**. *Dev Cell* 2009, **16**(1):21-34.
52. Hayakawa Y, Itoh M, Yamada A, Mitsuda T, Nakagawa T: **Expression and localization of Cayman ataxia-related protein, Caytaxin, is regulated in a developmental- and spatial-dependent manner**. *Brain Res* 2007, **1129**(1):100-109.
53. Xiao J, Ledoux MS: **Caytaxin deficiency causes generalized dystonia in rats**. *Brain Res Mol Brain Res* 2005, **141**(2):181-192.
54. Low BC, Seow KT, Guy GR: **Evidence for a novel Cdc42GAP domain at the carboxyl terminus of BNIP-2**. *J Biol Chem* 2000, **275**(19):14415-14422.
55. Zhou YT, Guy GR, Low BC: **BNIP-2 induces cell elongation and membrane protrusions by interacting with Cdc42 via a unique Cdc42-binding motif within its BNIP-2 and Cdc42GAP homology domain**. *Exp Cell Res* 2005, **303**(2):263-274.
56. Gasteiger E, Gattiker A, Hoogland C, Ivanyi I, Appel RD, Bairoch A: **ExPASy: The proteomics server for in-depth protein knowledge and analysis**. *Nucleic Acids Res* 2003, **31**(13):3784-3788.
57. Blom N, Sicheritz-Ponten T, Gupta R, Gammeltoft S, Brunak S: **Prediction of post-translational glycosylation and phosphorylation of proteins from the amino acid sequence**. *Proteomics* 2004, **4**(6):1633-1649.
58. Ao Li XG, Jian Ren, Changjiang Jin, and Yu Xue: **BDM-PUB: Computational Prediction of Protein Ubiquitination Sites with a Bayesian Discriminant Method**. In.; 2009.
59. Monigatti F, Gasteiger E, Bairoch A, Jung E: **The Sulfinator: predicting tyrosine sulfation sites in protein sequences**. *Bioinformatics* 2002, **18**(5):769-770.

60. Kiemer L, Bendtsen JD, Blom N: **NetAcet: prediction of N-terminal acetylation sites**. *Bioinformatics* 2005, **21**(7):1269-1270.
61. Johansen MB, Kiemer L, Brunak S: **Analysis and prediction of mammalian protein glycation**. *Glycobiology* 2006, **16**(9):844-853.
62. Hecht K, Bailey JE, Minas W: **Polycistronic gene expression in yeast versus cryptic promoter elements**. *FEMS Yeast Res* 2002, **2**(2):215-224.
63. Zhang T, Cheng T, Wei L, Cai Y, Yeo AE, Han J, Yuan YA, Zhang J, Xia N: **Efficient inhibition of HIV-1 replication by an artificial polycistronic miRNA construct**. *Virol J* 2012, **9**(1):118.
64. Banerjee A, Roy S, Tarafdar J: **The large intergenic region of Rice tungro bacilliform virus evolved differentially among geographically distinguished isolates**. *Virus Genes* 2012, **44**(2):312-318.
65. Kozak M: **Pushing the limits of the scanning mechanism for initiation of translation**. *Gene* 2002, **299**(1-2):1-34.
66. Matynia A, Ng CH, Dansithong W, Chiang A, Silva AJ, Reddy S: **Muscleblind1, but not Dmpk or Six5, contributes to a complex phenotype of muscular and motivational deficits in mouse models of myotonic dystrophy**. *PLoS One* 2010, **5**(3):e9857.
67. Hann SR, King MW, Bentley DL, Anderson CW, Eisenman RN: **A non-AUG translational initiation in c-myc exon 1 generates an N-terminally distinct protein whose synthesis is disrupted in Burkitt's lymphomas**. *Cell* 1988, **52**(2):185-195.
68. Spotts GD, Patel SV, Xiao Q, Hann SR: **Identification of downstream-initiated c-Myc proteins which are dominant-negative inhibitors of transactivation by full-length c-Myc proteins**. *Mol Cell Biol* 1997, **17**(3):1459-1468.
69. Hann SR: **Methionine deprivation regulates the translation of functionally-distinct c-Myc proteins**. *Adv Exp Med Biol* 1995, **375**:107-116.
70. Crawley JN, Belknap JK, Collins A, Crabbe JC, Frankel W, Henderson N, Hitzemann RJ, Maxson SC, Miner LL, Silva AJ *et al*: **Behavioral phenotypes of inbred mouse strains: implications and recommendations for molecular studies**. *Psychopharmacology (Berl)* 1997, **132**(2):107-124.
71. Kozak M: **Point mutations define a sequence flanking the AUG initiator codon that modulates translation by eukaryotic ribosomes**. *Cell* 1986, **44**(2):283-292.
72. Goossen B, Hentze MW: **Position is the critical determinant for function of iron-responsive elements as translational regulators**. *Mol Cell Biol* 1992, **12**(5):1959-1966.
73. Wang L, Wessler SR: **Role of mRNA secondary structure in translational repression of the maize transcriptional activator Lc(1,2)**. *Plant Physiol* 2001, **125**(3):1380-1387.

74. Kozak M: **Circumstances and mechanisms of inhibition of translation by secondary structure in eucaryotic mRNAs**. *Mol Cell Biol* 1989, **9**(11):5134-5142.
75. Kochetov AV, Prayaga PD, Volkova OA, Sankararamakrishnan R: **Hidden coding potential of eukaryotic genomes: nonAUG started ORFs**. *J Biomol Struct Dyn* 2012.
76. Nishikawa T, Ota T, Isogai T: **Prediction whether a human cDNA sequence contains initiation codon by combining statistical information and similarity with protein sequences**. *Bioinformatics* 2000, **16**(11):960-967.
77. Johnson WG MW, and Bloom AD: **Recessive congenital cerebellar disorder in a genetic isolate: CPD Type II?** *Neurology* 1978, **28**:351-352.
78. Meisler MH: **Insertional mutation of 'classical' and novel genes in transgenic mice**. *Trends Genet* 1992, **8**(10):341-344.
79. Palmiter RD, Brinster RL: **Germ-line transformation of mice**. *Annu Rev Genet* 1986, **20**:465-499.
80. Dellaire G, Chartrand P: **Direct evidence that transgene integration is random in murine cells, implying that naturally occurring double-strand breaks may be distributed similarly within the genome**. *Radiat Res* 1998, **149**(4):325-329.
81. Silvers W: **The Coat Colors of Mice: A Model for Mammalian Gene Action and Interaction**, 1 edn. New York: Springer Verlag; 1979.
82. Hatcher JP, Jones DN, Rogers DC, Hatcher PD, Reavill C, Hagan JJ, Hunter AJ: **Development of SHIRPA to characterise the phenotype of gene-targeted mice**. *Behav Brain Res* 2001, **125**(1-2):43-47.
83. Van Keuren ML, Gavrilina GB, Filipiak WE, Zeidler MG, Saunders TL: **Generating transgenic mice from bacterial artificial chromosomes: transgenesis efficiency, integration and expression outcomes**. *Transgenic Res* 2009, **18**(5):769-785.
84. Crawley J: **What's Wrong with my Mouse? Behavioral Phenotyping of Transgenic and Knockout Mice**. New York: John Wiley & Sons; 2000.
85. Crawley JN: **Behavioral phenotyping of rodents**. *Comp Med* 2003, **53**(2):140-146.
86. Crawley JN: **Exploratory behavior models of anxiety in mice**. *Neurosci Biobehav Rev* 1985, **9**(1):37-44.
87. Crawley JN, Paylor R: **A proposed test battery and constellations of specific behavioral paradigms to investigate the behavioral phenotypes of transgenic and knockout mice**. *Horm Behav* 1997, **31**(3):197-211.
88. Rustay NR, Wahlsten D, Crabbe JC: **Influence of task parameters on rotarod performance and sensitivity to ethanol in mice**. *Behav Brain Res* 2003, **141**(2):237-249.
89. Crawley JN: **Behavioral phenotyping strategies for mutant mice**. *Neuron* 2008, **57**(6):809-818.

90. Henikoff S: **Conspiracy of silence among repeated transgenes**. *Bioessays* 1998, **20**(7):532-535.
91. Chandler KJ, Chandler RL, Broeckelmann EM, Hou Y, Southard-Smith EM, Mortlock DP: **Relevance of BAC transgene copy number in mice: transgene copy number variation across multiple transgenic lines and correlations with transgene integrity and expression**. *Mamm Genome* 2007, **18**(10):693-708.
92. Kaufman RM, Pham CT, Ley TJ: **Transgenic analysis of a 100-kb human beta-globin cluster-containing DNA fragment propagated as a bacterial artificial chromosome**. *Blood* 1999, **94**(9):3178-3184.
93. Lo CW: **Localization of low abundance DNA sequences in tissue sections by in situ hybridization**. *J Cell Sci* 1986, **81**:143-162.
94. Stinnakre MG, Soulier S, Schibler L, Lepourry L, Mercier JC, Vilotte JL: **Position-independent and copy-number-related expression of a goat bacterial artificial chromosome alpha-lactalbumin gene in transgenic mice**. *Biochem J* 1999, **339 (Pt 1)**:33-36.
95. Giraldo P, Montoliu L: **Size matters: use of YACs, BACs and PACs in transgenic animals**. *Transgenic Res* 2001, **10**(2):83-103.
96. Wutz A: **Gene silencing in X-chromosome inactivation: advances in understanding facultative heterochromatin formation**. *Nat Rev Genet* 2011, **12**(8):542-553.
97. Insel TR, Young LJ: **The neurobiology of attachment**. *Nat Rev Neurosci* 2001, **2**(2):129-136.
98. Crawley JN: **Unusual behavioral phenotypes of inbred mouse strains**. *Trends Neurosci* 1996, **19**(5):181-182; discussion 188-189.
99. Rogers DC, Jones DN, Nelson PR, Jones CM, Quilter CA, Robinson TL, Hagan JJ: **Use of SHIRPA and discriminant analysis to characterise marked differences in the behavioural phenotype of six inbred mouse strains**. *Behav Brain Res* 1999, **105**(2):207-217.
100. Altmann J: **Observational study of behavior: sampling methods**. *Behaviour* 1974, **49**(3):227-267.
101. Daily DK, Ardinger HH, Holmes GE: **Identification and evaluation of mental retardation**. *Am Fam Physician* 2000, **61**(4):1059-1067, 1070.
102. Porsolt RD, Bertin A, Jalfre M: **Behavioral despair in mice: a primary screening test for antidepressants**. *Arch Int Pharmacodyn Ther* 1977, **229**(2):327-336.
103. Smith JP, Hicks PS, Ortiz LR, Martinez MJ, Mandler RN: **Quantitative measurement of muscle strength in the mouse**. *J Neurosci Methods* 1995, **62**(1-2):15-19.
104. Rayavarapu S, Van der meulen JH, Gordish-Dressman H, Hoffman EP, Nagaraju K, Knoblach SM: **Characterization of Dysferlin Deficient SJL/J Mice to Assess Preclinical Drug Efficacy: Fasudil Exacerbates Muscle Disease Phenotype**. *PLoS ONE* 2010, **5**(9):e12981.
105. Livak KJ, Schmittgen TD: **Analysis of relative gene expression data using real-time quantitative PCR and the 2(-Delta Delta C(T)) Method**. *Methods* 2001, **25**(4):402-408.

106. Owczarzy R, Tataurov AV, Wu Y, Manthey JA, McQuisten KA, Almabrazi HG, Pedersen KF, Lin Y, Garretson J, McEntaggart NO *et al*: **IDT SciTools: a suite for analysis and design of nucleic acid oligomers**. *Nucleic Acids Res* 2008, **36**(Web Server issue):W163-169.
107. Concepcion D, Flores-Garcia L, Hamilton BA: **Multipotent genetic suppression of retrotransposon-induced mutations by Nxf1 through fine-tuning of alternative splicing**. *PLoS Genet* 2009, **5**(5):e1000484.
108. Losson R, Lacroute F: **Interference of nonsense mutations with eukaryotic messenger RNA stability**. *Proc Natl Acad Sci U S A* 1979, **76**(10):5134-5137.
109. Baker KE, Parker R: **Nonsense-mediated mRNA decay: terminating erroneous gene expression**. *Curr Opin Cell Biol* 2004, **16**(3):293-299.
110. Chang YF, Imam JS, Wilkinson MF: **The nonsense-mediated decay RNA surveillance pathway**. *Annu Rev Biochem* 2007, **76**:51-74.
111. Seoighe C, Gehring C: **Heritability in the Efficiency of Nonsense-Mediated mRNA Decay in Humans**. *PLoS ONE* 2010, **5**(7):e11657.
112. Zetoune AB, Fontaniere S, Magnin D, Anczukow O, Buisson M, Zhang CX, Mazoyer S: **Comparison of nonsense-mediated mRNA decay efficiency in various murine tissues**. *BMC Genet* 2008, **9**:83.
113. Linde L, Boelz S, Neu-Yilik G, Kulozik AE, Kerem B: **The efficiency of nonsense-mediated mRNA decay is an inherent character and varies among different cells**. *Eur J Hum Genet* 2007, **15**(11):1156-1162.
114. Linde L, Boelz S, Neu-Yilik G, Kulozik AE, Kerem B: **The efficiency of nonsense-mediated mRNA decay is an inherent character and varies among different cells**. *Eur J Hum Genet* 2007, **15**(11):1156-1162.
115. Kamath KS, Vasavada MS, Srivastava S: **Proteomic databases and tools to decipher post-translational modifications**. *J Proteomics* 2011, **75**(1):127-144.
116. Antoch MP, Song EJ, Chang AM, Vitaterna MH, Zhao Y, Wilsbacher LD, Sangoram AM, King DP, Pinto LH, Takahashi JS: **Functional identification of the mouse circadian Clock gene by transgenic BAC rescue**. *Cell* 1997, **89**(4):655-667.
117. Koetsier PA, Mangel L, Schmitz B, Doerfler W: **Stability of transgene methylation patterns in mice: position effects, strain specificity and cellular mosaicism**. *Transgenic Res* 1996, **5**(4):235-244.
118. Vergara GJ, Irwin MH, Moffatt RJ, Pinkert CA: **In vitro fertilization in mice: Strain differences in response to superovulation protocols and effect of cumulus cell removal**. *Theriogenology* 1997, **47**(6):1245-1252.
119. Casola S: **Mouse Models for miRNA Expression: The ROSA26 Locus**. In., vol. 667; 2010: 145-163.
120. Shakkottai VG, Xiao M, Xu L, Wong M, Nerbonne JM, Ornitz DM, Yamada KA: **FGF14 regulates the intrinsic excitability of cerebellar Purkinje neurons**. *Neurobiol Dis* 2009, **33**(1):81-88.
121. Brodskii LI, Ivanov VV, Kalaidzidis Ia L, Leontovich AM, Nikolaev VK, Feranchuk SI, Drachev VA: **[GeneBee-NET: An Internet based server for biopolymer structure analysis]**. *Biokhimiia* 1995, **60**(8):1221-1230.

122. Zheng CY, Petralia RS, Wang YX, Kachar B: **Fluorescence recovery after photobleaching (FRAP) of fluorescence tagged proteins in dendritic spines of cultured hippocampal neurons**. *J Vis Exp* 2011(50).
123. Curthoys NP, Shapiro RA: **Mechanism of glutamate and alpha-ketoglutarate inhibition of rat renal phosphate-dependent glutaminase**. *Contrib Nephrol* 1982, **31**:71-76.